Non-Monotonic Pricing Kernels and Risk-Neutral Bounds for Expected Returns*

Stefanos Delikouras†

March 17, 2025

Abstract

This paper studies how non-monotonicities and VIX-dependence of the stochastic discount factor affect the option-based physical distribution of market returns and the accuracy of risk-neutral bounds for expected returns. I show that monotonic and non-monotonic pricing kernels generate similar option-based physical distributions of returns. However, when non-monotonicities are combined with VIX-dependent risk aversion in the discount factor, the resulting physical densities are very different. Similarly, option-based expected returns from both monotonic and non-monotonic fixed-parameter pricing kernels are aligned with the variance-based risk-neutral bounds. Yet, when the parameters of the pricing kernel depend on the VIX, the resulting option-based expected returns largely deviate from the risk-neutral bounds.

Keywords: options, risk-neutral density, physical density, expected-returns, risk-neutral bounds, non-monotonic pricing kernels
JEL classification: G10, G13, D84

*I would like to thank Alexandros Kostakis and Lykourgos Alexiou. I am responsible for all errors and omissions.

†Department of Finance, Miami Herbert Business School, University of Miami, email: *sdelikouras@bus.umiami.edu*

Non-Monotonic Pricing Kernels and Risk-Neutral Bounds for Expected Returns

Abstract

This paper studies how non-monotonicities and VIX-dependence of the stochastic discount factor affect the option-based physical distribution of market returns and the accuracy of risk-neutral bounds for expected returns. I show that monotonic and non-monotonic pricing kernels generate similar option-based physical distributions of returns. However, when non-monotonicities are combined with VIX-dependent risk aversion in the discount factor, the resulting physical densities are very different. Similarly, option-based expected returns from both monotonic and non-monotonic fixed-parameter pricing kernels are aligned with the variance-based risk-neutral bounds. Yet, when the parameters of the pricing kernel depend on the VIX, the resulting option-based expected returns largely deviate from the risk-neutral bounds.

Keywords: options, risk-neutral density, physical density, expected-returns, risk-neutral bounds, non-monotonic pricing kernels
JEL classification: G10, G13, D84

1 Introduction

Conditional stock market expected returns are one of the most important yet elusive objects in finance. Conditional expected returns are important because they are a basic component of almost all asset pricing models. From the capital asset pricing model (Lintner (1965)) to the alternative factor specifications (Merton (1974), Fama and French (2015), Hou et al. (2019)) and the life-cycle income models in household finance (Viceira (2001)), conditional expected stock market returns are a key variable in financial decision making. Conditional expected returns are elusive because there is no direct way of measuring forward-looking expectations. Traditionally, expected returns for the aggregate stock market are obtained via time-series (predictability) regressions, while expected returns at the firm-level are derived from cross-sectional (factor) regressions.[1]

In either case, the derived conditional expected returns cannot be considered truly forward-looking because they are are based on contemporaneous or lagged historical data (e.g., asset pricing factors, price-dividend ratio, dividend growth), and are estimated using backward-looking relations that require strong assumptions. An alternative approach to estimating expected returns are surveys (e.g., Gallup/UBS Survey of Investor Optimism, Duke's CFO survey) that directly ask investors about their expectations for the stock market (e.g., Vissing-Jorgensen (2004)). However, these surveys tend to have a limited time-span, and focus on subsets of individuals or professionals that do not encompass the aggregate expectations of market participants.

In recent years, one of the most prominent methodologies for deriving forward-looking conditional expected market returns is using option prices and option-implied risk-neutral densities. For instance, Martin (2017) derives bounds for market-level expected returns that are based on the risk-neutral market variance and the risk-free rate. In a subsequent paper, Martin and Wagner (2019) derive variance-based bounds for firm-level expected returns, while Chabi-Yo and Loudis (2020) and Chabi-Yo et al. (2022) derive bounds for expected returns that are based on high-order risk-neutral moments.

Conditional expected market returns based on risk-neutral bounds are important because they rely on forward-looking option prices as opposed to the traditional backwards-looking regression approach. Despite this innovative methodology, option-derived bounds for expected returns are subject to criticism because they are based on risk-neutral moments, and

[1]Predictability tests: Campbell and Shiller (1988), Stambaugh (1999), Lettau and Ludvigson (2001a), Goyal and Welch (2003), Goyal and Welch (2008), Ang and Bekaert (2007), van Binsgergen and Koijen (2010), Lewellen (2015), Kostakis et al. (2015). Cross-sectional tests: Fama and French (1993), Fama and French (2015), Hou et al. (2019), Liu et al. (2009), Lettau and Ludvigson (2001b), Yogo (2006), Delikouras (2017), Delikouras and Kostakis (2019). These papers constitute a very small sample of a vast literature.

ignore the physical measure. One way to resolve the issue of deriving expected returns using risk-neutral moments is by assuming a pricing kernel that reflects investors' risk-return preferences. To this end, Bliss and Panigirtzoglou (2004) estimate the standard power utility discount factor from option prices, while Linn et al. (2018) estimate a non-parametric pricing kernel. Based on this approach, it is quite straightforward to multiply the option-based risk-neutral density by the inverse of the estimated discount factor and derive the option-based distribution of stock market returns under the physical measure. Using this physical density, one could then calculate forward-looking expected returns.

Even in this case, however, there are several issues regarding the properties of the true stochastic discount factor that need to be addressed. To begin with, discount factors are not observable. Secondly, the structural parameters of the discount factor (e.g., elasticity of intertemporal substitution, risk aversion, discount rate) can be time-varying (e.g., Schreindorfer and Sischert (2022)). Thirdly, contrary to the standard monotonicity assumptions for marginal utility in economics and finance, option-derived pricing kernels can be non-monotonic (e.g., Cuesdeanu and Jackwerth (2018)). Motivated by these observations, in this paper I jointly examine two important and contentious issues in the asset pricing literature. First, I investigate the implications of non-monotonicities and time-variation in the parameters of the pricing kernel for the moments of the physical density. Second, I examine the accuracy of the risk-neutral bounds across monotonic and non-monotonic discount factors.

To examine the effects of non-monotonicities and time-variation of the pricing kernel on the option-based physical distribution of returns, I estimate four alternative specifications for the discount factor: standard power utility (monotonic marginal utility with fixed parameters), power utility with VIX-dependent risk aversion (monotonic marginal utility with time-varying parameters), power utility with quadratic exponent (non-monotonic marginal utility with fixed parameters), power utility with VIX-dependent quadratic exponent (non-monotonic marginal utility with time-varying parameters). These pricing kernels expand the standard power utility specification and allow for non-monotonicities, as well as the possibility of time-varying parameters in the discount factor. Hence, these parametric pricing kernels are quite versatile, and allow for a rich set of risk preferences.

In estimating these pricing kernels, I calculate the option-based risk-neutral density across four different maturities (1-, 2-, 3-, and 6-month) using the standard methodology in Figlewski (2008), Linn et al. (2018), and Alexiou et al. (2024), which identifies the risk-neutral density from the second derivative of option prices with respect to the strike price (Huang and Litzenberger (1989)). Then, I use a GMM system that combines the moment restrictions in Linn et al. (2018) with rational expectations. Specifically, I estimate the parameters in the four discount factors using the fact that any cumulative distribution function

is a standard uniform random variable. Further, I combine these uniform moments with a rational expectations moment restriction according to which average option-based expected returns should be equal to average realized returns over the sample period. Finally, I multiply the inverse of the four alternative discount factors with the common risk-neutral density to derive alternative option-based physical distributions across the four expirations.

To address the issue of the importance of non-monotonicities and VIX-dependence (time-variation) in the pricing kernel, first I examine, through standard GMM hypothesis testing, the statistical significance of the linear and quadratic parameters of the pricing kernel as well as the significance of the VIX-dependence parameters. My results indicate, that the evidence in support of non-monotonicities are relatively weak since the parameters in the quadratic terms of the pricing kernel are statistically insignificant. Similar results also hold for the significance of the VIX-dependence parameters, which appear to be statistically insignificant in most cases. To the contrary, the standard linear coefficients (risk aversion) that capture monotonic marginal utility are statistically significant.

In addition to hypothesis testing, I examine whether the resulting physical distributions from the four discount factors are similar, and whether the alternative discount factors generate significantly different distributions than the standard monotonic pricing kernel. To this end, I use Kolmogorov-Smirnov tests for the pairwise equality of two distribution functions. My results indicate that the monotonic pricing kernels with either fixed or VIX-dependent parameters generate quite similar physical distributions, which are in turn relatively close to the physical distribution from the non-monotonic discount factor with fixed-parameters. To the contrary, the physical densities generated by the non-monotonic pricing kernel with VIX-dependent parameters are substantially different from the densities of the other pricing kernels. Importantly, the effects of the VIX, which for the purposes of this estimation is normalized by its sample average, on risk-aversion is non-linear. Hence, my results suggest that non-monotonicities need to be combined with time-variation of parameters to generate substantially different physical densities from the standard monotonic (power utility) model.

I further identify the causes of these differences among the physical distributions by examining the relation, both in levels and in comovement, among the option-based physical moments (expected value, variance, skewness, and kurtosis) from the various discount factor specifications. Regarding first moments, all discount factors are able to generate expected returns that are higher than the ones implied by the risk-neutral density. This is because the GMM moments for the estimation of the alternative pricing kernels force the average option-based expected returns to be equal to the average realized return (rational expectations).

Although variances are not a target moment in the GMM estimation of the discount factors, variance levels are consistent across pricing kernels, and are similar, albeit lower, to the

risk-neutral variance. The discount factor that generates the lowest forward-looking variance is the non-monotonic pricing kernel with VIX-dependent parameters. Similar results hold for skewness and kurtosis. The non-monotonic specification with VIX-dependent parameters generates the least amount of variance, skewness, and kurtosis for the physical measure due to the time-variation in its parameters, which depend on the VIX. In other worlds, the non-monotonic pricing kernel with VIX-dependent parameters is the only pricing kernel that can transform a risk-neutral density with large (in absolute value) variance, skewness, and kurtosis into a physical distribution with moderate high-order moments. In fact, the physical moments implied by the non-monotonic discount factor with VIX-dependent risk aversion are too low and exhibit too little time-variation compared to the moments of the risk-neutral density or to realized moments.

In addition to studying the levels of the option-based physical moments across pricing kernels, I also examine their comovement using coefficients of determination (R^2's) from pairwise regressions of the physical moments from one pricing kernel to the same moments form the rest of the discount factors. The results from these tests suggest that variances are highly correlated both across pricing kernels and with the corresponding risk-neutral moments. To the contrary, odd physical moments, i.e., expected values and skewess, are less correlated across discount factors and from the corresponding risk-neutral moments. This is the first paper to show that the effects of monotonic and non-monotonic pricing kernels differ across variances and the rest of the moments. Even moments, especially variances, are strongly correlated across discount factors, whereas odd moments (means and skewness), differ across pricing kernels, and this divergence in physical moments is mainly driven by the non-monotonic discount factor with VIX dependent parameters.

Overall, my findings from comparing the physical densities across the different pricing kernels suggest that the monotonic, monotonic with VIX-dependence, and non-monotonic pricing kernels seem to generate somewhat similar moments, which are positively correlated. To the contrary, the non-monotonic discount factor with VIX-dependent parameters implies vastly different physical moments, which are almost orthogonal to the moments from rest of the discount factors. Hence, non-monotonicity and VIX-dependence of the pricing kernel alone do not generate substantially different physical moments from the standard monotonic discount factor with fixed-parameters. To the contrary, the combination of non-monotonicity with VIX-dependence, implies a unique physical distribution, which is different to those from the alternative discount factors.

To complement these novel empirical results, I provide additional theoretical insights, which explain the differential effects of non-monotonicities and VIX-dependence on the option-based physical moments. To this end, I combine elements from actuarial science,

termed linear and quadratic Esscher transforms (Esscher (1932), Monfort and Pegoraro (2010)), with normal or skew-normal assumptions for the risk-neutral density. This is one of the first attempts to theoretically explain how monotonicity and VIX-dependence of the discount factor affect option-based physical moments.

Based on these results, the second contentious issue addressed in this paper is the accuracy of the risk-neutral bounds for expected returns. Specifically, having derived option-based distributions under the physical measure for various pricing kernels, I examine whether the risk-neutral bounds proposed by the literature, e.g., bounds based on risk-neutral variances, can accurately capture expected returns under the physical measure.

Expected returns are unobservable. Hence, deriving expected returns from options requires assumptions for the pricing kernel. To avoid such assumptions, the existing literature (e.g., Martin (2017)) has argued that forward-looking expected returns can be measured using option-based risk-neutral moments (e.g., risk-neutral variance) via an (almost) assumption-free approach. Importantly, Martin (2017) and Chabi-Yo and Loudis (2020) provide empirical evidence that risk-neutral bounds are accurate proxies for expected returns by regressing realized returns on these risk-neutral bounds. More recently however Back et al. (2022), using a different methodology, cast doubt on whether these risk-neutral bounds are tight enough to accurately capture expected returns.

I further expand these regression tests for the accuracy of risk-neutral bounds along the following dimensions. First, I provide summary statistics and correlations for the risk-neutral bounds to verify whether these bounds, i.e, the risk-neutral variances, are aligned with average realized returns or average expected returns from the option-based physical densities. Secondly, in addition to the regressions of realized returns on risk-neutral variances, which have been extensively used by the existing literate to empirically validate these bounds, I regress option-based expected returns from the different pricing kernels on risk-neutral variances. For these tests, in addition to realized returns or option-based expected returns, I use backward-looking fitted returns, which are based on predictive regressions of realized returns on the dividend yield, the dividend growth, and the risk-free rate.

Finally, I examine whether realized returns and option-based expected returns from the different pricing kernels tend to violate the risk-neutral bounds. Specifically, the risk-neutral bounds proposed by the literature are lower bounds for expected returns. Hence, I investigate whether there are instances where the risk-neutral bounds are greater than the realized returns or the option-based expected returns.

The results from this analysis highlight four important findings. First, longer option maturities adversely affect the tightness of the risk-neutral bounds. Secondly, realized returns and fitted returns are not appropriate for testing the accuracy of risk-neutral bounds

via regressions. This is because binding risk neutral bounds would imply high R^2's and a very accurate fit for the regressions of expected returns on risk-neutral bounds. To the contrary, the risk-neutral bound regressions with realized returns as the dependent variable have almost zero fit, standard errors are very large, and realized returns often violate the risk-neutral lower bounds, which are strictly positive, due to their large negative values.

Thirdly, for the baseline monotonic power utility pricing kernel with constant parameters, regression results of option-based expected returns on risk-neutral variances show that slope estimates are close to one (e.g., 1.2-1.3), intercepts are zero (e.g., 0.01%), and the R^2's are large (e.g., 99%). These results imply that, even if the slope coefficients are not equal to one, risk-neutral variances are an accurate proxy for expected returns derived from the standard monotonic power utility pricing kernel with constant parameters. These findings run against the results in Back et al. (2022), who show that risk-neutral bounds are not binding.

Finally, for discount factors with VIX-dependent coefficients, the intercepts from regressing option-based expected returns on risk-neutral bounds are significant and the slope estimates are different than one. Hence, for these cases, the risk-neutral bounds are not binding. The finding that the accuracy of the risk-neutral bounds for expected returns depends on VIX-dependence (time-variation) of risk aversion is a novel empirical result that has not been previously studied by the literature.

Interestingly, non-monotonicity does not seem to affect the tightness of the risk-neutral bounds as much as the VIX-dependence of risk aversion since expected returns from the non-monotonic pricing kernel with fixed parameters seem to be closely aligned to the risk-neutral variance bounds. This is because non-monotonicities occur over sets of returns that are assigned very low probabilities either in the left or right tail of the distribution of returns, whereas VIX-dependence affects the entire distribution of returns.

Overall, this paper adds to the expanding literature that uses option markets to study investor preferences and assess the accuracy of competing macroeconomic asset pricing models. Specifically, Ait-Sahalia and Lo (2000) and Rosenberg and Engle (2000) have motivated a series of papers on the monotonicity of discount factors derived from option prices. They document that the option derived-kernels can be increasing over a certain moneyness range (U-shaped marginal utility). Linn et al. (2018) and Kim (2021) introduce conditional estimation of their non-parametric discount factor during periods of high and low VIX values, and, similar to Barone-Adesi et al. (2020), cannot find evidence in support of non-monotonicities in option-derived marginal utility.

Driessen et al. (2022) examine the topic of non-monotonic pricing kernel using a cross-section of option maturities to generate forward pricing kernels. Schreindorfer and Sischert (2022) examine the issue of non-monotonicity through the lens of VIX-dependent param-

eters. Beason and Schreindorfer (2022) use option prices to decompose risk premia and examine which macroeconomic asset pricing model (e.g., long-run risk, habit, disappointment aversion) is consistent with this decomposition. Chabi-Yo et al. (2022) repeat this exercise for conditional risk premia. In a closely related paper by Heston et al. (2023), the authors estimate option-based pricing kernels by imposing restrictions such as monotonicity and path-independence (recovery theory) to achieve good option fit and reasonable estimates of equity and variance risk premiums, while resolving pricing kernel anomalies.

The findings in this paper complement these works by simultaneously examining the implied physical densities from alternative pricing kernels (power utility, power utility with VIX-dependent parameters, power utility with quadratic exponent, and power utility with quadratic exponent and VIX-based parameters). Additionally, my empirical analysis is able to identify the specific effects of non-monotonicity and VIX-dependence on the physical density by examining the first four moments (mean, variance, skewness, kurtosis) of the resulting physical distributions. Importantly, this is one of the first papers to theoretically explain the effects of the different pricing kernel characteristics on the different moments using results from actuarial science involving Esscher transforms (Esscher (1932), Monfort and Pegoraro (2010)) and the skew-normal assumption for the risk-neutral density.

From the perspective of risk-neutral bounds for expected returns, Martin (2017) is the seminal paper that establishes the relation between risk-neutral variance and expected returns for the aggregate stock market. Chabi-Yo and Loudis (2020) expand this bound with additional higher-order risk-neutral moments, while Martin and Wagner (2019) derive the relation between risk premia and risk-neutral moments for individual stocks. Back et al. (2022) conduct a thorough empirical investigation on the validity of these risk-neutral bounds, and conclude that although the direction of the bounds is correct (lower bounds), these bounds are not binding. Finally, Gandhi et al. (2023) relate option-based expected returns to return expectations from investor surveys (UBS/Gallup survey for investor optimism, Duke's CFO survey), and show that the two sets of expected returns are quite different.

This paper adds to our understanding of the relation between expected returns and risk-neutral moments by using alternative pricing kernels to obtain option-based expected returns under the physical measure. I then test the validity of the risk-neutral bounds by examining their summary statistics and comparing them to summary statistics of realized and expected returns. Importantly, I provide theoretical explanations as to why the expected returns from certain discount factors, e.g., monotonic marginal utility, satisfy the risk neutral bounds while in other cases, e.g., expected returns from non-monotonic utility with VIX-dependent parameters, do not.

The fact that the accuracy of risk-neutral bounds depends on option expiration and

on time-variation of risk aversion but not on the monotonicity of the discount factor is a novel finding that has not been previously examined by the literature. Although risk-neutral bounds for expected returns may not be perfect, especially for long maturities (e.g., 6-month), my results indicate that these bounds are superior to alternative measures of expected returns such as average realized returns or fitted returns using predictive factors (e.g., price-dividend ratio, dividend growth, etc.). This is mainly due to the forward-looking aspect of option-based risk-neutral bounds.

The rest of the paper is organized as follows. Section 2 provides the theoretical framework and discusses the alternative pricing kernels used in this study. Section 3 introduces the data and estimation methodology for the risk-neutral density from option prices. Section 4 discusses the estimation results for the different discount factors. Section 5 presents the empirical results regarding the various forward-looking physical densities generated by the alternative pricing kernels. Section 6 examines the validity of risk-neutral bounds for expected returns, and Section 7 concludes.

2 Theoretical Background

To set the stage for the empirical analysis on how the different stochastic discount factors affect the moments under the physical measure and the accuracy of risk neutral bounds for expected returns, I first discuss the various pricing kernels used to derive option-based moments. These discount factors can be broadly classified into monotonic and non-monotonic groups. For each group, I assume both constant and time-varying parameters.

2.1 Monotonic Pricing Kernel

The baseline specification used in my tests is the power utility discount factor defined over stock market wealth W_t:

$$U_1(W_t) = \frac{W_t^{1-\gamma_1}}{1-\gamma_1}.$$

Based on the above functional form, the intertemporal marginal rate of substitution between dates t and $t+T$ is given by

$$M_{1,t,t+T}(R_{t,t+T}) = \beta \frac{U'(W_{t+T})}{U'(W_t)} \quad = \quad exp\{log\beta - \gamma_1 lnR_{t,t+T}\}. \tag{1}$$

The constant β is the rate of time preference, and $R_{t,t+T} = \frac{W_{t+T}}{W_t}$ is the return on total equity wealth. The parameter $\gamma_1 > 0$ describes (relative) risk aversion since

$$-\frac{R_{t,t+T}}{M_{1,t,t+T}}\frac{\partial M_{1,t,t+T}}{\partial R_{t,t+T}} = \gamma_1.$$

A natural extension to the standard power-utility pricing kernel of equation (1) is to assume that risk aversion is time-varying depending on observable variables that are known at time t. To this end, Linn et al. (2018) and Kim (2021) introduce conditional estimation of their non-parametric discount factor during periods of high and low VIX values. Given the importance of the VIX in option-pricing and the recent results in Schreindorfer and Sischert (2022), I assume an extension of the monotonic pricing kernel of equation (1) for which γ_1 is time-varying with an explicit dependence on the VIX:

$$M_{2,t,t+T}(R_{t,t+T}) = \beta\frac{U_2'(W_{t+T})}{U_2'(W_t)} = exp\{log\beta - \gamma_1 nvix_{t,t+T}^{\gamma_3} lnR_{t,t+T}\}. \tag{2}$$

Risk aversion in the above discount factor is given by $\gamma_1 nvix_{t,t+T}^{\gamma_3}$, where $nvix_{t,t+T}$ is the VIX ($VIX_{t,t+T}$) normalized by its unconditional average ($\overline{VIX_{t,t+T}}$) and scaled by $\sqrt{T}$, the number of days in 1-, 2-, 3-, and 6-month intervals ($T \approx 30, 60, 90, 180$), over $\sqrt{365}$:

$$nvix_{t,t+T} = \frac{VIX_{t,t+T}\sqrt{T}}{\overline{VIX_{t,t+T}}\sqrt{365}} \tag{3}$$

The intuition behind this formulation is that there is a natural level of risk associated with investing in the stock market, which is captured by the average VIX. When VIX is greater or lower than its average, risk aversion will be affected depending on the signs of γ_1 and γ_3. Similarly, since VIX is a percentage, I opt for the specification $nvix_{t,t+T}^{\gamma_3}$ in equation (2) instead of the term $VIX_{t,t+T}^{\gamma_3}$ to avoid extreme values for risk aversion when the VIX is very low (high) and γ_3 is a negative (positive) number. The VIX and the normalized VIX ($nvix$) are known to the investor at time t. Hence, to avoid any look-ahead bias, the average VIX, $\overline{VIX}$ in equation (3), is estimated over the 1986-1995 period before the start of our sample. The values for the average VIX are 5.356%, 7.818%, 10.186%, and 13.119% for the 1-, 2-, 3-, and 6-month maturities respectively.[2]

Given the positivity of the VIX and $nvix$, a well-defined risk aversion coefficient would require a positive γ_1 parameter. The constant γ_3 captures the procyclicality of risk-aversion

[2]The VIX values before 1990 were fitted by estimating the regression of the VIX on the old methodology VIX at the daily frequency. The estimates of this regression are: intercept = 0.240% (t-stat= 1.04), OLS coefficient = 0.987 (t-stat=71.01), R^2 = 96%. Standard errors were calculated with a 30-lag Newey-West correction for autocorellation and heteroscedasticity.

with respect to the $nvix$. For positive γ_1, if γ_3 is positive (negative), risk aversion is procyclical (counter-cyclical) with respect to the $nvix$. Empirically, we would expect γ_3 to be positive so that risk aversion raises with the $nvix$. If γ_3 is zero, equation (2) collapses to the utility function with constant risk aversion (equation (1)).

2.2 Non-monotonic Pricing Kernel

One contentious aspect of the option-derived pricing kernel is its monotonicity. Although Linn et al. (2018) cannot find evidence in support of non-monotonicities in option-based marginal utility, the existing literature has advocated for U-shaped discount factors (e.g., Ait-Sahalia and Lo (2000), Rosenberg and Engle (2000)). Given the recent findings in Schreindorfer and Sischert (2022) and Driessen et al. (2022), I also allow for non-monotonicities in the pricing kernel. The non-monotonic pricing kernel is described by a power utility function with a quadratic exponent.

Specifically, I assume the following quadratic intertemporal marginal rate of substitution

$$M_{3,t,t+T}(R_{t,t+T}) = exp\{log\beta - \gamma_1 lnR_{t,t+T} - \gamma_2 ln^2 R_{t,t+T}\}. \tag{4}$$

The non-monotonicity of the pricing kernel is captured by the square term $ln^2 R_{t,t+T}$ and the parameter γ_2. A possible interpretation of the non-monotonic model is a power utility specification with a risk-aversion coefficient that depends on the stock market since

$$-\frac{R_{t,t+T}}{M_{3,t,t+T}}\frac{\partial M_{3,t,t+T}}{\partial R_{t,t+T}} = \gamma_1 + 2\gamma_2 lnR_{t,t+T}. \tag{5}$$

Based on the above relation, the coefficient γ_2 determines the procyclicality of the coefficient of risk aversion with respect to stock market returns. If γ_2 is positive (negative) then risk aversion is procyclical (counter-cyclical) with respect to the stock market. According to Bakshi and Madan (2007) and Bakshi et al. (2010), another possible interpretation of the quadratic term is that it captures risk aversion of investors who are shorting the market. Cuesdeanu and Jackwerth (2018) provide an thorough analysis of the possible causes of the non-monotonic pricing kernel.

Finally, similar to the VIX-dependent model of equation (2), in addition to non-monotonicities, I introduce a more complicated pricing kernel, which is characterized by dependence of the quadratic preference parameters on the normalized VIX ($nvix$). Specifically, I assume that the discount factor is

$$M_{4,t,t+T}(R_{t,t+T}) = exp\{log\beta - \gamma_1 nvix_{t,t+T}^{\gamma_3} lnR_{t,t+T} - \gamma_2 nvix_{t,t+T}^{\gamma_3} ln^2 R_{t,t+T}\}. \tag{6}$$

The dependence of the above pricing kernel on the normalized VIX ($nvix$) is regulated by the constant γ_3. In this case, risk aversion depends both on the VIX and on stock market returns since

$$-\frac{R_{t,t+T}}{M_{4,t,t+T}}\frac{\partial M_{4,t,t+T}}{\partial R_{t,t+T}} = \gamma_1 nvix_{t,t+T}^{\gamma_3} + 2\gamma_2 nvix_{t,t+T}^{\gamma_3} lnR_{t,t+T}. \tag{7}$$

Because the VIX is positive, the coefficient γ_2 in equation (6) determines the procyclicality of risk aversion with respect to stock market as in the non-monotonic discount factor with fixed parameters of equation (4). If γ_2 is positive (negative) then risk aversion is procyclical (counter-cyclical) relatively to the stock market. Nevertheless, the introduction of a quadratic term complicates the dependence of risk aversion on the normalized VIX $nvix$, which is given by

$$\gamma_1\gamma_3 nvix_{t,t+T}^{\gamma_3-1} + 2\gamma_2\gamma_3 nvix_{t,t+T}^{\gamma_3-1} lnR_{t,t+T}.$$

In this case, the procyclicality of risk aversion with respect to the VIX also depends on the level of stock market returns.

The dependence of option-based pricing kernels on the VIX has gained considerable traction in the existing literature (e.g., Linn et al. (2018), Kim (2021)). To the contrary, the existence and significance of non-monotonic (quadratic) terms in the pricing kernel is a controversial topic with evidence both in support (e.g., Schreindorfer and Sischert (2022), Driessen et al. (2022)) and against (e.g., Linn et al. (2018), Barone-Adesi et al. (2020)). To further advance this discussion, the GMM estimation in my empirical analysis is unconstrained, and the preference parameters are dictated by the data.

Overall, I opt for parametric specifications of the pricing kernel as opposed a non-parametric one (e.g., Linn et al. (2018)) for two reasons. First, the parametric discount factor is based on solid economic foundations, and allows me to derive risk-return relations that involve structural parameters (e.g., risk aversion). Secondly, and more importantly, parametric discount factors allow me to examine how different properties, e.g, non-monotonicities or time-variation of parameters, affect the resulting option-based physical measures. In general, my assumptions for the parametric pricing kernels are quite versatile, and allow for a rich set of risk attitudes. Finally, as shown in Sichert (2023) non-monotonicities in option-based pricing kernels can be accurately captured by quadratic functions, and it is not necessary to resort to higher-order models.

2.3 Estimation of the Pricing Kernel and the Forward-looking Physical Measure

In estimating the moments under the physical distribution across different pricing kernels, I assume that $Q(R)$ is the cumulative distribution function for gross equity returns, R, under the risk-neutral measure. The risk-neutral density can be estimated from option prices. I also assume that $P(R)$ is the forward-looking continuous cumulative distribution function for equity returns under the physical measure, and $dP(R)/dQ(R)$ is the Radon-Nikodym derivative between the two measures. The forward-looking physical measure is unobservable. However, assuming that the conditions in Linn et al. (2018) hold, the Radon-Nikodym derivative is unique, and is equal to the inverse of the discount factor

$$\frac{dP(R)}{dQ(R)} = M_{t,t+T}(R)^{-1}. \tag{8}$$

The forward-looking physical measure can therefore be calculated as the product of the risk-neutral measure with the inverse of the pricing kernel

$$dP(R) = M_{t,t+T}(R)^{-1} dQ(R). \tag{9}$$

In general, the pricing kernel is also unobservable. However, I can use equations (1) - (6) in a GMM system to estimate the unknown parameters of the discount factor. To this end, I employ two sets of GMM moment conditions. The first one, which is introduced in Linn et al. (2018), is based on the fact that any continuous density function is a standard uniform random variable, $P(R) \sim U[0,1]$, and thus

$$\mathbb{E}\Big[\Big(\int_0^{R^*_{t,t+T}} M_{t,t+T}(R)^{-1} dQ_{t,t+T}(R)\Big)^n\Big] = \frac{1}{n+1},\ n = 1, 2, ... \tag{10}$$

The variable $R^*_{t,t+T}$ above is the realized gross equity return between dates t and $t+T$.

The second set of target GMM moments is a rational expectations restriction where the unconditional average of option-based expected returns according to the physical measure are equal to the unconditional averages of realized returns $\big(\mathbb{E}\big[R^*_{t,t+T}\big]\big)$:

$$\mathbb{E}\Big[\int_0^{+\infty} R\ M_{t,t+T}(R)^{-1} dQ_{t,t+T}(R)\Big] = \mathbb{E}\big[R^*_{t,t+T}\big]. \tag{11}$$

By equating average realized returns to average expected returns, I establish a link between realized and option-based expected returns. The rational expectations moment condition of

equation (11) is a novel component in the GMM estimation of option-based discount factors that has not been used before.

Following Bliss and Panigirtzoglou (2004), I further impose the normalisation

$$\Big(\int_0^{+\infty} M_{t,t+T}(R)^{-1} dQ_{t,t+T}(R) \Big)^{-1} \tag{12}$$

in the above theoretically-derived moment conditions to guarantee that the estimated parameters imply well-behaved conditional physical density functions for every date in my sample. After this normalization, the GMM system from equations (10) and (11) becomes

$$\begin{bmatrix} \mathbb{E}\Big[\Big(\frac{\int_0^{R^*_{t,t+T}} M_{t,t+T}(R)^{-1} dQ_{t,t+T}(R)}{\int_0^{+\infty} M_{t,t+T}(R)^{-1} dQ_{t,t+T}(R)} \Big)^n \Big] - \frac{1}{n+1}, \ n = 1, 2, ..., \\ \mathbb{E}\Big[\frac{\int_0^{+\infty} R \ M_{t,t+T}(R)^{-1} dQ_{t,t+T}(R)}{\int_0^{+\infty} M_{t,t+T}(R)^{-1} dQ_{t,t+T}(R)} \Big] - \mathbb{E}\big[R^*_{t,t+T} \big] \end{bmatrix}. \tag{13}$$

As in Bliss and Panigirtzoglou (2004), due to this normalization, the discount rate parameter β in equations (1), (2), (4), and (6) cannot be identified and will be dropped. The normalisation in equation (13) is equivalent to imposing an additional time-varying parameter in the discount factor as in Schreindorfer and Sischert (2022), which forces every estimated physical density to integrate to one.

I estimate the parameters in the pricing kernels of equations (1), (2), (4), and (6) with an exactly identified single-stage GMM, i.e., n is equal to $m - 1$ in equation (13), where m is the number of parameters in the discount factor. For the case that $m = 1$, namely the estimation of the simple power utility model from equation (1), GMM is conducted with an over-identified 2×2 system with one degree of freedom. This over-identification stems from the fact that I force the simple one-parameter discount factor to satisfy both the uniform moments (equation (10)) and the rational expectations (equation (11)) condition.

For all pricing kernels, I use an $m \times m$ diagonal weighting matrix with diagonal elements $\{1, 1, ..., 100\}$. The weighting matrix assigns a weight of one to the uniform moments (equation (10)), and a weight of 100 to the rational expectations condition (equation (11)). This is because the scale of the rational expectations condition is much lower than that of the uniform moment. The gradient of the GMM objective function is obtained numerically by differentiating equation (13) with respect to the parameters of each discount factor. Standard errors are corrected for autocorrelation and heteroscedasticity using the Newey and West (1987) formula with 12, 6, 4, and 2 lags for the 1-, 2-, 3-, and 6-month expirations, respectively. For the over-identified GMM system that corresponds to the standard power utility model of equation (1), I also calculate the χ^2-test for GMM errors. The estimation of the remaining discount factors (equations (2) to (6)) is based on exactly-identified GMM

systems for which the χ^2-test has zero degrees of freedom.

After estimating the preference parameters via GMM, I can multiply the inverse of the estimated pricing kernel with the option based risk-neutral density to derive the option-based physical measure. Specifically, the option-based physical density, distribution function, and corresponding physical moments are given by

$$\begin{aligned}
dP_{t,t+T}(R)/dR &= \frac{M_{t,t+T}(R)^{-1}dQ_{t,t+T}(R)}{\int_0^{+\infty} M_{t,t+T}(R)^{-1}dQ_{t,t+T}(R)}/dR \qquad (14)\\
P_{t,t+T}(R^*_{t,t+T}) &= \frac{\int_0^{R^*_{t,t+T}} M_{t,t+T}(R)^{-1}dQ_{t,t+T}(R)}{\int_0^{+\infty} M_{t,t+T}(R)^{-1}dQ_{t,t+T}(R)}\\
\mathbb{E}_t[R_{t,t+T}] &= \frac{\int_0^{+\infty} R\ M_{t,t+T}(R)^{-1}dQ_{t,t+T}(R)}{\int_0^{+\infty} M_{t,t+T}(R)^{-1}dQ_{t,t+T}(R)}\\
var_t(R_{t,t+T}) &= \frac{\int_0^{+\infty}(R-\mathbb{E}_t[R])^2\ M_{t,t+T}(R)^{-1}dQ_{t,t+T}(R)}{\int_0^{+\infty} M_{t,t+T}(R)^{-1}dQ_{t,t+T}(R)}\\
skew_t((R)_{t,t+T}) &= \frac{\int_0^{+\infty}(R-\mathbb{E}_t[R])^3\ M_{t,t+T}(R)^{-1}dQ_{t,t+T}(R)}{var_t(R_{t,t+T})^{3/2}\int_0^{+\infty} M_{t,t+T}(R)^{-1}dQ_{t,t+T}(R)}\\
kurt_t(R_{t,t+T}) &= \frac{\int_0^{+\infty}(R-\mathbb{E}_t[R])^4\ M_{t,t+T}(R)^{-1}dQ_{t,t+T}(R)}{var_t(R_{t,t+T})^{4/2}\int_0^{+\infty} M_{t,t+T}(R)^{-1}dQ_{t,t+T}(R)}.
\end{aligned}$$

The same approach without the term $\frac{M_{t,t+T}(R)^{-1}}{\int_0^{+\infty} M_{t,t+T}(R)^{-1}dQ_{t,t+T}(R)}$ is used to calculate moments of the risk-neutral density. Finally, log-return moments are calculated by replacing the terms $(R-\mathbb{E}_t[R])^n$ above with $(lnR-\mathbb{E}_t[lnR])^n$, both for the physical and the risk-neutral measures.

3 Option Data and the Risk-Neutral Density

In this section, I discuss the options data used in my empirical analysis that examines how different pricing kernels affect the moments of the physical distribution and the accuracy of risk-neutral bounds for expected returns.

3.1 Data

For my tests, I use option data with expirations of one, two, three, and six months. Choosing a cross-section of expirations is done for two reasons. First, it helps verify the robustness of my results across expirations. Second, it allows for term-structure implications across preference parameters similar to Driessen et al. (2022). The sample of option contracts on the S&P500 is from OptionMetrics, and is summarized in Table 1. I do not to include

high-frequency options (0DTE's) in my sample so that the time-series of my options dataset spans a long period of time characterized by a wealth of events (Great Recession, Covid, etc.). Tothe contrary, high-frequency options were introduced after 2015: 2016 for weekly's and 2022 for daily's. Finally, in selecting option contracts, I impose the following filters: non-missing implied volatility, positive volume, and bid price above \$3/8. After imposing these criteria, I also require that outside the ±2% moneyness range, there are at least six option contracts for each date, with at least three puts and at least three calls.

There are two nonconsecutive 2-month observations and eleven nonconsecutive 3-month observations at the beginning of the sample for which the risk-neutral distributions could not be estimated. For these dates, there were not enough option contracts satisfying the sample selection criteria. Further, consecutive observations are required to calculate autocorrelations for Newey-West standard errors in the GMM estimation. Hence, for the 2- and 3-month options additional observations had to be deleted. The resulting sample is from January 1996 to December 2022 for 1-month expiration options, May 1998 to November 2022 for 2-month expiration, January 2002 to October 2022 for 3-month expiration, and June 1996 to June 2022 for 6-month options.

3.2 Derivation of the Risk-neutral Density

The derivation of the risk-neutral density (RND) follows the methodology in Figlewski (2008), Birru and Figlewski (2012), Linn et al. (2018), and Alexiou et al. (2024). The first step is to construct the implied volatility (IV) curve across strike prices. For strike prices (K) outside the ±2% range of the underlying spot price (S_t), I use IV's provided by OptionMetrics. For strike prices inside the ±2% range of the underlying spot price, I combine the IV's of OptionMetrics for puts (IV_p) and calls (IV_c) with the same strike price into a single point

$$IV\big(K \in (1 \pm 2\%)S_t\big) = \omega IV_p\big(K \in (1 \pm 2\%)S_t\big) + (1-\omega)IV_c\big(K \in (1 \pm 2\%)S_t\big),$$

where $\omega = (K_{max} - K)/(K_{max} - K_{min})$, and K_{max} and K_{min} are respectively the maximum and minimum strike prices in the ±2% moneyness range. As in Alexiou et al. (2024), this is done to avoid an artificial jump at the ATM region, which could arise from ATM puts potentially trading at higher IV relative to ATM calls.

Based on these IV points, I construct the IV curve by fitting a quintic spline with 1,000 moneyness nodes. Using the Black and Scholes (1973) formula, the IV curve is then converted into a curve of call option prices, $C_{t,t+T}(S_t R_{i,t}, S_t, \widetilde{r}_{f,t,t+T}, IV_{t,t+T}(K), div_{t,t+T})$, where $R_{i,t} = K_{i,t}/S_t$ is the moneyness (or gross return) for every strike price, $\widetilde{r}_{f,t,t+T}$ is the

continuously-compounded risk-free rate (Federal funds rate), and $div_{t,t+T}$ is the continuously-compounded dividend yield from OptionMetrics. The risk-neutral density, $\widetilde{q}_{t,t+T}(SR) = d\widetilde{Q}_{t,t+T}(SR)/d(SR)$, is derived using the result in Breeden and Litzenberger (1978) where

$$\widetilde{q}_{t,t+T}(S_t R_{t,t+T}) = e^{T\ \widetilde{r}_{f,t,t+T}} \frac{\partial^2 C_{t,t+T}(S_t R_{t,t+T}, S_t, \widetilde{r}_{f,t,t+T}, IV_{t,t+T}(K), div_{t,+T})}{\partial (S_t R_{t,t+T})^2}.$$

The chain rule implies that the risk-neutral density for gross returns is

$$\widetilde{q}_{t,t+T}(R_{t,t+T}) = S_t e^{T\ \widetilde{r}_{f,t,t+T}} \frac{\partial^2 C_{t,t+T}(S_t R_{t,t+T}, S_t, \widetilde{r}_{f,t,t+T}, IV_{t,t+T}(K), div_{t,+T})}{\partial (S_t R_{t,t+T})^2}.$$

The second derivative above is calculated using a second-order centered difference approximation. Further, I can rescale the RND with the factor

$$\widehat{q}_{t,t+T}(R_{i,t}) = \frac{\widetilde{q}_{t,t+T}(R_{i,t})}{\sum_{i=1}^{1,000} \widetilde{q}_{t,t+T}(R_{i,t})(R_{i+1,t} - R_{i,t})}.$$

In this case, $\widehat{q}_{t,t+T}(R_{i,t})$ is a well-defined density function for gross returns (moneyness) since

$$\sum_{i=1}^{1,000} \widehat{q}_{t,t+T}(R_{i,t})(R_{i+1,t} - R_{i,t}) = \sum_{i=1}^{1,000} \frac{\widetilde{q}_{t,t+T}(R_{i,t})(R_{i+1,t} - R_{i,t})}{\sum_{i=1}^{1,000} \widetilde{q}_{t,t+T}(R_i)(R_{i+1,t} - R_{i,t})} = 1.$$

The derived density is truncated at its tails because options for extreme values of the stock market index are dropped from the sample ($< \$3/8$) or the corresponding prices are zero. Hence, as in Figlewski (2008) and Linn et al. (2018), the final step in the derivation of the RND is adjusting its tails by appending heavy-tailed distributions. To this end, I assume that the left (l) and right (r) tails of the RND are given by two-parameter Pareto density functions, $f_l(R)$ and $f_r(R)$:

$$f_l(R) = \frac{\alpha_l(\lambda_l - R)^{-\alpha_l - 1}}{\lambda_l^{-\alpha_l}}, R \leq \lambda_l, \quad f_r(R) = \frac{\alpha_r R^{-\alpha_r - 1}}{\lambda_r^{-\alpha_r}}, R \geq \lambda_r. \tag{15}$$

The two parameters, α_l and λ_l (α_r and λ_r) are identified by solving a 2×2 system of non-linear equations where I set the left (right) Pareto density above equal to the values of the derived empirical RND at the 2% and 5% (95% and 98%) percentiles. Finally, using the solutions for the parameters in the tail distributions, I extend the domain of moneyness by approximately 60% (30% in the left tail and 30% in the right tail) from 1,000 to 1,600 nodes and re-normalize the RND to obtain a well-defined density that integrates to one:

$$q_{t,t+T}(R_i) = \frac{\widehat{q}_{t,t+T}(R_i)}{\sum_{i=1}^{1,400} \widehat{q}_{t,t+T}(R_i)(R_{i+1} - R_i)}.$$

Overall, I obtain 323 RND's for the 1-month expiration, 147 for the 2-month, 83 for the 3-month, and 52 RND's for the 6-month expiration. Figure A.1 in the Appendix shows the average RND, with and without tail adjustments, obtained from option prices for different expirations. These graphs are very similar to the ones in Linn et al. (2018).

4 Estimation of the Alternative Pricing Kernels

Using the GMM estimation methodology from Section 2.3 and the RND's from Section 3.2, I estimate the parameters in the various discount factors from equations (1), (2), (4), and (6). The estimated pricing kernels will help us identify how different functional forms of the pricing kernel affect physical moments and the accuracy of risk-neutral bounds.

4.1 Monotonic Pricing Kernels

Table 2 reports the estimates for the standard monotonic power utility model (equation (1)). The risk aversion parameters are positive across expirations, and range from 1.266 (2-month) to 1.524 (6-month). The values of these parameters are consistent with the ones reported in Bliss and Panigirtzoglou (2004), and imply that risk aversion is stable across expirations.

Table 3 reports the results for the monotonic pricing kernel with time-varying risk aversion coefficients that depend on the normalized VIX ($nvix$) from equation (2). γ_1 estimates are positive across all expirations implying positive risk aversion. The γ_1 estimate for the 1-month options is 0.518. To the contrary, the γ_1 estimates for the 2-,3-, and 6-months options range from 1.295 to 1.661. These discrepancies in γ_1 for the VIX-dependent pricing kernel across expirations can be explained he coefficient that regulates the dependence of risk aversion on the normalized VIX, γ_3, which is positive for the 1-month expiration (1.936) and negative (from -0.817 to -0.559) for the 2-, 3-, and 6-month expirations.

The above estimates imply that risk aversion is procyclical with respect to the VIX for the 1-month expiration, and counter-cyclical for the remaining expirations. The finding that risk aversion increases with VIX for the 1-month expiration is intuitive. However, the fact that risk aversion decreases with VIX for the 2-, 3-, and 6-month expirations might appear counter-intuitive. Nevertheless, this finding is consistent with the results in Schreindorfer and Sischert (2022) regarding counter-cyclical risk aversion with respect to the VIX.

4.2 Non-Monotonic Pricing Kernels

Table 4 reports the GMM results for the non-monotonic discount factor of equation (4) with constant parameters. For the 1-month expiration, the linear coefficient γ_1 is positive (0.814) and the quadratic parameter γ_2 is negative (-7.412). This implies that risk-aversion is counter-cyclical with respect to market returns (equation (5)), and that marginal utility is U-shaped. To the contrary, for 2-, 3-, and 6-month expirations, both the linear γ_1 parameter and the quadratic γ_2 coefficients are positive ($\gamma_1 = 1.386$-1.672, $\gamma_2 = 0.334$-0.779). According to equation (5), this finding implies that risk aversion for these expirations is pro-cyclical, and that marginal utility is inverse U-shaped. For the 2-, 3-, and 6-month expirations, the procyclicality of risk aversion with respect to the stock market is counter-intuitive. However, this procyclicality with respect to the stock market is consistent with the counter-cyclicality of risk aversion with respect to the *nvix* for the VIX-dependent model of equation (2), which was documented in Table 3.

Finally, Table 5 reports estimation results for the non-monotonic pricing kernel with VIX-dependent parameters from equation (6). In this case, the linear coefficient γ_1 is positive (0.129 to 1.991) and the quadratic coefficient γ_2 is negative (-47.470 to -2.143) across all expirations. These estimates imply U-shaped marginal utility and counter-cyclical risk aversion with respect to the stock market. The parameter γ_3 that determines the dependence of the linear and quadratic coefficients on the *nvix* is also negative (γ_3 = -9.720 to -4.421). However, negative estimates for the VIX-dependence coefficients γ_3 do not necessarily mean that risk aversion is decreasing in the VIX. As shown in equation (7), the overall cyclicality of risk aversion with respect to the *nvix* in the VIX-dependent quadratic discount factor also depends on the level of stock market returns.

Based on the standard errors and t-statistics of the estimates in Table 2 to Table 5, the option-implied pricing kernel is probably monotonic since the quadratic terms are mostly statistical insignificant. To the contrary, the t-statistics (t-stats: 4.43 to 6.83 in Table 2, 0.31 to 5.12 in Table 3, and 0.23 to 4.08 in Table 5) for the linear γ_1 coefficients in the monotonic and non-monotonic discount factors of equations (1), (2), and (6) are much larger, in absolute magnitude, than those for the quadratic γ_2 coefficients (-1.38 to -0.30 in Table 5) in the pricing kernels of equations (4) and (6). Regarding VIX-dependence the evidence most likely points towards VIX-independence with the exception of two instances in Table 5: the 1- and 2-month expirations for the non-monotonic VIX-dependent model of equation (6) with t-statistics for γ_3 equal to -2.21 and -2.29. In all other cases in Table 3 and Table 5, the estimates for the VIX-dependence parameter γ_3 are statistically insignificant.

Figure 1 plots the various pricing kernels based on the GMM results from Table 2 through

Table 5. In these plots, the *nvix* in the VIX-dependent discount factors is set equal to its sample average for each expiration. With the exception of the 2-, 3-, and 6-month expirations for the fixed parameters non-monotonic pricing kernel (equation (4)), the remaining discount factors appear to be monotonically decreasing for most moneyness values. The fixed-parameters non-monotonic model for 2-, 3-, and 6-month expirations has an inverse U-shape because the estimates both for the linear γ_1 and the quadratic γ_2 coefficients are positive (Table 4). Nevertheless, the increasing part of this pricing kernel corresponds to very low values for market returns (e.g., -100% to -50%), which are assigned almost zero probabilities in practice. For realistic market returns (e.g., -50% to 30%), the non-monotonic pricing kernel of equation (4) is decreasing.

The VIX-dependent non-monotonic specification of equation (6) is decreasing for most moneyness values. There is a small increasing portion for this discount factor that corresponds to large, positive values for market returns. The U-shape of the non-monotonic pricing kernel with VIX-dependent parameters is due the fact that the quadratic parameter γ_2 is negative (Table 5). According to equation (7), for negative γ_2 and large positive values of stock market returns, risk aversion turns negative. In this case, the pricing kernel is increasing, and the risk-return relation is negative. Regardless of whether non-monotonic pricing kernels are U-shaped on inverse U-shaped, these non-monotonicities appear in either extremely large or extremely low returns, which are assigned near zero probabilities in the far-left or far-right of the distribution of returns. This shows that non-monotonicities may not be particularly important in affecting the moments of the physical density. We shed more light on this conjecture in our empirical analysis below, where we compare the resulting physical densities and corresponding moments from the various estimated pricing kernels, regardless of the statistical significance of their coefficients.

5 Physical Densities from Alternative Pricing Kernels

Using the estimation results for the discount factors from the previous section, I derive the corresponding option-based physical densities and moments for gross returns according to equation (14). This will allow me to identify how different functional forms of the pricing kernel affect physical moments and the accuracy of risk-neutral bounds for expected returns. For comparison, I also derive the distribution and density functions of realized returns by fitting a kernel-density estimator on the set on realized returns, and then interpolating the density values over the entire range of moneyness using a piecewise cubic hermite polynomial.

Figure 2 plots the average option-based physical densities across pricing kernels and expirations to verify that these densities are well-defined. Most of the resulting physical

distribution functions appear to be quite similar with the exception of the density for the non-monotonic VIX-dependent discount factor from equation (6) and the density for realized returns. To this end, for my first set of tests, I run pairwise Kolmogorov-Smirnov statistics that examine the equality of option-based physical distributions across discount factors.[3] In these tests, I also compare the option-based physical distributions to the risk-neutral ones and the distribution of realized returns.

5.1 Kolmogorov-Smirnov Tests

Results for the Kolmogorov-Smirnov tests are reported in Table 6, where option-based physical densities are identified by the exponents of the corresponding discount factors: $\gamma_1 r$ for equation (1), $\gamma_1 nvix^{\gamma_3} r$ for equation (2), $\gamma_1 r + \gamma_2 r^2$ for equation (4), and $\gamma_1 nvix^{\gamma_3} r + \gamma_2 nvix^{\gamma_4} r^2$ for equation (6). Based on the percentage of rejections of these tests over the sample period, the most similar option-based distributions are those derived from the two monotonic specifications (equations (1) and (2)) with rejections ranging from 3% (2-month) to 23% (6-month).

The option-based physical distributions from the non-monotonic model with fixed parameters (equation (4)) are somewhat different to those from the monotonic specifications with rejections of the Kolmogorov-Smirnov tests ranging from 2% (2-month) to 77% (1-month). Finally, the option-based distributions from the non-monotonic discount factor with VIX-depended parameters (equation (6)) are quite different to the rest of the distributions with very high rejection percentages (84% to 96%) across all expirations.

These results shed additional light on a very contentious literature (e.g., Linn et al. (2018), Schreindorfer and Sischert (2022)) regarding the importance of VIX-dependent parameters and non-monotonicities in the pricing kernel from the perspective of equality of the resulting physical distributions. Specifically, the VIX-dependent quadratic pricing kernel from equation (6) induces much different option-based physical distributions than the rest of the discount factors. To the contrary, the VIX-dependent monotonic pricing kernel of equation (2), and to a lesser extend the constant parameter non-monotonic discount factor of equation (2), imply physical distributions that are quite similar to the fixed-parameter monotonic discount factor of equation (1). In other words, non-monotonic pricing kernels with constant parameters or monotonic pricing kernels with VIX-dependent risk aversion yield relatively similar physical distributions to those from the standard monotonic discount factor. To the contrary, combining non-monotonicities with VIX-dependence of preference parameters generates vastly different physical densities than the rest of the discount factors.

[3] In untabulated results, I also run the Cramer-von Mises test. The results are quantitative similar.

According to the results in Table 6, all specifications generate physical-distribution that are different than the risk-neutral measure with rejections of the Kolmogorov-Smirnov test ranging from 23% to 100%. Interestingly, the average option-based physical distribution is quite different to the distribution of realized returns across all discount factors and expirations. To identify which moments cause the Kolmogorov-Smirnov tests to reject equality of distributions across distributions, I further compare the values and comovement of the first four moments of these distributions.

5.2 Moments of the Physical Distribution

Table 7 reports summary statistics for the first four moments of the option-based physical distributions across expirations and pricing kernels. Table 7 also reports summary statistics for the first four moments of the risk-neutral distribution as well as the sample moments of the realized distribution. Panel A shows the results for expected returns across distributions.

All discount factors are characterized by the same average expected returns (0.63% for 1-month to 4.25% for 6-month), which are identical to the average realized return, since this moment is part of the GMM objective function (equation (2.3)). Similarly, the physical expected returns across all pricing kernels are larger than the risk-neutral ones (-0.06% for 1-month to 0.46% for 6-month). Although average expected returns are the same across models, the volatility of expected returns differs significantly across discount factors, with the VIX-dependent non-monotonic model of equation (6) yielding less volatile expected returns than the remaining models across all maturities, with the exception of the 3-month expected returns for the VIX-dependent monotonic specification of equation (6).

Panel B, Table 7 reports the variances of the option-based physical densities across discount factors and expirations. Although the variance is not a target moment in the GMM estimation, the resulting physical variances are quite consistent across pricing kernels ($0.34\% - 0.43\%$ for 1-month to $1.33\% - 2.23\%$ for 6-month), and are less than the risk-neutral ones. The option-based physical densities result in average variances that are larger than the variance of realized returns (0.24% for 1-month to 1.13% for 6-month). According to Panel B, among the different discount factors, the non-monotonic pricing kernel with VIX-dependent parameters (equation (6)) generates the lowest physical variances.

Panel C, Table 7 reports the results for physical skewness, which is negative across all expirations and discount factors (-1.45 to -0.59 for 1-month and -0.91 to -0.15 for 6-month). Option-based physical skewness is, in absolute value, less than the risk-neutral one (-1.51 for 1-month to -0.98 for 6-month). Similar to the variance case, the non-monotonic VIX-dependent model (equation (6)) generates the lowest, in absolute magnitude, physical skew-

ness (-0.59 for 1-month to -0.15 for 6-month). To the contrary, the rest of the discount factors imply physical skewness that is large in absolute value and similar in magnitude, albeit smaller, to the risk-neutral one. The results are similar for physical kurtosis in Panel D of Table 7, where the non-monotonic model with VIX-dependent parameters generates the least amount of kurtosis (3.24 or 6-month to 4.37 for 1-month).

In general, the risk-neutral density has negative skewness and positive excess kurtosis (7.67 for 1-month to 4.49 for 6-month), and these characteristics carry over to the physical densities as well. Interestingly, the non-monotonic specification with VIX-dependent parameters generates the least amount of negative skewness and excess kurtosis for the physical measure. In fact, skewness and kurtosis from the VIX-dependent non-monotonic discount factor are too low compared to the corresponding risk-neutral and realized moments. Finally, Table A.2 in the Appendix reports moments for the physical and risk-neutral distributions for log-returns ($lnR_{t,t+T}$). The results are qualitatively similar to the ones in Table 7 with a key difference that skewness (in absolute value) and kurtosis for log-returns are larger than for gross returns.

Overall, the results in this section constitute an out-of-sample analysis for the option-based physical moments from the various pricing kernels. The GMM system of equation (13) estimates the various discount factors by matching higher-order moments of the physical distribution function to moments from the uniform distribution and average expected returns to average realized returns (equations (10) and (11)). Hence, the results in Table 7 examine the "out-of-sample" plausibility of the resulting high-order physical moments (e.g., variance, skewness) although these high-order moments are not part of the estimation.

The various discount factors generate plausible and consistent higher-order moments. For example, in all cases risk-neutral variance and skeweness are larger than physical ones. Yet, risk-neutral kurtosis is similar to the physical one. Notably, the VIX-dependent non-monotonic pricing kernel of equation (6) not only generates the lowest higher order moments across discount factors, but also yields moments with the least amount of time-variation. This is because the combination of non-monotonicity with VIX-dependence results in a discount factor, whose times-series volatility is much larger than that of the remaining specifications with fixed parameters or with monotonic VIX-dependence.

The pronounced movements of the non-monotonic VIX-dependent pricing kernel soak up most of the time variation of the risk-neutral density and result is a fairly stable physical distribution. This might be an important argument regarding the plausibility of this discount factor. The fact that the VIX-dependent non-monotonic pricing kernel generates very low, in absolute magnitude, moments for the physical density than the rest of the specifciations (fixed-parameter non-monotonic, VIX-dependent monotonic, fixed-parameter monotonic) is

a novel result that has not been studied by the literature.

5.3 Coefficients of Determination for Physical Moments

To complement the findings regarding the levels of the first four moments of the option-based physical densities, Table 8 reports the adjusted coefficients of determination (R^2's) from regressing the physical moments of each pricing kernel to the same moments implied by the other pricing kernels and the risk-neutral measure. These tests examine the comevement across the option-based physical moments from the various discount factors.

First, the option-based variances across pricing kernels are highly correlated with R^2's much higher than 80% across all expirations (average R^2 93% to 97%). To the contrary, the moments with the highest degree of divergence across discount factors are expected returns, with average R^2's between 33% and 43% across expirations (42% and 50% if we exclude the R^2's from regressions of the risk-neutral expected returns). Skewness and kurtosis exhibit similar degrees of divergence across discount factors. Specifically, the results from Table 8 suggest that expected returns, skewness, and kurtosis are strongly correlated (R^2's from 62% to 99%) across the monotonic pricing kernels of equations (1) and (2). The moments from these two monotonic pricing kernels are also strongly correlated (R^2's from 55% to 99%) to those from the fixed-parameter non-monotonic pricing kernel of equation (4). To the contrary, expected returns, skewness, and kurtosis from the VIX-dependent non-monotonic discount factor (equation (6)) are almost completely orthogonal (R^2's from 0% to 23%) to the corresponding moments from the remaining pricing kernels.

Nevertheless, the most striking result in Table 8 is that the physical variance is near-perfectly correlated across all four discount factors and the risk-neutral density (R^2's from 82% to 99%). In sum, physical variances are highly correlated both across pricing kernels and with the corresponding risk-neutral moments. To the contrary, the rest of the physical moments are less correlated across discount factors and from the risk-neutral ones. This divergence in the comovement of physical moments is mainly driven by the non-monotonic discount factor with VIX dependence.

This is the first paper to show that the effects of monotonic and non-monotonic pricing kernels vary considerably across moments. The option-implied variances are strongly correlated across discount factors, whereas the rest of the moments, especially odd moments such as expected returns and skewness, differ significantly across pricing kernels. The differential effects of the various pricing kernels on odd and even moments are clearly illustrated in Table 9, which shows the coefficients of determination across pricing kernels for the third and fourth central moments (skewness and variances without the variance scaling). The R^2's for

the third moments range from 46% (1-month) to 86% (3-month), whereas the R^2's for the fourth moments range from 87% (1-month) to 93% (3-month). For all expirations, the co-movenemnt of fourth moments is much more similar across pricing kernels than that of third moments. Hence, Table 8 and Table 9 highlight the differential effects of the various pricing kernels across odd and even moments: even moments, especially variances, are strongly correlated across pricing kernels, whereas odd moments are exhibit a weaker relation across discount factors.[4]

Overall, the findings from Table 7 and Table 8 suggest that the monotonic (equation (1)), monotonic with VIX-dependence (equation (2)), and non-monotonic (equation (4)) pricing kernels seem to generate somewhat similar moments, which are strongly correlated. To the contrary, the non-monotonic discount factor with VIX-dependent parameters implies vastly different physical moments that are almost orthogonal to the moments from rest of the discount factors. A notable exception is the physical variance, which is similar and strongly correlated across all discount factors, including the VIX-dependent non-monotonic model. Hence, Table 7 and Table 8 indicate that non-monotonicity (equation (4)) and VIX-dependence (equation (2)) of the pricing kernel alone cannot generate substantially different physical moments from the standard monotonic discount factor with fixed-parameters (equation (1)). To the contrary, the combination of non-monotonicity with VIX-dependence, implies a unique physical distribution, which is quite different to those obtained from the remaining discount factors.

5.4 Pricing Kernels and Moments of the Physical Distribution: Theoretical Explanation

The above empirical findings regarding the differential effects of the various pricing kernels on physical moments can be explained using standard results from the normal distribution. Most of the theoretical results in this section are about the moments of log-returns from log-normal or skew log-normal distributions. These results can be applied to gross returns either using the approximation $lnR \approx R-1$ or using the exact formulas from the log-normal and skew log-normal distributions.

In actuarial science, the baseline monotonic utility of equations (1) and (2) with the normalization of equation (13) are referred to as a linear Esscher (1932) transform. More recently, Monfort and Pegoraro (2010) introduced the concept of the second-order Esscher transform, which is related to the quadratic pricing kernels of equations (4) and (6). Within

[4]Table A.3 and Table A.4 report adjusted R^2's from regressions of option-based physical moments for log-returns across pricing kernels. These results are similar to the ones presented here for gross returns.

this framework, if the risk-neutral density for log-returns is normal with mean $\widetilde{r}^{f}_{t,t+T}$ and variance $\sigma^2_{RND,t,t+T}$, the monotonic discount factors from equations (1) and (2) preserve normality and result in physical densities which are normal with mean and variance respectively given by

$$\mathbb{E}_t[lnR_{t,t+T}] = \widetilde{r}^{f}_{t,t+T} + \gamma_{1,t}\sigma^2_{RND,t,t+T} \tag{16}$$

$$var_t\big(lnR_{t,t+T}\big) = \sigma^2_{RND,t,t+T}. \tag{17}$$

Above, $\gamma_{1,t}$ captures risk aversion, which can either be a fixed parameter, $\gamma_{1,t} = \gamma_1$ as in equation (1), or a time-varying coefficient, $\gamma_{1,t} = \gamma_1 nvix^{\gamma_3}_{t,t+T}$ as in equation (2). Hence, when the risk-neutral density is normal, linear discount factors, with either constant or time-varying coefficients, shift expected returns by the product of the risk aversion with the variance, but leave the risk-neutral variance unaltered (see Appendix A.1). Equations (16) and (17) illustrate why option-based expected returns and variances are so similar, both in levels (Table 7) and in comovement (Table 8), across the two monotonic pricing kernels of equations (1) and (2).

On the other hand, when the risk-neutral density is normal, the quadratic pricing kernels from equations (4) and (6) preserve normality but alter both the mean and the variance of log-returns. Specifically, as shown in Appendix A.1, if the risk-neutral density for log-returns is normal, the quadratic discount factors, with either constant or time-varying coefficients, yield normal physical densities with mean and variance equal to

$$\mathbb{E}_t[lnR_{t,t+T}] = \frac{\widetilde{r}^{f}_{t,t+T} + \gamma_{1,t}\sigma^2_{RND,t,t+T}}{1 - 2\gamma_{2,t}\sigma^2_{RND,t,t+T}} \tag{18}$$

$$var_t\big(lnR_{t,t+T}\big) = \frac{\sigma^2_{RND,t,t+T}}{1 - 2\gamma_{2,t}\sigma^2_{RND,t,t+T}}. \tag{19}$$

In this case, the physical variance is less than the risk-neutral one only if the non-monotonic discount factor has a negative quadratic $\gamma_{2,t}$ parameter. The fixed-parameter non-monotonic pricing kernel from equation (4) for 1-month options and the VIX-dependent non-monotonic discount factor from equation (6) across all expirations are characterized by negative $\gamma_{2,t}$ parameters (Table 4). Thus, according to equations (5) and (19), these discount factors imply risk-aversion that is counter-cyclical to market returns and generate low values for the physical variance compared to the risk-neutral one (Table 7 and Table A.2 in the Appendix).

To the contrary, the fixed-parameter non-monotonic pricing kernel from equation (4) with positive $\gamma_{2,t}$ coefficients for the 2-, 3-, and 6-month expirations (Table 4) yields pro-cyclical risk aversion (equation (5)) and relatively large physical variances (see Table 7 and Table A.2

in the Appendix). Nevertheless, even for the non-monotonic pricing kernels, the denominator in equation (19), $1-\gamma_{2,t}\sigma^2_{RND,t,t+T}$, is a number close to one for both the fixed- and the VIX-dependent specification due to the low values of $\sigma^2_{RND,t,t+T}$ (Table 7). This could explain the findings in Table 7 through Table 8 for gross returns and Table A.2 through Table A.3 in the Appendix for log-returns, according to which physical variances are quite similar across pricing kernels and highly correlated with each other and with the risk-neutral one.

On the other hand, expected returns vary both across pricing kernels and from the risk-neutral density due to the $\gamma_{1,t}\sigma^2_{RND,t,t+T}$ term in equation (16) and in the numerator of (18). Specifically, for the non-monotonic VIX-dependent pricing kernel of equation (6), the non-linear relation of equation (18) is amplified by VIX-dependence. Hence, the resulting expected returns are orthogonal to the expected returns of the remaining discount factors (Table 8) although their levels are the same and equal to average realized returns (Table 7).

As highlighted in Table 7 (and Table A.2 of the Appendix), the risk-neutral density for both gross and log-returns is negatively skewed with excess kurtosis across all expirations. Hence, even if the assumption of normality provides helpful insights, it is is quite restrictive. To this end, I further examine the results from Table 7 and Table 8 for gross returns under the assumption that the risk-neutral density is skewed log-normal with location, scale, and shape parameters respectively given by ω_t, σ_t, λ_t, and θ_t. For these parameters, according to the log skew-normal specification of Henze (1986), the density function, up to a normalisation constant, is

$$dQ_t(R) = \frac{1}{R}Exp\Big[\frac{lnR-\omega_t}{2\sigma^2_{RND,t}}\Big]\Phi\Big(\lambda_t\frac{lnR-\omega_t}{\sigma_t}+\xi_t\Big).$$

The sign of λ_t determines the sign of skewness, and $\xi_t(>0)$ amplifies skewness and kurtosis. In this case, the risk-neutral expected log-return is

$$\mathbb{E}^{RND}_t[lnR_{t,t+T}] = \omega_t + \big(\lambda_t/\sqrt{1+\lambda_t^2}\big)\Big(\phi\big(-\frac{\xi_t}{\sqrt{1+\lambda_t^2}}\big)/\Big[1-\Phi\big(-\frac{\xi_t}{\sqrt{1+\lambda_t^2}}\big)\Big]\Big)\sigma_t, \quad (20)$$

where $\phi(x)/(1-\Phi(x))$ is the inverse Mills ratio. Based on the results for the risk-neutral density for gross- and log-returns in Table 7 and Table A.2 of the Appendix respectively, λ_t should be negative and ξ_t should be positive for the option-based RND across all expirations.

As shown in Appendix A.6, applying a linear pricing kernel with positive risk-aversion parameter $\gamma_{1,t}$ to the above skew log-normal RND implies that the mean under the physical density becomes

$$\mathbb{E}_t[lnR_{t,t+T}] = \omega_t + \gamma_{1,t}\sigma_t^2 + \frac{\lambda_t}{\sqrt{1+\lambda_t^2}} \frac{\phi\big(-\frac{\xi_t+\lambda_t\gamma_{1,t}\sigma_t^2}{\sqrt{1+\lambda_t^2}}\big)}{1-\Phi\big(-\frac{\xi_t+\lambda_t\gamma_{1,t}\sigma_t^2}{\sqrt{1+\lambda_t^2}}\big)}\sigma_t. \tag{21}$$

Hence under non-normality, the linear pricing kernel increases the risk-neutral expected return by the term $\gamma_{1,t}\sigma_t^2$, as in the case of a normal RND (equation (16)), and by decreasing the absolute value of the negative skewness term in equation (20) from

$$\frac{\lambda_t}{\sqrt{1+\lambda_t^2}} \frac{\phi\big(-\frac{\xi_t}{\sqrt{1+\lambda_t^2}}\big)}{1-\Phi\big(-\frac{\xi_t}{\sqrt{1+\lambda_t^2}}\big)}\sigma_t \qquad \text{to} \qquad \frac{\lambda_t}{\sqrt{1+\lambda_t^2}} \frac{\phi\big(-\frac{\xi_t+\lambda_t\gamma_{1,t}\sigma_t^2}{\sqrt{1+\lambda_t^2}}\big)}{1-\Phi\big(-\frac{\xi_t+\lambda_t\gamma_{1,t}\sigma_t^2}{\sqrt{1+\lambda_t^2}}\big)}\sigma_t. \tag{22}$$

Since the parameter λ_t is negative for a negatively-skewed RND, and the inverse Mills ratio is positive and monotonically increasing (see Appendix A.5), the terms in equation (22) are negative. A positive risk aversion coefficient combined $\gamma_{1,t}$ with a negative λ_t parameter decrease the argument in the inverse Mills ratio from $\frac{\xi_t}{\sqrt{1+\lambda_t^2}}$ to $\frac{\xi_t+\lambda_t\gamma_{1,t}\sigma_t^2}{\sqrt{1+\lambda_t^2}}$. Given the monotonicity of the inverse Mills ratio, the decrease in the argument of the inverse Mills ration decreases the absolute value of the negative term in equation (22), and increases the expected value of the physical density (equation (21)) relative to the expected value of the risk-neutral measure (equation (20)).

In Appendix A.6 (equation (a.3)), I also derive the physical variance for skew log-normal RND's and linear discount factors. These results confirm that when the RND is non-normal, the linear pricing kernel affects both the mean and the variance of the RND, and explain why the levels of the physical variances of the monotonic pricing kernels are different to that of the risk-neutral ones (Table 7). To the contrary, in the case of normality, the linear pricing kernel only alters the mean of the risk-neutral distribution but not its variance (equations (16) and (17)).

Regarding the quadratic pricing kernels and the skew log-normal RND, an interesting result from Appendix A.6 is that as long as the quadratic parameter $\gamma_{2,t}$ in equations (4) and (6) is negative, the mean of the physical density could still increase relatively to the mean of the RND, as shown in Table 7, even if the linear term in the quadratic pricing kernel $\gamma_{1,t}$ is low, such as the estimates in Table 5, or negative. This is because, according to equations (a.4) and (a.5) of the Appendix, a negative $\gamma_{2,t}$ parameter in the quadratic discount factor decreases the absolute magnitude of the negative term in equation (22), and thus increases physical expected returns relative to risk-neutral ones.

In sum, the theoretical results derived in this section can help explain the empirical

regularities reported in Table 7 through Table 8 for gross returns (and Table A.2 through Table A.3 of the Appendix for log-returns). One of the most important results of this section is that if the RND is normal, then linear pricing kernels (equations (1) and (2)) do not change the risk-neutral variance. To the contrary, if the RND is non-normal, then linear pricing kernels can affect higher moments of the physical distribution as well.

Regarding the non-monotonic pricing kernels, the findings in this section highlight the importance of negative values for the quadratic parameter $\gamma_{2,t}$ in equations (4) and (6) to generate plausible physical variances, skewness, and kurtosis that are smaller in absolute magnitude than the RND ones. Negative $\gamma_{2,t}$ parameters in quadratic pricing kernels are also important for generating option-based physical means that are greater than RND means, when the RND is either normal or negatively skewed. These theoretical results cast doubt on the plausibility of the fixed parameter non-monotonic pricing kernel with positive quadratic γ_2 parameters (2-, 3-, 6-month expirations in Table 4).

6 Option-based Expected Returns and Risk-Neutral Lower Bounds

Physical expected returns are unobservable, and their extraction from option prices requires assumptions for the pricing kernel. Nevertheless, recent works (Martin (2017), Chabi-Yo and Loudis (2020)) have argued that forward-looking expected returns can be proxied by risk-neutral moments via an assumption-free approach. I can assess the accuracy of these risk-neutral bounds for expected returns using the option-based physical expected returns from the various pricing kernels. Specifically, Martin (2017) derives a lower bound for risk premia that depends on the risk-neutral variance

$$\mathbb{E}_t[R_{t,t+T}] - R^f_{t,t+T} \geq var^{RND}(R_{t,t+T})/R^f_{t,t+T}. \tag{23}$$

Chabi-Yo and Loudis (2020) derive a similar lower bound for expected returns that depends on high-order risk-neutral moments

$$\mathbb{E}_t[R_{t,t+T}] - R^f_{t,t+T} \geq \frac{\frac{m^2_{t,t+T}}{R^f_{t,t+T}} - \frac{m^3_{t,t+T}}{(R^f_{t,t+T})^2} + \frac{m^4_{t,t+T}}{(R^f_{t,t+T})^3}}{1 - \frac{m^2_{t,t+T}}{(R^f_{t,t+T})^2} + \frac{m^3_{t,t+T}}{(R^f_{t,t+T})^3}}, \tag{24}$$

where the terms $m^n_{t,t+T}$ above are risk-neutral moments of excess returns

$$m^n_{t,t+T} = \int_0^{+\infty} \left(R - R^f_{t,t+T}\right)^n dQ_{t,t+T}(R).$$

The above risk-neutral bounds are not completely assumption-free. Martin's bound assumes that the covariance $cov_t(M_{t,t+T}R_{t,t+T}, R_{t,t+T})$ is non-positive, while Chabi-Yo and Loudis impose restrictions on preferences.

To empirically assess whether the risk-neutral bounds are binding, the existing literature regresses realized excess returns on these bounds, e.g.,

$$R_{t,t+T} - R^f_{t,t+T} = a + b \cdot var^{RND}(R_{t,t+T})/R^f_{t,t+T} + \epsilon_t \tag{25}$$

If a is statistically insignificant and b is statistically equal to one, then the inequalities (23) and (24) are in fact equalities, and the lower bounds are binding. I further expand these tests along the following dimensions.

First, in addition to the regression results, I provide summary statistics and correlations for the risk-neutral variances to verify whether these bounds are aligned with average realized returns or average expected returns from the option-based physical densities. Secondly, although Martin (2017) derives the lower-bound condition in terms of the risk-neutral variance (equation (23)), in his empirical tests he uses the SVIX, which is defined as $var^{RND}\left(\frac{R_{t,t+T}}{R^f_{t,t+T}}\right)$.[5] For consistency with the rest of my tests, I measure the risk-neutral lower bound for expected returns using the risk-neutral variance from equation (14), which is consistent in Martin's original framework (equation ((23)) here and equation (4) in his paper). In untabulated tests, I find that using SVIX does not affect the results, which are similar to the ones reported here with the risk-neutral variance.

Thirdly, in addition to using realized returns as the dependent variable in equation (25), I test whether the risk-neutral bounds are binding by regressing option-based risk premia from the different pricing kernels on these variances, i.e.,

$$\mathbb{E}_t[R_{t,t+T}] - R^f_{t,t+T} = a + b \cdot var^{RND}(R_{t,t+T})/R^f_{t,t+T} + \epsilon_t. \tag{26}$$

Further, I consider a specification where the dependent variable in equation (26) is fitted returns based on predictive regressions of realized returns on the dividend yield, the dividend growth, and the risk-free rate.

[5]The SVIX is equal to $\frac{2R^f_{t,t+T}}{T \cdot F_{t,t+T}}\left\{\int_0^{F_{t,t+T}} Put_{t,t+T}dK + \int_{F_{t,t+T}}^{\infty} Call_{t,t+T}dK\right\}$, where $F_{t,t+T}$ is the forward price of the underlying asset with $F_{t,t+T} = \mathbb{E}_t[S_{t+T}]$.

Finally, I test whether the realized returns and the option-based risk premia from the different pricing kernels violate these risk-neutral lower bounds. That is, I test whether there are instances where the inequality (23) is reversed. For all these tests, I only report the results for the risk-neutral variance bound of Martin (2017) (equation (23)). This is because my findings suggest that the risk-neutral bound in Chabi-Yo and Loudis (2020) (equation (24)) is dominated by the second moment term ($M^2_{t,t+T}$), and is indistinguishable from the variance bound of Martin (2017).

6.1 Summary Statistics for Risk-Neutral Lower Bounds

Table 10 reports summary statistics and correlations for Martin's risk-neutral bounds from equation (23), where the risk-free rate, $R^f_{t,t+T}$, is measured by the mean of the risk-neutral distribution. The results in Table 10 for the summary statistics of the option-based variance bounds should be compared to the summary statistics in Panel A, Table 7 for expected returns across pricing kernels and expirations, and to the summary statistics for realized returns in Panel B, Table A.1 of the Appendix. According to these results, the levels of the risk-neutral bounds from equation (23) (0.45% for 1-month, 1.05% for 2-month, 1.37% for 3-month and 3.23% for 6-month) somewhat diverge from the level of average expected and realized returns (0.63% for 1-month, 1.28% for 2- months, 1.66 % for 3-month, and 4.25% for 6-month) in Tables 7 and A.1, respectively. Importantly, this divergence increases as the option expiration increases, especually for 6-month maturities.

Nevertheless, the correlations of risk-neutral bounds with expected returns are quite large across all pricing kernels and expirations, with values ranging from 0.8 to 1. The notable exception is the VIX-dependent non-monotonic pricing kernel whose expected returns are negatively correlated to the risk-neutral variance bounds. Taken together these results suggest that for short-maturities, the risk-neutral variance bounds are a valid proxy for expected returns for all pricing kernels with the exception of the VIX-dependent non-monotonic specification. Importantly, regardless of the stochastic discount factor, as the expiration increases, the level of risk-neutral bounds diverges from expected returns (Panel A in Table 10).

This is the first paper to highlight that the validity of the risk-neutral bounds as a measure of expected returns under the physical measure depends on option expiration and the VIX-dependence of preference parameters. These results are important because they complement the existing literature, which either unconditionally accepts (Martin (2017)) or unconditionally rejects (Back et al. (2022)) the tightness of these bounds.

6.2 Regressions of Expected Returns on Risk-Neutral Lower Bounds

Table 11 reports results from regressing realized and option-based expected returns on the risk-neutral bound of equation (23). Consistent with the findings in Martin (2017) and Chabi-Yo and Loudis (2020), when regressing realized returns on the risk-neutral bound (Panel A in Table 11), I cannot reject the hypothesis that the intercept in equation (26) is zero (t-stats: -0.47 to 1.06) or that the slope is one (t-stats: -0.66 to 0.89).

However, the results of these regressions, which test the accuracy of risk-neutral bounds using realized returns, should be interpreted with caution for several reasons. First, as indicated by the low R^2's (0.13% to 4.63%), the fit of these regressions is quite poor. This means that realized returns are not aligned with risk-neutral bounds contrary to the strict lower-bound theoretical relation from equation (23), which implies that the coefficients of determination between returns and risk-neutral variances should be large. Secondly, the slope estimates for these regressions are marginally statistically significant (t-stats: 0.25 to 2.06). Hence, these parameters are not informative regarding the relation between returns and risk-neutral bounds.

Regression results become more reliable in Panel B of Table 11, where realized returns are replaced by fitted returns based on regressions of realized returns on the dividend yield, the dividend growth, and the risk-free rate. The estimation of fitted returns is described in Table A.1 of the Appendix. Compared to realized returns, fitted returns yield more accurate slope estimates (t-stats: 2.97 to 4.73) in regressions with the risk-neutral bounds. In this case, the null hypothesis that risk-neutral bounds for expected returns are binding (slope is one, zero intercept) is rejected for short expirations (1- and 2-month options) with t-statistics equal to -4.15 and -4.16 for slopes, and 2.65 and 2.83 for the intercepts. To the contrary, the null hypothesis cannot be rejected for 3- and 6-month expirations (t-stats: -1.71 and 0.03 for slopes, 1.32 and 0.57 for intercepts). Consistent with these statistics, the slope estimates for short expirations are 0.532 and 0.409, whereas the slope estimates for long expirations are closer to one, with values 0.625 and 1.011.

The accuracy of the regressions with fitted returns in Panel B of Table 11 is much better than those with realized returns (Panel A) with R^2's between 10.33% to 14.68%. Yet, the low values for the coefficient of determination continues to cast doubt on the overall explanatory power of these regressions. A tight risk-neutral bound in equation (23) should be able to explain a large part of the variation in physical expected returns.

Relative to realized and fitted returns, the accuracy of the regressions tests for risk-neutral bounds increases dramatically when I consider the option-based expected returns from equation (14) across the different pricing kernels. First, the R^2's in regression (26)

increase substantially across all expirations and pricing kernels (R^2's = 70% to 99%), with the exception of the VIX-dependent non-monotonic discount factor of equation (6).

As shown in Panel C of Table 11, the best fit in the regressions of physical expected returns on risk-neutral variances corresponds to the baseline power utility model of equation (1) with constant coefficients. For this discount factor, the intercept in equation (26) is economically insignificant across all expirations (0.01% to 0.10%) despite its large statistical significance (t-stat: 4.78 to 7.23). Further, even though I can reject the null hypothesis that the slope is equal to one (t-stat: 23.19 to 67.13), the estimated slopes are economically close to one: 1.195 to 1.371. Similar results hold in Panel E of Table 11 for the non-monotonic pricing kernel with constant coefficients from equation (4), even though in this case, intercepts are economically more significant: 0.1% to 0.5% for the non-monotonic model in Panel E against 0.01% to 0.1% for the monotonic model in Panel C.

For the both the monotonic and the non-monotonic VIX-dependent pricing kernels from equations (2) and (6), the null hypothesis in equation (26) that the risk-neutral bounds are binding is rejected (Panels D and F). This is because the intercepts are both statistically significant (t-stat absolute value: -4.80 to 13.44) and economically meaningful (intercepts 0.51% to 4%). Importantly, most of the slope estimates are quite different than one with values ranging from 0.623 to 4 for the VIX-dependent monotonic pricing kernel of equation (2) and from -0.276 to -0.081 for the VIX-dependent non-monotonic model of equation (6).

For the majority of the regressions in Table 11, the economic magnitude and statistical significance of the intercept in equation (26) increases across expiration, not always monotonically though. This result implies that longer option expiration adversely affects the accuracy of the risk-neutral bound for expected returns. This is consistent with the the summary statistics of the risk-neutral bounds from (Table 10), which show that the alignment between average risk-neutral variances and average expected returns across pricing kernels from Panel A, Table 7 is negatively affected by option expiration: for longer option maturities, e.g., 6-month, this alignment deteriorates.

6.3 Violations of Risk-Neutral Lower Bounds

The fact that realized or fitted returns are not suitable for testing risk-neutral lower bounds is also confirmed in Table 12 that reports the percentage of instances where realized and expected returns violate the risk-neutral lower bound of equation (23).[6]

The percentage of violations of the risk-neutral lower-bound by realized and fitted returns is approximately 40% and remains constant across expirations. The frequency of violations of

[6]Similar results hold for the risk-neutral bound of equation (24).

the lower bound in equation (23) by expected returns from the fixed-parameter monotonic (equation (1)) and the non-monotonic (equation (4)) discount factors is near zero across all maturities. To the contrary, expected returns from the VIX-dependent pricing kernels (equations (2) and (6)) violate the risk-neutral lower bounds. This is particularly true for the VIX-dependent quadratic pricing kernel of equation (6), whose excepted returns violate the risk-neutral bounds 40% of the time across expirations. In sum, the evidence from Table 12 suggest that realized and fitted returns are not reliable sources for testing the risk-neutral lower bounds because realized and fitted returns violate risk-neutral bounds 40% of the time. To the contrary, option-based expected returns rarely violate the risk neutral lower bounds with the exception of the expected returns from the VIX-dependent non-monotonic pricing kernel of equation (6).

Overall, the results in this section highlight four important findings. First, longer option maturities adversely affect the tightness of the risk-neutral bounds. Secondly, realized returns (or fitted returns) are not appropriate for testing the accuracy of risk-neutral bounds via the OLS regression of equation (26). This is because regressions with realized returns have almost zero fit, standard errors are very large, and realized returns often violate risk-neutral lower bounds, which are strictly positive, due to their negative values. Thirdly, for the baseline monotonic pricing kernel with constant parameters (equation (1)), regressions of expected returns on risk-neutral bounds show that slope estimates are close to one, intercepts are zero, and the R^2's are large. These findings imply that risk-neutral variances are an accurate proxy for expected returns derived from the pricing kernel of equation (1), and run against the findings in Back et al. (2022), who show that risk-neutral bounds are not binding.

Finally, non-monotonicity of the pricing kernel does not affect the tightness of the risk-neutral bounds as both the mononotonic and non-monotonic discount factors with fixed parameters (equations (1) and (4))) seem to generate expected returns that are aligned with the risk-neutral variance bounds (Panels C and E Table 11). To the contrary, VIX-dependent risk aversion regardless of monotonicity of the discount factor (equations (2) and (6)) distorts the alignment between expected returns and the risk-neutral variance-based bounds (Panels D and F in Table 11). Specifically, for pricing kernels with VIX-dependent parameters, intercepts are economically and statistically significant, and slope estimates are different than one across all expirations, implying that the risk-neutral bounds are not binding. The fact that the accuracy of the risk-neutral bounds is mostly affected by the VIX-dependence of risk aversion and not by the monotonicity of marginal utility is a novel finding that has been shown before. This finding can be explained by the fact that non-monotonicities occur over events that are assigned very low probabilities either in the left or right tail of the distribution (Figure 1). To the contrary, VIX-dependence affects the entire distribution.

Despite the shortcomings of the risk-neutral lower bounds, these bounds seem to be able to track expected returns quite well for the fixed-parameters discount factors of equations (1) and (4). Hence, if we take the stance that preference parameters are constant over time, then, according the to the results in Table 10 and Panels C and E of Table 11, the variance-based risk-neutral bounds do an excellent job in tracking expected returns. In this case, the relation between risk-neutral variances and expected returns is stronger than any predictive regression (e.g., Table A.1 in the Appendix) despite the fact that the coefficient of the risk neutral bound is not identically equal to one as predicted by the theory, but slightly larger (e.g., 1.2 from Panels C and E of Table 11).

6.4 Risk-neutral Bounds and Pricing Kernels: Theoretical Explanation of Results

The tight alignment between risk-neutral bounds and expected returns for the fixed-parameters linear pricing kernel of equation (1) documented in Table 11 can be explained by the basic equation in Martin (2017) for the derivation of the risk-neutral bound in equation (23). According to Martin (2017), expected returns are equal to risk-neutral moments minus a covariance term, which is assumed negative

$$\mathbb{E}_t[R_{t,t+T}] - R^f_{t,t+T} = var^{RND}(R_{t,t+T})/R^f_{t,t+T} - cov_t\big(M_{t,t+T}R_{t,t+T}, R_{t,t+T}\big). \tag{27}$$

As explained in Martin (2017), the covariance term is zero for log-preferences. According to the results in Table 2 for the linear pricing kernel, γ_1 estimates across expirations are close to one. Hence, for this discount factor, the risk aversion estimates imply log preferences. Hence, the covariance in equation (27) is zero, and expected returns are tightly linked to risk-neutral bounds even if regression estimates are statistically different than one.

Similarly, as shown by the frequency of risk-neutral bound violations in Table 12, for pricing kernels with VIX-dependent parameters, the covariance term in equation (27) is non-trivial. In fact, for the VIX-dependent pricing kernels, the covariance term in equation (27) might become positive, implying that the bound in equation (23) becomes an upper bound and not a lower one. For those pricing kernels that the covariance in equation (27) is non-zero or even positive, the results in Table 12 suggest that the risk-neutral bound is not binding, and might even be reversed, i.e., an upper bound instead of a lower one, at least for short maturities. For this reason, the regressions in Table 11 for the VIX-dependent pricing kernels (equations (2) and (6)) yield economically and statistically significant intercepts as well as slope coefficients that are different than one. These regression results suggest that the risk-neutral bounds of equation (23) are not binding for expected returns from VIX-

dependent models.

7 Conclusion

The goal of this paper is two-fold. The first part of the analysis identifies how different pricing kernels interact with the option-based risk-neutral density across different option maturities (1-month options, 2-, 3-, and 6-months) to generate different forward-looking distributions for stock market returns under the physical measure. The theoretical framework of this analysis is based on four power-utility pricing kernels, whose exponents are either linear (monotonic) or quadratic (non-monotonic), and whose risk aversion parameters are either fixed or dependent on the VIX. In the second part of my analysis, I use the resulting option-based physical distributions from the various pricing kernels to test the accuracy of the risk-neutral variance bounds for expected market returns proposed by the literature (e.g., Martin (2017), Chabi-Yo and Loudis (2020)).

Results from Kolmogorov-Smirnov tests indicate that option-based physical distributions derived from the fixed-parameter monotonic, VIX-dependent monotonic, and fixed-parameter non-monotonic discount factors are quite similar. Instead, the physical distribution from the the non-monotonic pricing kernel with VIX-dependent parameters is different to those from the rest of the discount factors. Hence, my results suggest that non-monotonicities need to be combined with time-variation of parameters to generate substantially different physical densities from the standard fixed-parameter monotonic (power utility) specification. Additional tests focusing on the first four physical moments from the different pricing kernels show that the variances of the option-based physical distributions are highly correlated. To the contrary, odd moments (expected returns and skewness) are the least correlated moments across pricing kernels. This is one of the first attempts to explain how different discount factors affect the moments of the option-based physical distribution.

Regarding the risk-neutral bounds for expected returns, I find that these bounds are only aligned to expected returns from pricing kernels with fixed parameters regardless of monotonicity. To the contrary, for discount factors with VIX-dependent parameters, monotonic and non-monotonic, my tests do not support the hypothesis that risk-neutral bounds are binding and aligned with option-based expected returns. Similarly, my results indicate that risk-neutral bounds diverge from the option expected returns across all discount factors as option expiration increases, e.g., from 1-month to 6-months.

These results highlight that option-expiration and VIX-dependence of the pricing kernel affect the accuracy of the risk-neutral bounds, which have proposed by the literature as a proxy for forward-looking expected returns. To the contrary, non-monotonicities do not seem

to impact the tightness of these bounds. I conclude that caution should be exerted when risk-neutral moments are used as a proxy of stock market expected returns. Although risk-neutral bounds may not be perfect, my results also indicate that these bounds are superior to alternative measures of expected returns such as average realized returns or fitted returns using predictive factors (e.g., price-dividend ratio, dividend growth, etc.).

References

Ait-Sahalia, Y. and A. W. Lo (2000). Non-parametric risk management and implied risk aversion. *Journal of Econometrics 94*, 9–51.

Alexiou, L., A. Goyal, A. Kostakis, and L. Rompolis (2024). Pricing event risk: Evidence from concave implied volatility curves. *Working Paper*.

Ang, A. and G. Bekaert (2007). Stock return predictability: Is it there? *Review of Financial Studies 20*, 651–707.

Back, K., K. Crotty, and S. M. Kazempour (2022). Validity, tightness, and forecasting power of risk premium bounds. *Journal of Financial Economics 144*, 732–760.

Bakshi, G. and D. B. Madan (2007). Investor heterogeneity, aggregation, and the non-monotonicity of the aggregate marginal rate of substitution in the price of market-equity. *Working paper*.

Bakshi, G., D. B. Madan, and G. Panayotov (2010). Returns of claims on the upside and the viability of u-shaped pricing kernels. *Journal of Financial Economics 97*, 130–154.

Barone-Adesi, G., N. Fusari, A. Mira, and C. Sala (2020). Option market trading activity and the estimation of the pricing kernel: A bayesian approach. *Journal of Econometrics 216*, 430–449.

Beason, T. and D. Schreindorfer (2022). Dissecting the equity premium. *Journal of Polictical Economy 130*, 2203–2222.

Birru, J. and S. Figlewski (2012). Anatomy of a meltdown: The risk neutral density for the S&P 500 in the fall of 2008. *Journal of Financial Markets*, 151–180.

Black, F. and M. Scholes (1973). The pricing of options and corporate liabilities. *Journal of Political Economy 81*(3), 637–654.

Bliss, R. R. and N. Panigirtzoglou (2004). Option-implied risk aversion estimates. *Journal of Finance 59*(1), 407–444.

Breeden, D. and R. Litzenberger (1978). Prices of state-contigent claims implicit in option prices. *Journal of Business 51*(4), 621–51.

Campbell, J. Y. and R. J. Shiller (1988). Stock prices, earnings, and expected dividends. *Journal of Finance 43*(3), 661–76.

Chabi-Yo, F., C. Dim, and G. Vilkov (2022). Generalized bounds on the conditional expected excess return on individual stocks. *Management Science 69*(2), 922–939.

Chabi-Yo, F. and J. Loudis (2020). The conditional expected market return. *Journal of Financial Economics 137*(3), 752–786.

Cuesdeanu, H. and J. C. Jackwerth (2018). The pricing kernel puzzle: Survey and outlook. *Annals Finance 14*, 289–329.

Delikouras, S. (2017). Where's the kink? disappointment events in consumption growth and equilibrium asset prices. *Review of Financial Studies 30*(8), 2851–2889.

Delikouras, S. and A. Kostakis (2019). A single factor consumption-based asset pricing model. *Journal of Financial and Quantitative Analysis 54*(2), 789–827.

Driessen, J., J. Koëter, and O. Wilms (2022). Horizon effects in the pricing kernel: How investors price short-term versus long-term risks. *Working Paper*.

Esscher, F. (1932). Onn the probability function in the collective theory of risk. *Skandinavisk Aktuarietidskrift 15*(3), 175–195.

Fama, E. F. and K. R. French (1993). Common risk factors in the returns on stocks and bonds. *Journal of Financial Economics 33*(1), 3–56.

Fama, E. F. and K. R. French (2015). A five-factor asset pricing model. *Journal of Financial Economics 116*(1), 1–22.

Figlewski, S. (2008). Estimating the implied risk neutral density.

Gandhi, M., N. J. Gormsen, and E. Lazarus (2023). Forward return expectations. *Working Paper*.

Goyal, A. and I. Welch (2003). Predicting the equity premium with dividend ratios. *Management Science 49*, 639–654.

Goyal, A. and I. Welch (2008). A comprehensive look at the empirical performance of the equity premium prediction. *Review of FInancial Studies 21*, 1455–1508.

Henze, N. (1986). A probabilistic representation of the 'skew-normal' distribution. *Scandinavian Journal of Statistics 13*(4), 271–275.

Heston, S., K. Jacobs, and H. J. Kim (2023). The pricing kernel in options. *Working Paper*.

Hou, K., C. Xue, and L. Zhang (2019). Which factors? *Review of Finance 23*(1), 1–35.

Huang, C.-F. and R. H. Litzenberger (1989). *Foundations for Financial Economics*. New York, NY: North-Holland.

Kim, H. J. (2021). Characterizing the conditional pricing kernel: A new approach. *Working Paper*.

Kostakis, A., T. Magdalinos, and M. P. Stamatogiannis (2015). Robust econometric inference for stock return predictability. *Review of Financial Studies 28*, 1506–1553.

Lettau, M. L. and S. C. Ludvigson (2001a). Consumption, aggregate wealth, and expected stock returns. *Journal of Finance 56*(3), 815–49.

Lettau, M. L. and S. C. Ludvigson (2001b). Resurrecting the (c)capm: A cross-sectional test when risk premia are time-varying. *Journal of Political Economy 109*(6), 1238–1287.

Lewellen, J. (2015). The cross-section of expected stock returns. *Critical Finance Review 4*, 1–44.

Linn, M., S. Shive, and T. Shumway (2018). Pricing kernel monotonicity and conditional infromation. *Review of Financial Studies 31*(2), 493–531.

Lintner, J. (1965). The valuation of assets and the selection of risky investments in stock portfolios and capital budgets. *Review of Economics and Statistics 47*(1), 13–37.

Liu, L. X., T. M. Whited, and L. Zhang (2009). Investment-based expected stock returns. *Journal of Political Economy 117*, 1105–39.

Martin, I. (2017). What is the expected return on the market. *Quarterly Journal of Economics 132*(2), 367–433.

Martin, I. and C. Wagner (2019). What is the expected return on a stock. *Journal of Finance 74*(4), 1887–1929.

Merton, R. C. (1974). On the pricing of corporate debt: the risk structure of interest rates. *Journal of Finance 29*, 449–70.

Monfort, A. and F. Pegoraro (2010). Asset pricing with second-order esscher transforms. *Working paper*.

Newey, W. K. and K. D. West (1987). A simple, positive semi-definite, heteroskedasticity and autocorrelation consistent covariance matrix. *Econometrica 55*, 703–8.

Rosenberg, J. V. and R. F. Engle (2000). Empirical pricing kernels. *Journal of Financial Economics 64*, 341–72.

Schreindorfer, D. and T. Sischert (2022). Volatility and the pricing kernel. Working Paper.

Sichert, T. (2023). The pricing kernel is u-shaped. *Working Paper*.

Stambaugh, R. F. (1999). Predictive regressions. *Journal of Financial Economics 54*, 375–421.

van Binsgergen, J. H. and R. S. J. Koijen (2010). Predictive ergressions: A present-value approach. *Journal of Finance 65*, 1439–1471.

Viceira, L. (2001). Optimal portfolio choice for long-horizon investors with nontradable labor income. *Journal of Finance 56*, 422–470.

Vissing-Jorgensen, A. (2004). Perspectives on behavioral finance: Does "irrationality" disappear with wealth? evidence from expectations and actions. *NBER Macroeconomics Annual 18*(139-208).

Yogo, M. (2006). A consumption-based explanation of expected stock returns. *Journal of Finance 61*(2), 539–80.

Figures

Figure 1 Pricing Kernels

This figure shows the monotonic and non-monotonic pricing kernels of equations (1), (2), (4), and (6) across the 1- (Panel A), 2- (Panel B), 3- (Panel C), and 6-month (Panel D) expirations. Estimation of the pricing kernels is reported in Table 2 through Table 5. In these graphs, I set the value of the normalized VIX ($nvix$) equal to its sample average for pricing kernels with VIX-dependent parameters (Panels B and D). The sample is from January 1996 to December 2022 for 1-month expiration options, May 1998 to November 2022 for 2-month expiration, January 2002 to October 2022 for 3-month expiration, and June 1996 to June 2022 for 6-month expiration options.

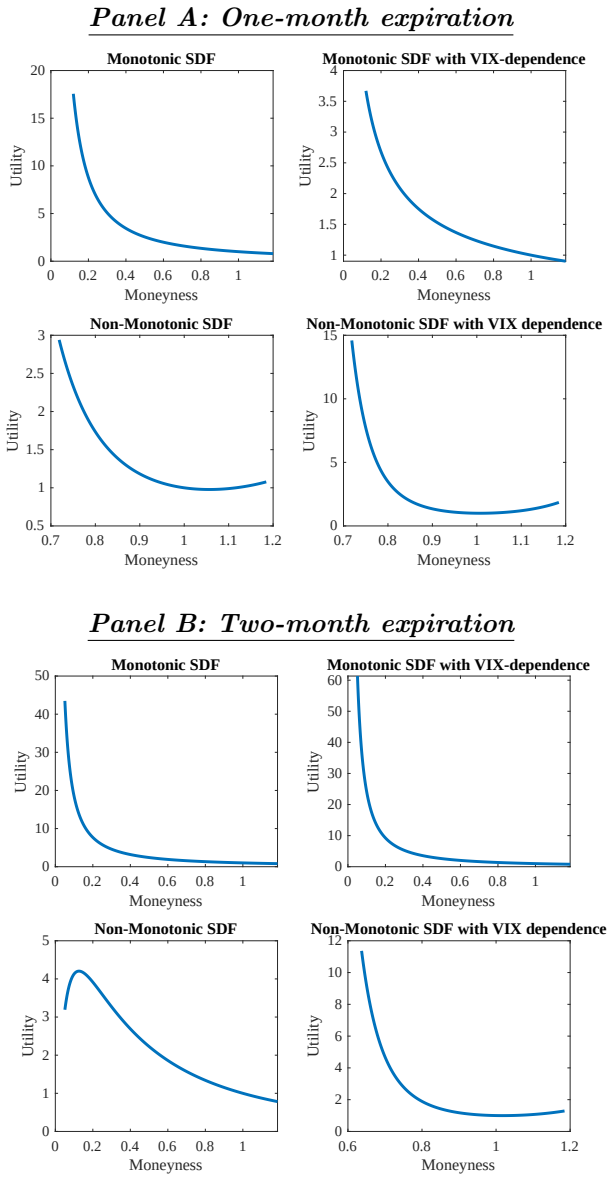

Panel C: Three-month expiration

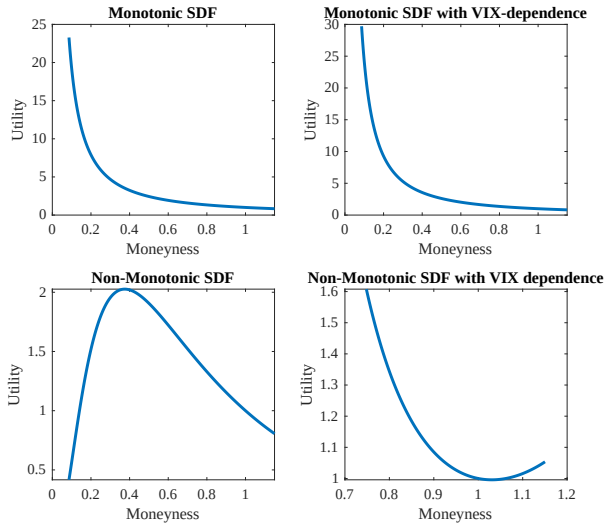

Panel D: Six-month expiration

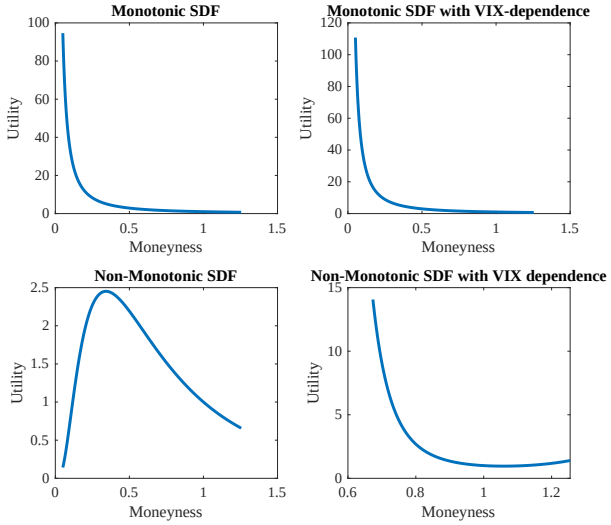

Figure 2 Option-based Physical Distribution and Density Functions

This figure shows the average distribution and density functions under the physical measure derived from the monotonic and non-monotonic pricing kernels of equations (1), (2), (4), and (6) across the 1- (Panel A), 2- (Panel B), 3-(Panel C), and 6-month (Panel D) expirations. The graphs are labeled according to the exponents of the corresponding pricing kernels: $\gamma_1 r$ (equation (1)), $\gamma_1 nvix^{\gamma_3} r$ (equation (2)), $\gamma_1 r + \gamma_2 r^2$ (equation (4)), and $\gamma_1 nvix^{\gamma_3} r + \gamma_2 nvix^{\gamma_3} r^2$ (equation (6)), where r denotes log returns, and $nvix$ is the normalized VIX, which is the VIX divided by its 1986-1995 average (to avoid look-ahead bias) and appropriately scaled for each expiration. *risk-neutral* denotes the risk-neutral density. Estimation of the pricing kernels is reported in Table 2 through Table 5. Estimation of the physical distribution and density functions is according to equation (14). I average the distribution and density functions for each expiration across dates. *realized* is the distribution of realized returns for each expiration. The realized distribution and density functions are derived by fitting a kernel-density estimator on the set of realized returns, and then interpolating the values for the entire range of moneyness using a piecewise cubic hermite interpolating polynomial. The sample is from January 1996 to December 2022 for 1-month expiration options, May 1998 to November 2022 for 2-month expiration, January 2002 to October 2022 for 3-month expiration, and June 1996 to June 2022 for 6-month expiration options.

Panel A: One-month expiration

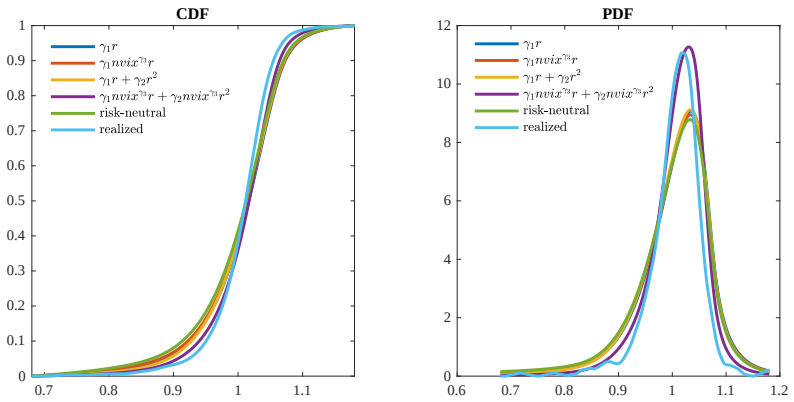

Panel B: Two-month expiration

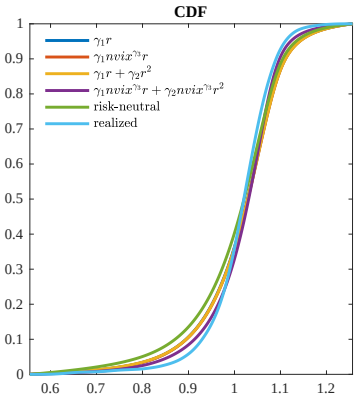

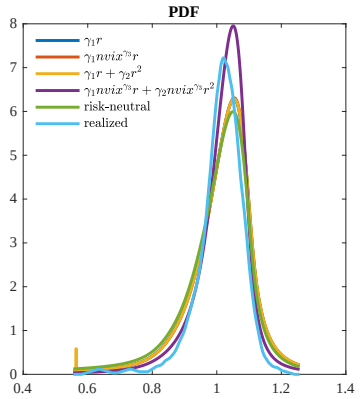

Panel C: Three-month expiration

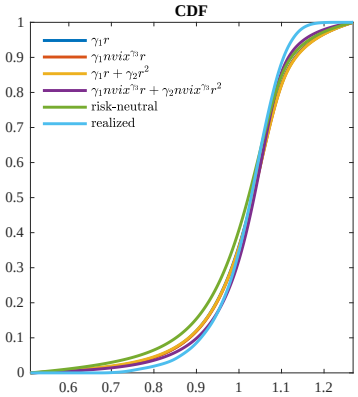

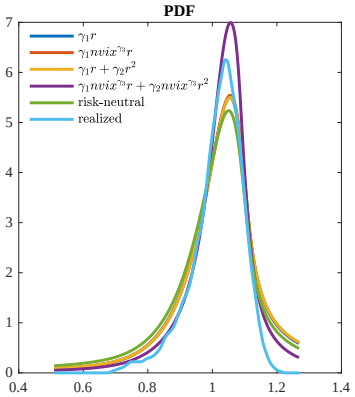

Panel D: Six-month expiration

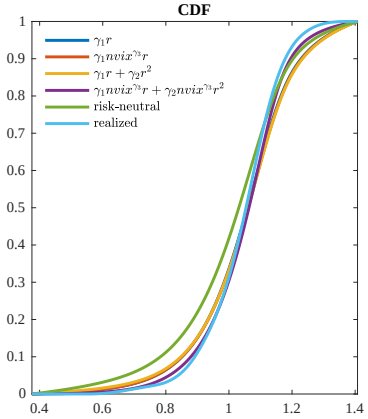

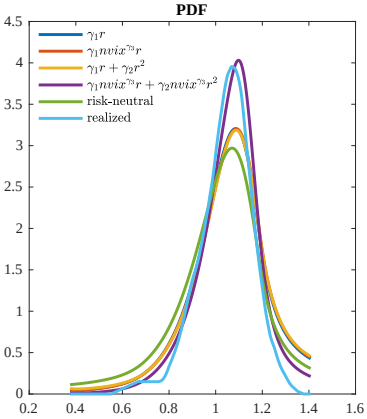

Tables

Table 1 Sample of Option Contracts

This table reports summary information for the S&P500 option contracts from OptionMetrics used to derive the forward-looking density for S&P500 under the physical measure. In selecting option contracts, I impose the following filters: non-missing implied volatility, positive volume, and bid price above \$3/8. I also require that there are at least six option contracts for each date, with at least three puts and at least three calls outside the $\pm 2\%$ moneyness range. There are two nonconsecutive 2-month observations and eleven nonconsecutive 3-month observations at the beginning of the sample for which the risk-neutral density could not be estimated. For these dates, there were not enough option contracts satisfying the sample selection criteria. Further, a sample of consecutive observations is required to calculate autocorrelations for Newey-West standard errors in the GMM estimation. Hence, for the 2- and 3-month contracts additional observations had to be deleted from the beginning of the sample. The resulting sample is from January 1996 to December 2022 for 1-month expiration, May 1998 to November 2022 for 2-month, January 2002 to October 2022 for 3-month, and June 1996 to June 2022 for 6-month expiration.

	1-month	2-month	3-month	6-month
Num. of Calls	38,577	14,329	6,141	3,368
Num. of Puts	46,420	18,980	8,432	3,574
Total	84,997	33,309	14,573	6,942
Num. of Expiration Dates (without filters)	323	161	107	52
Num. of Expiration Dates (with filters)	323	159	96	52
Num. of Expiration Dates (with filters and consecutive non-missing observations)	323	147	83	52

Table 2 GMM Estimation of the Option-based Monotonic Pricing Kernel

This table reports GMM results for the option-based monotonic pricing kernel of equation (1). γ_1 is the risk aversion parameter. The GMM moment conditions are given in equation (13). t-statistics in parentheses are corrected for heteroscedasticity and autocorrelation using Newey-West standard errors with 12, 6, 4, and 2 lags for the 1-, 2-, 3-, and 6-month maturities, respectively. χ^2, dof, and p are the χ^2 test, degrees of freedom, and p-value that all target moments are jointly zero. GMM is the minimized value of the GMM objective. The sample is from January 1996 to December 2022 for 1-month expiration options, May 1998 to November 2022 for 2-month expiration, January 2002 to October 2022 for 3-month expiration, and June 1996 to June 2022 for 6-month expiration options.

	1-month	2-month	3-month	6-month
γ_1	1.349	1.266	1.284	1.524
	(4.77)	(4.65)	(4.43)	(6.83)
χ^2	0.21	0.01	0.01	0.01
dof	1	1	1	1
p	0.64	0.90	0.91	0.89
GMM	$3.99e^{-05}$	$6.01e^{-06}$	$9.08e^{-06}$	$2.49e^{-05}$

Table 3 GMM Estimation of the Option-based Monotonic Pricing Kernel with VIX-dependent Parameters

This table reports GMM results of the option-based VIX-dependent monotonic pricing kernel of equation (2). γ_1 is the risk aversion parameter and γ_3 is the VIX-dependence coefficient. For the estimation, VIX is the normalized VIX ($nvix$), which is the VIX divided by its 1986-1995 average (to avoid look-ahead bias) and appropriately scaled for each expiration. The GMM moment conditions are given in equation (13). t-statistics in parentheses are corrected for heteroscedasticity and autocorrelation using Newey-West standard errors with 12, 6, 4, and 2 lags for the 1-, 2-, 3-, and 6-month maturities, respectively. χ^2, dof, and p are the χ^2 test, degrees of freedom, and p-value that all target moments are jointly zero. GMM is the minimized value of the GMM objective. The sample is from January 1996 to December 2022 for 1-month expiration options, May 1998 to November 2022 for 2-month expiration, January 2002 to October 2022 for 3-month expiration, and June 1996 to June 2022 for 6-month expiration options.

	1-month	2-month	3-month	6-month
γ_1	0.518	1.439	1.295	1.661
	(0.31)	(1.03)	(5.12)	(2.13)
γ_3	1.936	-0.558	-0.817	-0.813
	(0.47)	(-0.12)	(-0.11)	(-0.15)
χ^2	-	-	-	-
dof	0	0	0	0
p	-	-	-	-
GMM	$1.45e^{-13}$	$2.64e^{-13}$	$3.42e^{-17}$	$1.73e^{-15}$

Table 4 GMM Estimation of the Option-based Non-monotonic Pricing Kernel

This table reports GMM results of the option-based non-monotonic pricing kernel of equation (4). γ_1 is the parameter for the linear term and γ_2 is the parameter of the quadratic term in the discount factor. The GMM moment conditions are given in equation (13). t-statistics in parentheses are corrected for heteroscedasticity and autocorrelation using Newey-West standard errors with 12, 6, 4, and 2 lags for the 1-, 2-, 3-, and 6-month maturities, respectively. χ^2, dof, and p are the χ^2 test, degrees of freedom, and p-value that all target moments are jointly zero. GMM is the minimized value of the GMM objective. The sample is from January 1996 to December 2022 for 1-month expiration options, May 1998 to November 2022 for 2-month, January 2002 to October 2022 for 3-month, and June 1996 to June 2022 for 6-month expiration options.

	1-month	2-month	3-month	6-month
γ_1	0.814	1.386	1.439	1.672
	(0.57)	(1.27)	(0.92)	(1.35)
γ_2	-7.412	0.334	0.732	0.779
	(-0.32)	(1.83)	(0.16)	(0.29)
χ^2	-	-	-	-
dof	0	0	0	0
p	-	-	-	-
GMM	$9.70e^{-14}$	$1.11e^{-15}$	$1.86e^{-14}$	$5.32e^{-17}$

Table 5 GMM Estimation of the Option-based Non-monotonic Pricing Kernel with VIX-dependent Parameters

This table reports GMM results of the option-based VIX-dependent non-monotonic pricing kernel of equation (6). γ_1 is the parameter for the linear term and γ_2 is the parameter of the quadratic term in the discount factor. γ_3 is the VIX-dependence coefficient. For the estimation, the VIX is the normalized VIX ($nvix$), which is the VIX divided by its 1986-1995 average (to avoid look-ahead bias) and appropriately scaled for each expiration. The GMM moment conditions are given in equation (13). t-statistics in parentheses are corrected for heteroscedasticity and autocorrelation using Newey-West standard errors with 12, 6, 4, and 2 lags for the 1-, 2-, 3-, and 6-month maturities, respectively. χ^2, dof, and p are the χ^2 test, degrees of freedom, and p-value that all target moments are jointly zero. GMM is the minimized value of the GMM objective. The sample is from January 1996 to December 2022 for 1-month expiration options, May 1998 to November 2022 for 2-month expiration, January 2002 to October 2022 for 3-month expiration, and June 1996 to June 2022 for 6-month expiration options.

	1-month	2-month	3-month	6-month
γ_1	0.700	0.660	0.129	1.991
	(2.78)	(2.61)	(0.23)	(4.08)
γ_2	-47.470	-19.068	-2.143	-17.422
	(-1.26)	(-1.06)	(-0.30)	(-1.38)
γ_3	-8.153	-7.415	-9.720	-4.421
	(-2.21)	(-2.29)	(-0.43)	(-1.09)
χ^2	-	-	-	-
dof	0	0	0	0
p	-	-	-	-
GMM	$6.85e^{-13}$	$4.68e^{-14}$	$1.73e^{-14}$	$7.81e^{-14}$

Table 6 Kolmogorov-Smirnov Tests for the Option-based Physical Distribution Functions Across Pricing Kernels

This table reports the frequency of rejections of the null hypothesis that any two option-based physical distribution functions are equal according to the two-sample Kolmogorov-Smirnov test. The option-based physical distributions are derived from alternative pricing kernels, and are classified according to the exponents of the corresponding discount factors: $\gamma_1 r$ (equation (1)), $\gamma_1 nvix^{\gamma_3} r$ (equation (2)), $\gamma_1 r + \gamma_2 r^2$ (equation (4)), and $\gamma_1 nvix^{\gamma_3} r + \gamma_2 nvix^{\gamma_3} r^2$ (equation (6)), where r denotes log returns, and $nvix$ is the normalized VIX, which is the VIX divided by its 1986-1995 average (to avoid look-ahead bias) and appropriately scaled for each expiration. The estimation of the various pricing kernels is based on the GMM system of equation (13), and the results are reported in Table 2 through Table 5. *risk-neutral* is the risk-neutral distribution, and *realized* is the distribution of realized returns in the sample for each expiration. Option-based physical and risk-neutral distributions are derived according to equation (14). The realized distribution and density functions are derived by fitting a kernel-density estimator on the set of realized returns, and then interpolating the values for the entire range of moneyness using a piecewise cubic hermite interpolating polynomial. For the realized distribution, the Kolmogorov-Smirnov tests compare the density of realized returns to the averages of the option-option densities. Panel A reports the frequency of rejections of the Kolmogorov-Smirnov tests at the 1-month expiration. Panel B reports the results for the Kolmogorov-Smirnov tests at the 2-month expiration. Panel C shows frequency of rejections for the Kolmogorov-Smirnov tests at the 3-month expiration, and Panel D reports rejections at the 6-month expiration. The confidence level for the tests is set to 5%. The numbers in brackets are the average values for the Kolmogorov-Smirnov statistic. N is the number of observations. The sample is from January 1996 to December 2022 for 1-month expiration, May 1998 to November 2022 for 2-month expiration options, January 2002 to October 2022 for 3-month expiration, and June 1996 to June 2022 for 6-month expiration options.

Panel A: Rejections of the Kolmogorov-Smirnov tests, 1-month expiration (N=323)

N=323	$\gamma_1 r$	$\gamma_1 nvix^{\gamma_3} r$	$\gamma_1 r + \gamma_2 r^2$	$\gamma_1 nvix^{\gamma_3} r + \gamma_2 nvix^{\gamma_3} r^2$	risk-neutral
$\gamma_1 nvix^{\gamma_3} r$	22% [4%]				
$\gamma_1 r + \gamma_2 r^2$	50% [7%]	77% [9%]			
$\gamma_1 nvix^{\gamma_3} r + \gamma_2 nvix^{\gamma_3} r^2$	84% [26%]	87% [27%]	85% [25%]		
risk-neutral	65% [7%]	23% [4%]	88% [12%]	86% [27%]	
realized (N=1)	100% [14%]	100% [16%]	100% [10%]	100% [6%]	100% [19%]

Panel B: Rejections of the Kolmogorov-Smirnov tests, 2-month expiration (N=147)

N=147	$\gamma_1 r$	$\gamma_1 nvix^{\gamma_3} r$	$\gamma_1 r + \gamma_2 r^2$	$\gamma_1 nvix^{\gamma_3} r + \gamma_2 nvix^{\gamma_3} r^2$	risk-neutral
$\gamma_1 nvix^{\gamma_3} r$	3% [2%]				
$\gamma_1 r + \gamma_2 r^2$	2% [1%]	5% [2%]			
$\gamma_1 nvix^{\gamma_3} r + \gamma_2 nvix^{\gamma_3} r^2$	87% [26%]	85% [26%]	89% [27%]		
risk-neutral	87% [9%]	95% [10%]	90% [9%]	84% [29%]	
realized (N=1)	100% [11%]	100% [11%]	100% [12%]	100% [7%]	100% [18%]

Panel C: Rejections of the Kolmogorov-Smirnov tests, 3-month expiration (N=83)

N=83	$\gamma_1 r$	$\gamma_1 nvix^{\gamma_3} r$	$\gamma_1 r + \gamma_2 r^2$	$\gamma_1 nvix^{\gamma_3} r + \gamma_2 nvix^{\gamma_3} r^2$	risk-neutral
$\gamma_1 nvix^{\gamma_3} r$	15% [3%]				
$\gamma_1 r + \gamma_2 r^2$	20% [3%]	33% [5%]			
$\gamma_1 nvix^{\gamma_3} r + \gamma_2 nvix^{\gamma_3} r^2$	87% [26%]	84% [25%]	88% [27%]		
risk-neutral	86% [10%]	92% [11%]	87% [8%]	78% [27%]	
realized (N=1)	100% [23%]	100% [23%]	100% [24%]	100% [23%]	100% [25%]

Panel D: Rejections of the Kolmogorov-Smirnov tests, 6-month expiration (N=52)

N=52	$\gamma_1 r$	$\gamma_1 nvix^{\gamma_3} r$	$\gamma_1 r + \gamma_2 r^2$	$\gamma_1 nvix^{\gamma_3} r + \gamma_2 nvix^{\gamma_3} r^2$	risk-neutral
$\gamma_1 nvix^{\gamma_3} r$	23% [3%]				
$\gamma_1 r + \gamma_2 r^2$	40% [6%]	52% [7%]			
$\gamma_1 nvix^{\gamma_3} r + \gamma_2 nvix^{\gamma_3} r^2$	94% [27%]	90% [27%]	96% [30%]		
risk-neutral	100% [14%]	100% [15%]	100% [11%]	100% [32%]	
realized (N=1)	100% [18%]	100% [18%]	100% [19%]	100% [17%]	100% [21%]

Table 7 Summary Statistics of Option-based Moments under the Physical Measure Across Pricing Kernels

This table reports summary statistics for the option-based moments of returns under the physical measure across the different pricing kernels from equations (1), (2), (4), and (6). The pricing kernels are classified according to the their exponent: $\gamma_1 r$ (equation (1)), $\gamma_1 nvix^{\gamma_3} r$ (equation (2)), $\gamma_1 r + \gamma_2 r^2$ (equation (4)), and $\gamma_1 nvix^{\gamma_3} r + \gamma_2 nvix^{\gamma_3} r^2$ (equation (6)), where r denotes log returns, and $nvix$ is the normalized VIX, which is the VIX divided by its 1986-1995 average (to avoid look-ahead bias) and appropriately scaled for each expiration. The estimation of the various pricing kernels is based on the GMM system of equation (13), and the results are reported in Table 2 through Table 5. *risk-neutral* denotes the moments of the risk-neutral density. Option-based physical and risk-neutral moments are derived according to equation (14). *realized* denotes the unconditional sample moments of realized returns for each expiration. Panel A reports summary statistics for option-based expected returns. Panel B reports statistics for option-based variances. Panel C reports summary statistics for option-based skewness, and in Panel D for option-based kurtosis. The sample is from January 1996 to December 2022 for 1-month expiration options, May 1998 to November 2022 for 2-month expiration, January 2002 to October 2022 for 3-month expiration, and June 1996 to June 2022 for 6-month expiration options.

Panel A: Option-based expected returns across pricing kernels

i) $\gamma_1 r$	1-month	2-month	3-month	6-month
mean	0.61%	1.29%	1.67%	4.26%
st. deviation	0.77%	1.46%	1.41%	2.20%
N	323	147	83	52
ii) $\gamma_1 nvix^{\gamma_3} r$	1-month	2-month	3-month	6-month
mean	0.63%	1.28%	1.66%	4.25%
st. deviation	2.56%	1.04%	0.94%	1.46%
N	323	147	83	52
iii) $\gamma_1 r + \gamma_2 r^2$	1-month	2-month	3-month	6-month
mean	0.63%	1.28%	1.66%	4.25%
st. deviation	0.69%	1.29%	1.42%	2.18%
N	323	147	83	52
iv) $\gamma_1 nvix^{\gamma_3} r + \gamma_2 nvix^{\gamma_3} r^2$	1-month	2-month	3-month	6-month
mean	0.63%	1.28%	1.66%	4.25%
st. deviation	0.40%	0.74%	1.12%	1.16%
N	323	147	83	52
v) risk-neutral	1-month	2-month	3-month	6-month
mean	-0.06%	0.01%	0.11%	0.46%
st. deviation	0.44%	0.87%	0.97%	1.39%
N	323	147	83	52
vi) realized mean	1-month	2-month	3-month	6-month
	0.63%	1.28%	1.66%	4.25%

Panel B: Option-based physical variances across pricing kernels

i) $\gamma_1 r$	1-month	2-month	3-month	6-month
mean	0.42%	0.82%	0.97%	1.98%
st. deviation	0.44%	0.76%	0.70%	1.02%
N	323	147	83	52

ii) $\gamma_1 nvix^{\gamma_3} r$	1-month	2-month	3-month	6-month
mean	0.43%	0.82%	0.98%	2.00%
st. deviation	0.36%	0.88%	0.81%	1.19%
N	323	147	83	52

iii) $\gamma_1 r + \gamma_2 r^2$	1-month	2-month	3-month	6-month
mean	0.34%	0.89%	1.05%	2.23%
st. deviation	0.28%	1.37%	0.83%	1.39%
N	323	147	83	52

iv) $\gamma_1 nvix^{\gamma_3} r + \gamma_2 nvix^{\gamma_3} r^2$	1-month	2-month	3-month	6-month
mean	0.36%	0.70%	0.87%	1.33%
st. deviation	0.62%	1.17%	1.10%	1.31%
N	323	147	83	52

v) risk-neutral	1-month	2-month	3-month	6-month
mean	0.51%	1.04%	1.26%	2.67%
st. deviation	0.60%	1.12%	0.99%	1.52%
N	323	147	83	52

vi) realized variance	1-month	2-month	3-month	6-month
	0.24%	0.49%	0.54%	1.13%

Panel C: Option-based physical skewness across pricing kernels

i) $\gamma_1 r$	1-month	2-month	3-month	6-month
mean	-1.43	-1.34	-1.26	-0.72
st. deviation	0.77	0.71	0.62	0.29
N	323	147	83	52

ii) $\gamma_1 nvix^{\gamma_3} r$	1-month	2-month	3-month	6-month
mean	-1.45	-1.32	-1.23	-0.68
st. deviation	0.79	0.68	0.57	0.21
N	323	147	83	52

iii) $\gamma_1 r + \gamma_2 r^2$	1-month	2-month	3-month	6-month
mean	-1.17	-1.37	-1.39	-0.91
st. deviation	0.64	0.72	0.71	0.38
N	323	147	83	52

iv) $\gamma_1 nvix^{\gamma_3} r + \gamma_2 nvix^{\gamma_3} r^2$	1-month	2-month	3-month	6-month
mean	-0.59	-0.50	-0.56	-0.15
st. deviation	0.45	0.37	0.47	0.18
N	323	147	83	52

v) risk-neutral	1-month	2-month	3-month	6-month
mean	-1.51	-1.47	-1.41	-0.98
st. deviation	0.76	0.75	0.71	0.42
N	323	147	83	52

vi) realized skewness	1-month	2-month	3-month	6-month
	-1.24	-1.67	-1.15	-0.87

Panel D: Option-based physical kurtosis across pricing kernels

i) $\gamma_1 r$	1-month	2-month	3-month	6-month
mean	7.96	7.55	6.97	4.75
st. deviation	4.43	3.91	3.49	1.33
N	323	147	83	52

ii) $\gamma_1 nvix^{\gamma_3} r$	1-month	2-month	3-month	6-month
mean	7.78	7.54	6.92	4.61
st. deviation	4.16	3.91	3.37	1.06
N	323	147	83	52

iii) $\gamma_1 r + \gamma_2 r^2$	1-month	2-month	3-month	6-month
mean	6.84	7.73	7.58	5.45
st. deviation	3.36	4.10	4.16	2.00
N	323	147	83	52

iv) $\gamma_1 nvix^{\gamma_3} r + \gamma_2 nvix^{\gamma_3} r^2$	1-month	2-month	3-month	6-month
mean	4.37	4.01	4.12	3.24
st. deviation	1.51	1.14	1.55	0.23
N	323	147	83	52

v) risk-neutral	1-month	2-month	3-month	6-month
mean	7.67	7.39	6.92	4.99
st. deviation	3.94	3.69	3.44	1.75
N	323	147	83	52

vi) realized kurtosis	1-month	2-month	3-month	6-month
	9.10	9.36	4.71	4.55

Table 8 Coefficient of Determination for Option-based Moments under the Physical Measure across Pricing Kernels

This table reports coefficients of determination (R^2) from regressing option-based moments for returns across the different pricing kernels from equations (1), (2), (4), and (6). Option-based physical moments are derived according to equation (14). The pricing kernels are classified according to the their exponents: $\gamma_1 r$ (equation (1)), $\gamma_1 nvix^{\gamma_3} r$ (equation (2)), $\gamma_1 r + \gamma_2 r^2$ (equation (4)), and $\gamma_1 nvix^{\gamma_3} r + \gamma_2 nvix^{\gamma_3} r^2$ (equation (6)), where r denotes log returns, and $nvix$ is the normalized VIX, which is the VIX divided by its 1986-1995 average (to avoid look-ahead bias) and appropriately scaled for each expiration. The estimation of the various pricing kernels is based on the GMM system of equation (13), and the results are reported in Table 2 through Table 5. *risk-neutral* denotes the moments of the risk-neutral density. Panel A reports R^2's for option-based moment regressions for the 1-month expiration. Panel B reports R^2's for option-based moment regressions for the 2-month expiration. Panel C reports R^2's for the 3-month expiration, and Panel D shows R^2' for the 6-month expiration. N is the number of observations. The sample is from January 1996 to December 2022 for 1-month expiration options, May 1998 to November 2022 for 2-month expiration, January 2002 to October 2022 for 3-month expiration, and June 1996 to June 2022 for 6-month expiration.

Panel A: 1-month expiration

R^2's of option-based expected returns regressions (average R^2 = 33.72%; excl. risk-neutral: 49.51%)

	$\gamma_1 r$	$\gamma_1 nvix^{\gamma_3} r$	$\gamma_1 r + \gamma_2 r^2$	$\gamma_1 nvix^{\gamma_3} r + \gamma_2 nvix^{\gamma_3} r^2$
$\gamma_1 nvix^{\gamma_3} r$	74.28%			
$\gamma_1 r + \gamma_2 r^2$	95.80%	63.66%		
$\gamma_1 nvix^{\gamma_3} r + \gamma_2 nvix^{\gamma_3} r^2$	18.84%	21.39%	23.07%	
risk-neutral	8.43%	0.19%	4.97%	26.58%

R^2's of option-based variances regressions (average R^2 = 95.39%; excl. risk-neutral: 95.46%)

	$\gamma_1 r$	$\gamma_1 nvix^{\gamma_3} r$	$\gamma_1 r + \gamma_2 r^2$	$\gamma_1 nvix^{\gamma_3} r + \gamma_2 nvix^{\gamma_3} r^2$
$\gamma_1 nvix^{\gamma_3} r$	96.21%			
$\gamma_1 r + \gamma_2 r^2$	96.94%	94.82%		
$\gamma_1 nvix^{\gamma_3} r + \gamma_2 nvix^{\gamma_3} r^2$	98.14%	90.57%	96.06%	
risk-neutral	98.24%	92.60%	92.88%	97.43%

R^2's of option-based skewness regressions (average R^2 = 55.47%; excl. risk-neutral: 46.18%)

	$\gamma_1 r$	$\gamma_1 nvix^{\gamma_3} r$	$\gamma_1 r + \gamma_2 r^2$	$\gamma_1 nvix^{\gamma_3} r + \gamma_2 nvix^{\gamma_3} r^2$
$\gamma_1 nvix^{\gamma_3} r$	98.80%			
$\gamma_1 r + \gamma_2 r^2$	86.09%	86.23%		
$\gamma_1 nvix^{\gamma_3} r + \gamma_2 nvix^{\gamma_3} r^2$	0.66%	0.39%	4.93%	
risk-neutral	98.78%	97.17%	79.33%	2.34%

R^2's of option-based kurtosis regressions (average R^2 =55.87%; excl. risk-neutral: 45.63%)

	$\gamma_1 r$	$\gamma_1 nvix^{\gamma_3} r$	$\gamma_1 r + \gamma_2 r^2$	$\gamma_1 nvix^{\gamma_3} r + \gamma_2 nvix^{\gamma_3} r^2$
$\gamma_1 nvix^{\gamma_3} r$	99.66%			
$\gamma_1 r + \gamma_2 r^2$	84.24%	82.54%		
$\gamma_1 nvix^{\gamma_3} r + \gamma_2 nvix^{\gamma_3} r^2$	1.66%	2.27%	3.44%	
risk-neutral	99.44%	99.55%	83.64%	2.30%

Panel B: 2-month expiration

R^2's of option-based expected returns regressions (average R^2 = 38.60%; excl. risk-neutral: 42.98%)

	$\gamma_1 r$	$\gamma_1 nvix^{\gamma_3} r$	$\gamma_1 r + \gamma_2 r^2$	$\gamma_1 nvix^{\gamma_3} r + \gamma_2 nvix^{\gamma_3} r^2$
$\gamma_1 nvix^{\gamma_3} r$	91.44%			
$\gamma_1 r + \gamma_2 r^2$	74.54%	84.39%		
$\gamma_1 nvix^{\gamma_3} r + \gamma_2 nvix^{\gamma_3} r^2$	6.33%	0.25%	0.93%	
risk-neutral	16.64%	39.46%	33.79%	38.24%

R^2's of option-based variances regressions (average R^2 = 93.30%; excl. risk-neutral: 92.26%)

	$\gamma_1 r$	$\gamma_1 nvix^{\gamma_3} r$	$\gamma_1 r + \gamma_2 r^2$	$\gamma_1 nvix^{\gamma_3} r + \gamma_2 nvix^{\gamma_3} r^2$
$\gamma_1 nvix^{\gamma_3} r$	99.61%			
$\gamma_1 r + \gamma_2 r^2$	82.47%	86.20%		
$\gamma_1 nvix^{\gamma_3} r + \gamma_2 nvix^{\gamma_3} r^2$	98.57%	99.41%	87.28%	
risk-neutral	97.33%	98.01%	87.49%	96.62%

R^2's of option-based skewness regressions (average R^2 = 59.14%; excl. risk-neutral: 49.73%)

	$\gamma_1 r$	$\gamma_1 nvix^{\gamma_3} r$	$\gamma_1 r + \gamma_2 r^2$	$\gamma_1 nvix^{\gamma_3} r + \gamma_2 nvix^{\gamma_3} r^2$
$\gamma_1 nvix^{\gamma_3} r$	99.84%			
$\gamma_1 r + \gamma_2 r^2$	98.79%	99.13%		
$\gamma_1 nvix^{\gamma_3} r + \gamma_2 nvix^{\gamma_3} r^2$	0.02%	0.21%	0.39%	
risk-neutral	96.52%	97.20%	97.77%	1.49%

R^2's of option-based kurtosis regressions (average R^2 = 60.41%; excl. risk-neutral: 50.73%)

	$\gamma_1 r$	$\gamma_1 nvix^{\gamma_3} r$	$\gamma_1 r + \gamma_2 r^2$	$\gamma_1 nvix^{\gamma_3} r + \gamma_2 nvix^{\gamma_3} r^2$
$\gamma_1 nvix^{\gamma_3} r$	99.95%			
$\gamma_1 r + \gamma_2 r^2$	99.33%	99.23%		
$\gamma_1 nvix^{\gamma_3} r + \gamma_2 nvix^{\gamma_3} r^2$	1.44%	1.45%	2.94%	
risk-neutral	98.36%	98.26%	99.34%	3.79%

Panel C: 3-month expiration

R^2's of option-based expected returns regressions (average R^2 = 43.15%; excl. risk-neutral: 48.45%)

	$\gamma_1 r$	$\gamma_1 nvix^{\gamma_3} r$	$\gamma_1 r + \gamma_2 r^2$	$\gamma_1 nvix^{\gamma_3} r + \gamma_2 nvix^{\gamma_3} r^2$
$\gamma_1 nvix^{\gamma_3} r$	87.50%			
$\gamma_1 r + \gamma_2 r^2$	98.81%	89.70%		
$\gamma_1 nvix^{\gamma_3} r + \gamma_2 nvix^{\gamma_3} r^2$	8.30%	0.35%	6.06%	
risk-neutral	29.45%	59.03%	35.83%	16.53%

R^2's of option-based variances regressions (average R^2 = 97.33%; excl. risk-neutral: 97.95%)

	$\gamma_1 r$	$\gamma_1 nvix^{\gamma_3} r$	$\gamma_1 r + \gamma_2 r^2$	$\gamma_1 nvix^{\gamma_3} r + \gamma_2 nvix^{\gamma_3} r^2$
$\gamma_1 nvix^{\gamma_3} r$	99.65%			
$\gamma_1 r + \gamma_2 r^2$	98.40%	98.55%		
$\gamma_1 nvix^{\gamma_3} r + \gamma_2 nvix^{\gamma_3} r^2$	96.85%	97.72%	96.51%	
risk-neutral	96.25%	96.22%	99.08%	94.08%

R^2's of option-based skewness regressions (average R^2 = 58.31%; excl. risk-neutral: 48.50%)

	$\gamma_1 r$	$\gamma_1 nvix^{\gamma_3} r$	$\gamma_1 r + \gamma_2 r^2$	$\gamma_1 nvix^{\gamma_3} r + \gamma_2 nvix^{\gamma_3} r^2$
$\gamma_1 nvix^{\gamma_3} r$	99.09%			
$\gamma_1 r + \gamma_2 r^2$	93.10%	95.12%		
$\gamma_1 nvix^{\gamma_3} r + \gamma_2 nvix^{\gamma_3} r^2$	0.00%	0.73%	2.97%	
risk-neutral	94.59%	96.44%	98.51%	2.56%

R^2's of option-based kurtosis regressions (average R^2 = 54.91%; excl. risk-neutral: 55.11%)

	$\gamma_1 r$	$\gamma_1 nvix^{\gamma_3} r$	$\gamma_1 r + \gamma_2 r^2$	$\gamma_1 nvix^{\gamma_3} r + \gamma_2 nvix^{\gamma_3} r^2$
$\gamma_1 nvix^{\gamma_3} r$	62.33%			
$\gamma_1 r + \gamma_2 r^2$	54.35%	55.55%		
$\gamma_1 nvix^{\gamma_3} r + \gamma_2 nvix^{\gamma_3} r^2$	1.55%	0.90%	0.12%	
risk-neutral	62.03%	63.14%	79.68%	34.70%

Panel D: 6-month expiration

R^2's of option-based expected returns regressions (average R^2 = 39.67%; excl. risk-neutral: 46.68%)

	$\gamma_1 r$	$\gamma_1 nvix^{\gamma_3} r$	$\gamma_1 r + \gamma_2 r^2$	$\gamma_1 nvix^{\gamma_3} r + \gamma_2 nvix^{\gamma_3} r^2$
$\gamma_1 nvix^{\gamma_3} r$	82.06%			
$\gamma_1 r + \gamma_2 r^2$	98.07%	86.74%		
$\gamma_1 nvix^{\gamma_3} r + \gamma_2 nvix^{\gamma_3} r^2$	0.17%	0.12%	0.05%	
risk-neutral	13.86%	41.75%	21.63%	39.36%

R^2's of option-based variances regressions (average R^2 = 95.89%; excl. risk-neutral: 96.37%)

	$\gamma_1 r$	$\gamma_1 nvix^{\gamma_3} r$	$\gamma_1 r + \gamma_2 r^2$	$\gamma_1 nvix^{\gamma_3} r + \gamma_2 nvix^{\gamma_3} r^2$
$\gamma_1 nvix^{\gamma_3} r$	99.66%			
$\gamma_1 r + \gamma_2 r^2$	96.77%	97.32%		
$\gamma_1 nvix^{\gamma_3} r + \gamma_2 nvix^{\gamma_3} r^2$	94.60%	96.64%	93.20%	
risk-neutral	96.20%	96.18%	98.42%	89.91%

R^2's of option-based skewness regressions (average R^2 = 44.37%; excl. risk-neutral: 35.91%)

	$\gamma_1 r$	$\gamma_1 nvix^{\gamma_3} r$	$\gamma_1 r + \gamma_2 r^2$	$\gamma_1 nvix^{\gamma_3} r + \gamma_2 nvix^{\gamma_3} r^2$
$\gamma_1 nvix^{\gamma_3} r$	86.59%			
$\gamma_1 r + \gamma_2 r^2$	62.86%	62.75%		
$\gamma_1 nvix^{\gamma_3} r + \gamma_2 nvix^{\gamma_3} r^2$	1.11%	2.04%	0.14%	
risk-neutral	71.35%	61.75%	90.33%	4.75%

R^2's of option-based kurtosis regressions (average R^2 = 56.49%; excl. risk-neutral: 46.63%)

	$\gamma_1 r$	$\gamma_1 nvix^{\gamma_3} r$	$\gamma_1 r + \gamma_2 r^2$	$\gamma_1 nvix^{\gamma_3} r + \gamma_2 nvix^{\gamma_3} r^2$
$\gamma_1 nvix^{\gamma_3} r$	95.20%			
$\gamma_1 r + \gamma_2 r^2$	79.27%	83.71%		
$\gamma_1 nvix^{\gamma_3} r + \gamma_2 nvix^{\gamma_3} r^2$	2.85%	9.34%	9.42%	
risk-neutral	93.70%	92.96%	92.91%	5.50%

Table 9 Coefficient of Determination for 3rd and 4th Central Moments under the Physical Measure across Pricing Kernels

This table reports coefficients of determination (R^2) from regressing option-based third and fourth central moments across the different pricing kernels from equations (1), (2), (4), and (6). Option-based physical moments are derived according to equation (14). The pricing kernels are classified according to the their exponents: $\gamma_1 r$ (equation (1)), $\gamma_1 nvix^{\gamma_3} r$ (equation (2)), $\gamma_1 r + \gamma_2 r^2$ (equation (4)), and $\gamma_1 nvix^{\gamma_3} r + \gamma_2 nvix^{\gamma_3} r^2$ (equation (6)), where r denotes log returns, and $nvix$ is the normalized VIX, which is the VIX divided by its 1986-1995 average (to avoid look-ahead bias) and appropriately scaled for each expiration. The estimation of the various pricing kernels is based on the GMM system of equation (13), and the results are reported in Table 2 through Table 5. *risk-neutral* denotes the moments of the risk-neutral density. Panel A reports R^2's for option-based moment regressions for the 1-month expiration. Panel B reports R^2's for option-based moment regressions for the 2-month expiration. Panel C reports R^2's for the 3-month expiration, and Panel D shows R^2' for the 6-month expiration. N is the number of observations. The sample is from January 1996 to December 2022 for 1-month expiration options, May 1998 to November 2022 for 2-month expiration, January 2002 to October 2022 for 3-month expiration, and June 1996 to June 2022 for 6-month expiration options.

Panel A: 1-month expiration

R^2's of option-based third central moment regressions (average R^2 = 46.87%; excl. risk-neutral: 38.79%)

	$\gamma_1 r$	$\gamma_1 nvix^{\gamma_3} r$	$\gamma_1 r + \gamma_2 r^2$	$\gamma_1 nvix^{\gamma_3} r + \gamma_2 nvix^{\gamma_3} r^2$
$\gamma_1 nvix^{\gamma_3} r$	31.36%			
$\gamma_1 r + \gamma_2 r^2$	49.08%	45.05%		
$\gamma_1 nvix^{\gamma_3} r + \gamma_2 nvix^{\gamma_3} r^2$	81.39%	3.19%	22.70%	
risk-neutral	95.89%	20.85%	31.96%	87.29%

R^2's of option-based fourth central moment regressions (average R^2 =87.47%; excl. risk-neutral: 86.02%)

	$\gamma_1 r$	$\gamma_1 nvix^{\gamma_3} r$	$\gamma_1 r + \gamma_2 r^2$	$\gamma_1 nvix^{\gamma_3} r + \gamma_2 nvix^{\gamma_3} r^2$
$\gamma_1 nvix^{\gamma_3} r$	85.44%			
$\gamma_1 r + \gamma_2 r^2$	96.26%	82.88%		
$\gamma_1 nvix^{\gamma_3} r + \gamma_2 nvix^{\gamma_3} r^2$	93.86%	67.92%	89.78%	
risk-neutral	95.22%	77.93%	88.31%	97.07%

Panel B: 2-month expiration

R^2's of option-based third central moment regressions (average R^2 = 79.58%; excl. risk-neutral: 78.70%)

	$\gamma_1 r$	$\gamma_1 nvix^{\gamma_3} r$	$\gamma_1 r + \gamma_2 r^2$	$\gamma_1 nvix^{\gamma_3} r + \gamma_2 nvix^{\gamma_3} r^2$
$\gamma_1 nvix^{\gamma_3} r$	96.59%			
$\gamma_1 r + \gamma_2 r^2$	60.71%	69.90%		
$\gamma_1 nvix^{\gamma_3} r + \gamma_2 nvix^{\gamma_3} r^2$	81.39%	92.75%	70.85%	
risk-neutral	95.77%	93.19%	57.81%	76.83%

R^2's of option-based fourth central moment regressions (average R^2 = 88.55%; excl. risk-neutral: 86.75%)

	$\gamma_1 r$	$\gamma_1 nvix^{\gamma_3} r$	$\gamma_1 r + \gamma_2 r^2$	$\gamma_1 nvix^{\gamma_3} r + \gamma_2 nvix^{\gamma_3} r^2$
$\gamma_1 nvix^{\gamma_3} r$	99.44%			
$\gamma_1 r + \gamma_2 r^2$	70.50%	75.67%		
$\gamma_1 nvix^{\gamma_3} r + \gamma_2 nvix^{\gamma_3} r^2$	96.69%	98.69%	79.53%	
risk-neutral	97.61%	97.47%	75.94%	93.93%

Panel C: 3-month expiration

R^2's of option-based third central moment regressions (average R^2 = 86.45%; excl. risk-neutral: 86.57%)

	$\gamma_1 r$	$\gamma_1 nvix^{\gamma_3} r$	$\gamma_1 r + \gamma_2 r^2$	$\gamma_1 nvix^{\gamma_3} r + \gamma_2 nvix^{\gamma_3} r^2$
$\gamma_1 nvix^{\gamma_3} r$	93.89%			
$\gamma_1 r + \gamma_2 r^2$	89.38%	90.26%		
$\gamma_1 nvix^{\gamma_3} r + \gamma_2 nvix^{\gamma_3} r^2$	75.14%	90.17%	80.60%	
risk-neutral	89.23%	85.32%	97.07%	73.50%

R^2's of option-based fourth central moment regressions (average R^2 = 92.92%; excl. risk-neutral: 93.51%)

	$\gamma_1 r$	$\gamma_1 nvix^{\gamma_3} r$	$\gamma_1 r + \gamma_2 r^2$	$\gamma_1 nvix^{\gamma_3} r + \gamma_2 nvix^{\gamma_3} r^2$
$\gamma_1 nvix^{\gamma_3} r$	98.82%			
$\gamma_1 r + \gamma_2 r^2$	91.23%	91.47%		
$\gamma_1 nvix^{\gamma_3} r + \gamma_2 nvix^{\gamma_3} r^2$	92.58%	96.09%	90.85%	
risk-neutral	91.79%	90.15%	98.62%	87.57%

Panel D: 6-month expiration

R^2's of option-based third central moment regressions (average R^2 = 65.66%; excl. risk-neutral: 66.73%)

	$\gamma_1 r$	$\gamma_1 nvix^{\gamma_3} r$	$\gamma_1 r + \gamma_2 r^2$	$\gamma_1 nvix^{\gamma_3} r + \gamma_2 nvix^{\gamma_3} r^2$
$\gamma_1 nvix^{\gamma_3} r$	87.39%			
$\gamma_1 r + \gamma_2 r^2$	58.46%	76.48%		
$\gamma_1 nvix^{\gamma_3} r + \gamma_2 nvix^{\gamma_3} r^2$	44.83%	72.75%	60.47%	
risk-neutral	68.28%	69.88%	82.89%	35.09%

R^2's of option-based fourth central moment regressions (average R^2 = 91.74%; excl. risk-neutral: 92.26%)

	$\gamma_1 r$	$\gamma_1 nvix^{\gamma_3} r$	$\gamma_1 r + \gamma_2 r^2$	$\gamma_1 nvix^{\gamma_3} r + \gamma_2 nvix^{\gamma_3} r^2$
$\gamma_1 nvix^{\gamma_3} r$	99.40%			
$\gamma_1 r + \gamma_2 r^2$	91.09%	91.75%		
$\gamma_1 nvix^{\gamma_3} r + \gamma_2 nvix^{\gamma_3} r^2$	91.76%	94.98%	84.58%	
risk-neutral	93.70%	92.64%	96.15%	81.38%

Table 10 Summary Statistics of the Risk-neutral Variance Bounds for Expected Returns

Panel A of this table reports summary statistics for the Martin (2017) bound of expected returns, which is based on the risk-neutral variance according to equation (23), $R^f_{t,t+T} + var^{RND}(R_{t,t+T})/R^f_{t,t+T}$. The risk-free rate is the expected stock market return according to the risk-neutral density, $R^f_{t,t+T} = \mathbb{E}^{RND}_t[R_{t,t+T}]$. Panel B reports correlations between the risk-neutral variance bound for expected returns and the option-based expected returns from the different pricing kernels. The pricing kernels are classified according to the their exponents: $\gamma_1 r$ (equation (1)), $\gamma_1 nvix^{\gamma_3} r$ (equation (2)), $\gamma_1 r + \gamma_2 r^2$ (equation (4)), and $\gamma_1 nvix^{\gamma_3} r + \gamma_2 nvix^{\gamma_3} r^2$ (equation (6)), where r denotes log returns, and $nvix$ is the normalized VIX, which is the VIX divided by its 1986-1995 average (to avoid look-ahead bias) and appropriately scaled for each expiration. The estimation of the various pricing kernels is based on the GMM system of equation (13), and the results are reported in Table 2 through Table 5. *risk-neutral* denotes the moments of the risk-neutral density. Option-based physical and risk-neutral moments are derived according to equation (14). The sample is from January 1996 to December 2022 for 1-month expiration options, May 1998 to November 2022 for 2-month expiration, January 2002 to October 2022 for 3-month expiration, and June 1996 to June 2022 for 6-month expiration options.

Panel A: Risk-neutral bound for expected returns

$R^f_{t,t+T} + \frac{var^{RND}(R_{t,t+T})}{R^f_{t,t+T}} - 1$	1-month	2-month	3-month	6-month
mean	0.45%	1.05%	1.37%	3.12%
st. deviation	0.64%	1.28%	1.26%	1.77%
N	323	147	83	52

Panel B: Correlations of risk-neutral bound for expected returns with option-based expected returns

1-month expiration

	$\gamma_1 r$	$\gamma_1 nvix^{\gamma_3} r$	$\gamma_1 r + \gamma_2 r^2$	$\gamma_1 nvix^{\gamma_3} r + \gamma_2 nvix^{\gamma_3} r^2$	risk-neutral
$R^f_{t,t+T} + \frac{var^{RND}(R_{t,t+T})}{R^f_{t,t+T}}$	0.99	0.81	0.96	-0.33	0.42

2-month expiration

	$\gamma_1 r$	$\gamma_1 nvix^{\gamma_3} r$	$\gamma_1 r + \gamma_2 r^2$	$\gamma_1 nvix^{\gamma_3} r + \gamma_2 nvix^{\gamma_3} r^2$	risk-neutral
$R^f_{t,t+T} + \frac{var^{RND}(R_{t,t+T})}{R^f_{t,t+T}}$	0.99	0.97	0.87	-0.17	0.49

3-month expiration

	$\gamma_1 r$	$\gamma_1 nvix^{\gamma_3} r$	$\gamma_1 r + \gamma_2 r^2$	$\gamma_1 nvix^{\gamma_3} r + \gamma_2 nvix^{\gamma_3} r^2$	risk-neutral
$R^f_{t,t+T} + \frac{var^{RND}(R_{t,t+T})}{R^f_{t,t+T}}$	0.99	0.96	0.99	-0.20	0.63

6-month expiration

	$\gamma_1 r$	$\gamma_1 nvix^{\gamma_3} r$	$\gamma_1 r + \gamma_2 r^2$	$\gamma_1 nvix^{\gamma_3} r + \gamma_2 nvix^{\gamma_3} r^2$	risk-neutral
$R^f_{t,t+T} + \frac{var^{RND}(R_{t,t+T})}{R^f_{t,t+T}}$	0.98	0.95	0.99	0.09	0.53

Table 11 Regressions of Risk-Neutral Variances as a Binding Lower Bound for Option-based Expected Returns Across Pricing Kernels

This table reports regression results for equation (26), which examines whether the risk-neutral variance lower bound for risk premia from equation (23) is binding across the different pricing kernels. $var_t^{RND}(R_{t,t+T})$ is the risk-neutral variance and $R^f_{t,t+T}$ is the risk-free rate, which is measured by the mean of stock market returns under the risk-neutral distribution, $R^f_{t,t+T} = \mathbb{E}_t^{RND}[R_{t,t+T}]$. Panel A reports regression results for realized excess returns as the dependent variable, $R^e_{t,t+T} = R_{t,t+T} - R^f_{t,t+T}$, and Panel B shows results for backward-looking fitted excess return, $\widehat{R}^e_{t,t+T} = \widehat{R}_{t,t+T} - R^f_{t,t+T}$ as the dependent variable. Backward-looking fitted S&P500 returns, $\widehat{R}_{t,t+T}$, are fitted values from regressing realized returns on the price-dividend ratio, the dividend growth, and the risk-free rate. These regressions are reported in Table A.1 of the Appendix. Panels C and D report results where the dependent variable is the forward-looking option-based risk premium, $\mathbb{E}_t[R^e_{t,t+T}] = \mathbb{E}_t[R_{t,t+T}] - R^f_{t,t+T}$, according to the monotonic pricing kernels from equations (1), (2), (4), and (6). Panels E and F report results where the dependent variable is the forward-looking option-based risk premium based on the non-monotonic pricing kernels from equations (4) and (6). Option-based expected returns, $\mathbb{E}_t[R_{t,t+T}]$, are derived according to equation (14). The pricing kernels are classified according to the their exponents: $\gamma_1 r$ (equation (1)), $\gamma_1 nvix^{\gamma_3} r$ (equation (2)), $\gamma_1 r + \gamma_2 r^2$ (equation (4)), and $\gamma_1 nvix^{\gamma_3} r + \gamma_2 nvix^{\gamma_3} r^2$ (equation (6)), where r denotes log returns, and $nvix$ is the normalized VIX, which is the VIX divided by its 1986-1995 average (to avoid look-ahead bias) and appropriately scaled for each expiration. *risk-neutral* denotes the moments of the risk-neutral density. The estimation of the various pricing kernels is based on the GMM system of equation (13), and the results are reported in Table 2 through Table 5. All variables are contemporaneous, and all regressions are for non-overlapping intervals. t-statistics in parentheses are corrected for heteroscedasticity and autocorrelation using Newey-West standard errors with 12, 6, 4, and 2 lags for the 1-, 2-, 3-, and 6-month expirations, respectively. N is the number of observations. The sample is from January 1996 to December 2022 for 1-month expiration options, May 1998 to November 2022 for 2-month expiration, January 2002 to October 2022 for 3-month expiration, and June 1996 to June 2022 for 6-month expiration options.

Panel A: Realized returns

$R^e_{t,t+T}$	1-month	2-month	3-month	6-month
$\frac{var_t^{RND}(R_{t,t+T})}{R^f_{t,t+T}}$	1.763	1.106	0.280	1.196
	(2.06)	(1.39)	(0.25)	(1.82)
	{0.89}	{0.13}	{-0.66}	{0.30}
constant	-0.207%	0.120%	1.202%	0.604%
	(-0.47)	(0.14)	(1.06)	(0.28)
R^2	4.63%	3.18%	0.13%	2.88%
N	323	147	83	52

Panel B: Backward-looking fitted returns

$\widehat{R}^e_{t,t+T}$	1-month	2-month	3-month	6-month
$\frac{var_t^{RND}(R_{t,t+T})}{R^f_{t,t+T}}$	0.532	0.409	0.625	1.011
	(4.73)	(2.89)	(2.87)	(2.87)
	{-4.15}	{-4.16}	{-1.71}	{0.03}
constant	0.410%	0.823%	0.792%	0.653%
	(2.65)	(2.83)	(1.32)	(0.57)
R^2	12.38%	10.33%	10.77%	14.68%
N	321	146	82	50

Panel C: Option-based risk premia from pricing kernel in equation (1) ***($\gamma_1 r$)***

$\mathbb{E}_t[R^e_{t,t+T}]$	1-month	2-month	3-month	6-month
$\frac{var_t^{RND}(R_{t,t+T})}{R^f_{t,t+T}}$	1.282	1.195	1.219	1.371
	(172.37)	(141.76)	(204.61)	(247.90)
	{37.98}	{23.19}	{36.83}	{67.13}
constant	0.014%	0.033%	0.026%	0.148%
	(4.96)	(4.78)	(5.36)	(7.23)
R^2	99.96%	99.96%	99.94%	99.85%
N	323	147	83	52

Panel D: Option-based risk premia from pricing kernel in equation (2) ***($\gamma_1 nvix^{\gamma_3} r$)***

$\mathbb{E}_t[R^e_{t,t+T}]$	1-month	2-month	3-month	6-month
$\frac{var_t^{RND}(R_{t,t+T})}{R^f_{t,t+T}}$	3.993	0.725	0.623	0.735
	(7.34)	(23.09)	(10.94)	(16.41)
	{5.50}	{-8.75}	{-6.61}	{-5.91}
constant	-1.348%	0.517%	0.769%	1.834%
	(-4.80)	(12.33)	(10.59)	(13.44)
R^2	84.26%	96.84%	89.61%	89.11%
N	323	147	83	52

Panel E: Option-based risk premia from pricing kernel in equation (4) ***($\gamma_1 r + \gamma_2 r^2$)***

$\mathbb{E}_t[R^e_{t,t+T}]$	1-month	2-month	3-month	6-month
$\frac{var_t^{RND}(R_{t,t+T})}{R^f_{t,t+T}}$	1.192	0.773	1.146	1.257
	(16.20)	(2.66)	(26.41)	(43.10)
	{2.61}	{-0.78}	{3.38}	{8.81}
constant	0.084%	0.467%	0.110%	0.442%
	(2.30)	(1.83)	(3.04)	(6.62)
R^2	95.41%	69.95%	97.93%	97.26%
N	323	147	83	52

Panel F: Option-based risk premia from pricing kernel in equation (6) ***($\gamma_1 nvix^{\gamma_3} r + \gamma_2 nvix^{\gamma_3} r^2$)***

$\mathbb{E}_t[R^e_{t,t+T}]$	1-month	2-month	3-month	6-month
$\frac{var_t^{RND}(R_{t,t+T})}{R^f_{t,t+T}}$	-0.276	-0.271	-0.582	-0.081
	(-4.53)	(-3.66)	(-4.17)	(-1.08)
	{-20.92}	{-17.16}	{-11.34}	{-14.45}
constant	0.835%	1.557%	2.289%	4.009%
	(11.47)	(11.23)	(7.39)	(11.15)
R^2	16.20%	18.76%	25.08%	1.25%
N	323	147	83	52

Table 12 Violations of Risk-Neutral Lower Bounds for Option-based Expected Returns Across Pricing Kernels

This table reports how often realized returns and option-based risk-premia are lower than the risk-neutral variance lower bound from equation (23) Panel A reports the frequency of violations of the risk-neutral lower bound for the 1-month expiration. Panel B reports the frequency of violations for the 2-month expiration, Panel C shows the frequency of violations for the 3-month expiration, and Panel D for the 6-month expiration. We calculate the frequency of the lower bound violations for alternative measures of realized and expected returns. $R^e_{t,t+T} = R_{t,t+T} - R^f_{t,t+T}$ are excess returns. $\widehat{R}^e_{t,t+T} = \widehat{R}_{t,t+T} - R^f_{t,t+T}$ are backward-looking fitted excess return from regressing realized returns on the price-dividend ratio, the dividend growth, and the risk-free rate. These regressions are reported in Table A.1 of the Appendix. Option-based risk premia, $\mathbb{E}_t[R^e_{t,t+T}] = \mathbb{E}_t[R_{t,t+T}] - R^f_{t,t+T}$, are according to the pricing kernels from equations (1), (2), (4), and (6). The pricing kernels are classified based on the their exponents: $\gamma_1 r$ (equation (1)), $\gamma_1 nvix^{\gamma_3} r$ (equation (2)), $\gamma_1 r + \gamma_2 r^2$ (equation (4)), and $\gamma_1 nvix^{\gamma_3} r + \gamma_2 nvix^{\gamma_3} r^2$ (equation (6)), where r denotes log returns, and $nvix$ is the normalized VIX, which is the VIX divided by its 1986-1995 average (to avoid look-ahead bias) and appropriately scaled for each expiration. Estimation of the various pricing kernels is based on the GMM system of equation (13), and the results are reported in Table 2 through Table 5. Option-based physical moments are derived according to equation (14). N is the number of observations. In these tests, the risk-free rate for calculating risk premia is the expected stock market return according to the risk-neutral distribution, $R^f_{t,t+T} = \mathbb{E}^{RND}_t[R_{t,t+T}]$. The number in brackets are the average absolute differences between the alternative measures of excess returns and the risk-neutral variance bound. The sample is from January 1996 to December 2022 for 1-month expiration options, May 1998 to November 2022 for 2-month expiration, January 2002 to October 2022 for 3-month expiration, and June 1996 to June 2022 for 6-month expiration options.

Panel A: Violations of risk-neutral lower bounds for expected returns, 1-month expiration

$R^e_{t,T+T}$	$\widehat{R}^e_{t,T+T}$	$\mathbb{E}_t[R^e_{t,t+T}]$ $\gamma_1 r$	$\mathbb{E}_t[R^e_{t,t+T}]$ $\gamma_1 nvix^{\gamma_3} r$	$\mathbb{E}_t[R^e_{t,t+T}]$ $\gamma_1 r + \gamma_2 r^2$	$\mathbb{E}_t[R^e_{t,t+T}]$ $\gamma_1 nvix^{\gamma_3} r + \gamma_2 nvix^{\gamma_3} r^2$	N
41% [3.41%]	36% [0.76%]	0% [0.15%]	83% [0.41%]	5% [0.18%]	45% [0.54%]	323

Panel B: Violations of risk-neutral lower bounds for expected returns, 2-month expiration

$R^e_{t,T+T}$	$\widehat{R}^e_{t,T+T}$	$\mathbb{E}_t[R^e_{t,t+T}]$ $\gamma_1 r$	$\mathbb{E}_t[R^e_{t,t+T}]$ $\gamma_1 nvix^{\gamma_3} r$	$\mathbb{E}_t[R^e_{t,t+T}]$ $\gamma_1 r + \gamma_2 r^2$	$\mathbb{E}_t[R^e_{t,t+T}]$ $\gamma_1 nvix^{\gamma_3} r + \gamma_2 nvix^{\gamma_3} r^2$	N
40% [4.93%]	36% [1.26%]	0% [0.23%]	5% [0.31%]	1% [0.32%]	41% [0.96%]	147

Panel C: Violations of risk-neutral lower bounds for expected returns, 3-month expiration

$R^e_{t,T+T}$	$\widehat{R}^e_{t,T+T}$	$\mathbb{E}_t[R^e_{t,t+T}]$ $\gamma_1 r$	$\mathbb{E}_t[R^e_{t,t+T}]$ $\gamma_1 nvix^{\gamma_3} r$	$\mathbb{E}_t[R^e_{t,t+T}]$ $\gamma_1 r + \gamma_2 r^2$	$\mathbb{E}_t[R^e_{t,t+T}]$ $\gamma_1 nvix^{\gamma_3} r + \gamma_2 nvix^{\gamma_3} r^2$	N
40% [5.83%]	40% [1.64%]	0% [0.30%]	8% [0.43%]	1% [0.29%]	53% [1.44%]	83

Panel D: Violations of risk-neutral lower bounds for expected returns, 6-month expiration

$R^e_{t,T+T}$	$\widehat{R}^e_{t,T+T}$	$\mathbb{E}_t[R^e_{t,t+T}]$ $\gamma_1 r$	$\mathbb{E}_t[R^e_{t,t+T}]$ $\gamma_1 nvix^{\gamma_3} r$	$\mathbb{E}_t[R^e_{t,t+T}]$ $\gamma_1 r + \gamma_2 r^2$	$\mathbb{E}_t[R^e_{t,t+T}]$ $\gamma_1 nvix^{\gamma_3} r + \gamma_2 nvix^{\gamma_3} r^2$	N
36% [8.42%]	36% [3.15%]	0% [1.13%]	4% [1.19%]	0% [1.13%]	42% [2.10%]	52

Appendix

Appendix A Supplemental Figures

Figure A.1 Risk-neutral Density Functions

This figure shows the average risk-neutral density function across the different expirations with and without tail adjustment. The tail adjustment is done by appending a type-I (two-parameter) Pareto distribution to the tails of the risk-neutral distribution (equation (15)). The two parameters of the left-tail (right-tail) Pareto distribution are identified by matching the Pareto distribution to the empirical risk-neutral distributions at the 2% (98%) and 5% (95%). Details on the derivation of the risk-neutral distribution can be found in Section 3.2. For these plots, we average, across dates, the risk-neutral density functions (with and without tail adjustments) for each expiration. The sample is from January 1996 to December 2022 for 1-month expiration options, May 1998 to November 2022 for 2-month expiration, January 2002 to October 2022 for 3-month expiration, and June 1996 to June 2022 for 6-month expiration options.

Panel A: One-month expiration

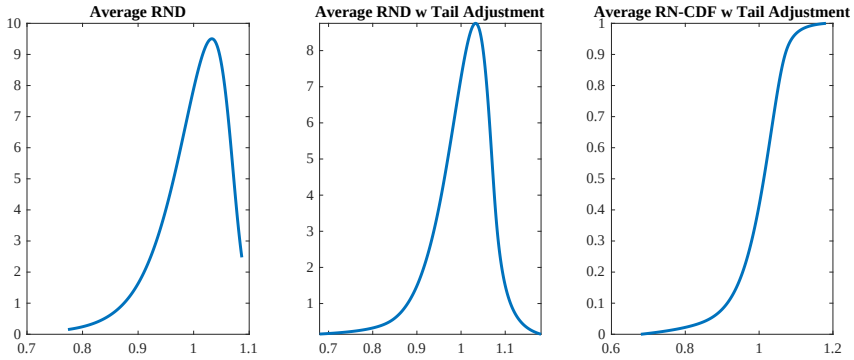

Panel B: Two-month expiration

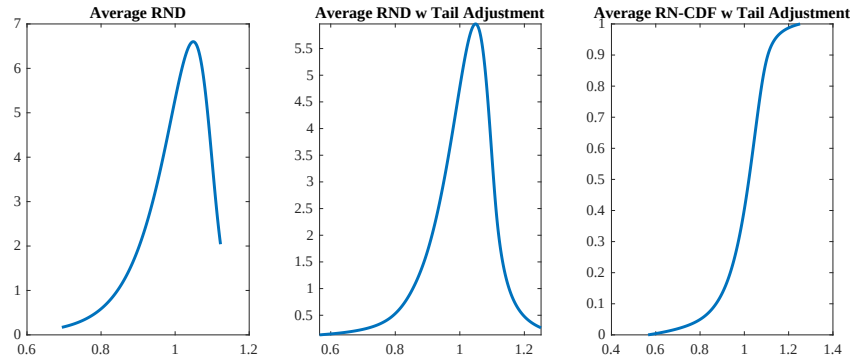

Panel C: Three-month expiration

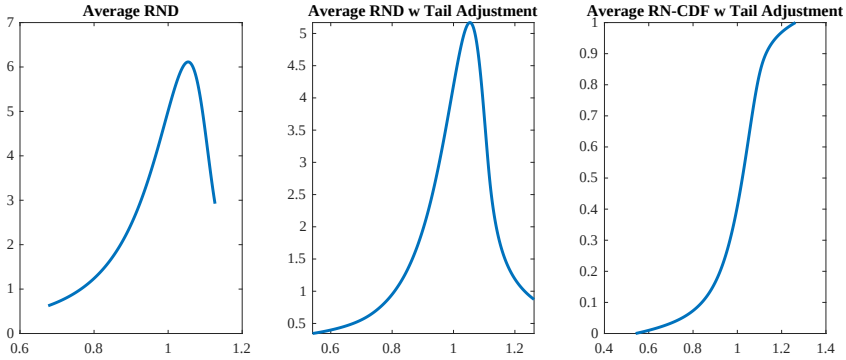

Panel D: Six-month expiration

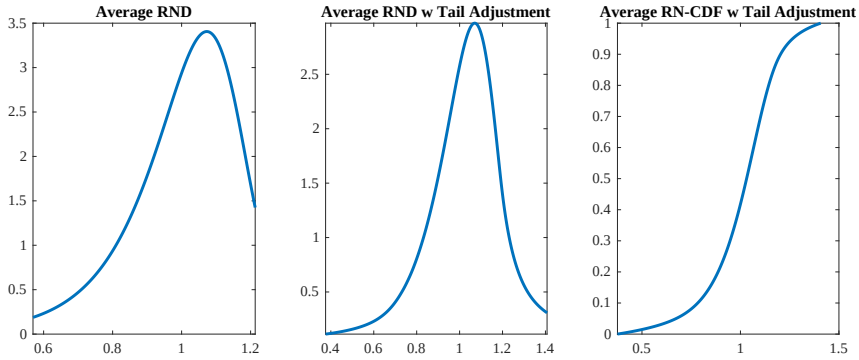

Appendix B Supplemental Tables

Table A.1 Backward-looking Fitted Returns

Panel A of this table reports four sets of regression results for the backward-looking fitted returns of the S&P500. Fitted returns, $\widehat{R}_{t,t+T} - 1$, are derived by regressing realized returns, $R_{t,t+T} - 1$, on the dividend-yield, $divp_t$, the lagged dividend growth, $\Delta div_{t-T,t}$, and the risk-free rate, $R^f_{t,t+T}$. Realized returns, dividends, and dividend yield are from the CRSP S&P Index files. The risk-free rate is the mean of the option-based RND ($\mathbb{E}^{RND}_t[R_{t,t+T} - 1]$). t-statistics in parentheses are corrected for heteroscedasticity and autocorrelation using Newey-West standard errors with 12, 6, 4, and 2 lags for the 1-, 2-, 3-, and 6-month expirations, respectively. All regressions are for non-overlapping intervals. Panel B reports summary statistics for realized and backward-looking fitted returns. Panel C reports correlations of realized and backward-looking returns with option-based expected returns according to the various pricing kernels. Option-based expected returns are classified according to the thee exponent of the corresponding discount factor: $\gamma_1 r$ (equation (1)), $\gamma_1 nvix^{\gamma_3} r$ (equation (2)), $\gamma_1 r + \gamma_2 r^2$ (equation (4)), and $\gamma_1 nvix^{\gamma_3} r + \gamma_2 nvix^{\gamma_3} r^2$ (equation (6)), where r denotes log returns, and $nvix$ is the normalized VIX, which is the VIX divided by its 1986-1995 average (to avoid look-ahead bias) and appropriately scaled for each expiration. The estimation of the various pricing kernels is based on the GMM system of equation (13), and the results are reported in Table 2 through Table 5. *risk-neutral* denotes the moments of the risk-neutral density. Option-based physical and risk-neutral moments are derived according to equation (14). *risk-neutral bound* is the expected returns according to Martin (2017) variance-based lower bound from equation (23). ρ^* is the correlation between realized and backward-looking fitted returns. The sample is from January 1996 to December 2022 for 1-month expiration, May 1998 to November 2022 for 2-month expiration, January 2002 to October 2022 for 3-month expiration, and December 1996 to June 2022 for 6-month expiration.

Panel A: Regressions for backward-looking expected returns

$R_{t,t+T}$	1-month	2-month	3-month	6-month
$divp_t$	12.954	16.092	10.930	14.037
	(1.56)	(1.24)	(0.84)	(1.22)
$\Delta div_{t-T,t}$	-0.011	-0.018	0.029	-0.028
	(-1.15)	(-0.57)	(0.28)	(-0.25)
$R^f_{t,t+T}$	-0.520	0.314	-0.719	-0.359
	(-0.66)	(0.35)	(-0.82)	(-0.21)
constant	-1.376%	-3.797%	-3.755%	-9.082%
	(-1.13)	(-0.97)	(-0.59)	(-0.84)
R^2	1.45%	2.25%	3.20%	8.59%
N	321	146	82	50

Panel B: Summary statistics for realized and backward-looking expected returns

i) $R_{t,t+T}$	1-month	2-month	3-month	6-month
mean	0.63%	1.28%	1.66%	4.25%
st. deviation	4.88%	7.01%	7.41%	10.72%
N	323	147	83	52

ii) $\widehat{R}_{t,t+T}$	1-month	2-month	3-month	6-month
mean	0.62%	1.24%	1.67%	3.78%
st. deviation	0.59%	1.05%	1.33%	3.11%
N	321	146	82	50

Panel C: Correlations of realized and backward-looking expected returns with option-based expected returns

1-month expiration

	$\gamma_1 r$ $\mathbb{E}_t[R_{t,t+T}]$	$\gamma_1 nvix^{\gamma_3} r$ $\mathbb{E}_t[R_{t,t+T}]$	$\gamma_1 r + \gamma_2 r^2$ $\mathbb{E}_t[R_{t,t+T}]$	$\gamma_1 nvix^{\gamma_3} r + \gamma_2 nvix^{\gamma_3} r^2$ $\mathbb{E}_t[R_{t,t+T}]$	risk-neutral $\mathbb{E}_t^{RND}[R_{t,t+T}]$	risk-neutral bound $R^f_{t,t+T} + \frac{var_t^{RND}(R_{t,t+T})}{R^f_{t,t+T}}$	ρ^*
$R_{t,t+T}$	0.15	0.20	0.14	-0.17	-0.06	0.14	
$\widehat{R}_{t,t+T}$	0.01	0.27	0.01	-0.41	-0.56	-0.07	0.12

2-month expiration

	$\gamma_1 r$ $\mathbb{E}_t[R_{t,t+T}]$	$\gamma_1 nvix^{\gamma_3} r$ $\mathbb{E}_t[R_{t,t+T}]$	$\gamma_1 r + \gamma_2 r^2$ $\mathbb{E}_t[R_{t,t+T}]$	$\gamma_1 nvix^{\gamma_3} r + \gamma_2 nvix^{\gamma_3} r^2$ $\mathbb{E}_t[R_{t,t+T}]$	risk-neutral $\mathbb{E}_t^{RND}[R_{t,t+T}]$	risk-neutral bound $r^{f*}_{t,t+T} + \frac{var_t^{RND}(R_{t,t+T})}{R^{f*}_{t,t+T}}$	ρ^*
$R_{t,t+T}$	0.14	0.10	0.04	-0.10	-0.01	0.13	
$\widehat{R}_{t,t+T}$	0.17	0.04	0.10	-0.24	-0.15	0.14	0.15

3-month expiration

	$\gamma_1 r$ $\mathbb{E}_t[R_{t,t+T}]$	$\gamma_1 nvix^{\gamma_3} r$ $\mathbb{E}_t[R_{t,t+T}]$	$\gamma_1 r + \gamma_2 r^2$ $\mathbb{E}_t[R_{t,t+T}]$	$\gamma_1 nvix^{\gamma_3} r + \gamma_2 nvix^{\gamma_3} r^2$ $\mathbb{E}_t[R_{t,t+T}]$	risk-neutral $\mathbb{E}_t^{RND}[R_{t,t+T}]$	risk-neutral bound $r^{f*}_{t,t+T} + \frac{var_t^{RND}(R_{t,t+T})}{R^{f*}_{t,t+T}}$	ρ^*
$R_{t,t+T}$	-0.05	-0.09	-0.05	-0.13	-0.10	-0.06	
$\widehat{R}_{t,t+T}$	-0.09	-0.31	-0.10	-0.26	-0.53	-0.15	0.18

6-month expiration

	$\gamma_1 r$ $\mathbb{E}_t[R_{t,t+T}]$	$\gamma_1 nvix^{\gamma_3} r$ $\mathbb{E}_t[R_{t,t+T}]$	$\gamma_1 r + \gamma_2 r^2$ $\mathbb{E}_t[R_{t,t+T}]$	$\gamma_1 nvix^{\gamma_3} r + \gamma_2 nvix^{\gamma_3} r^2$ $\mathbb{E}_t[R_{t,t+T}]$	risk-neutral $\mathbb{E}_t^{RND}[R_{t,t+T}]$	risk-neutral bound $r^{f*}_{t,t+T} + \frac{var_t^{RND}(R_{t,t+T})}{R^{f*}_{t,t+T}}$	ρ^*
$R_{t,t+T}$	0.05	-0.05	0.02	-0.17	-0.11	0.02	
$\widehat{R}_{t,t+T}$	-0.02	-0.26	-0.08	-0.40	-0.62	-0.14	0.29

Table A.2 Summary Statistics of Option-based Log-return Moments for the Physical Measure Across Pricing Kernels

This table reports summary statistics for the option-based moments of log-returns under the physical measure across the different pricing kernels from equations (1), (2), (4), and (6). The pricing kernels are classified based on the their exponents: $\gamma_1 r$ (equation (1)), $\gamma_1 nvix^{\gamma_3} r$ (equation (2)), $\gamma_1 r + \gamma_2 r^2$ (equation (4)), and $\gamma_1 nvix^{\gamma_3} r + \gamma_2 nvix^{\gamma_3} r^2$ (equation (6)), where r denotes log returns, and $nvix$ is the normalized VIX, which is the VIX divided by its 1986-1995 average (to avoid look-ahead bias) and scaled appropriately for each expiration. The estimation of the various pricing kernels is based on the GMM system of equation (13), and the results are reported in Table 2 through Table 5. *risk-neutral* denotes the moments of the risk-neutral density. *realized* denotes the moments of the distribution of the realized returns in the sample fro each expiration. Option-based physical and risk-neutral moments for log-returns are derived according to equation (14). Panel A reports summary statistics for option-based expected returns. Panel B reports statistics for option-based variances. Panel C reports summary statistics for option-based skewness, and in Panel D for option-based kurtosis. The sample is from January 1996 to December 2022 for 1-month expiration options, May 1998 to November 2022 for 2-month expiration, January 2002 to October 2022 for 3-month expiration, and June 1996 to June 2022 for 6-month expiration options.

Panel A: Option-based expected log-returns across pricing kernels

i) $\gamma_1 r$	1-month	2-month	3-month	6-month
mean	0.38%	0.83%	1.13%	3.14%
st. deviation	0.58%	1.11%	1.12%	1.71%
N	323	147	83	52

ii) $\gamma_1 nvix^{\gamma_3} r$	1-month	2-month	3-month	6-month
mean	0.38%	0.82%	1.11%	3.12%
st. deviation	2.19%	0.80%	0.78%	1.19%
N	323	147	83	52

iii) $\gamma_1 r + \gamma_2 r^2$	1-month	2-month	3-month	6-month
mean	0.45%	0.49%	1.04%	2.88%
st. deviation	0.57%	4.26%	1.13%	1.70%
N	323	147	83	52

iv) $\gamma_1 nvix^{\gamma_3} r + \gamma_2 nvix^{\gamma_3} r^2$	1-month	2-month	3-month	6-month
mean	0.43%	0.86%	1.13%	3.49%
st. deviation	0.74%	1.49%	1.69%	1.65%
N	323	147	83	52

v) risk-neutral	1-month	2-month	3-month	6-month
mean	-0.36%	-0.64%	-0.68%	-1.24%
st. deviation	0.67%	1.42%	1.32%	2.13%
N	323	147	83	52

vi) realized mean	1-month	2-month	3-month	6-month
	0.51%	1.01%	1.37%	3.60%

Panel B: Option-based physical variances of log-returns across pricing kernels

i) $\gamma_1 r$	1-month	2-month	3-month	6-month
mean	0.47%	0.94%	1.13%	2.19%
st. deviation	0.51%	0.90%	0.82%	1.08%
N	323	147	83	52

ii) $\gamma_1 nvix^{\gamma_3} r$	1-month	2-month	3-month	6-month
mean	0.47%	0.98%	1.17%	2.25%
st. deviation	0.32%	1.27%	1.08%	1.55%
N	323	147	83	52

iii) $\gamma_1 r + \gamma_2 r^2$	1-month	2-month	3-month	6-month
mean	0.36%	3.38%	1.37%	3.02%
st. deviation	0.28%	29.63%	1.29%	2.78%
N	323	147	83	52

iv) $\gamma_1 nvix^{\gamma_3} r + \gamma_2 nvix^{\gamma_3} r^2$	1-month	2-month	3-month	6-month
mean	0.44%	0.96%	1.15%	1.41%
st. deviation	0.95%	2.67%	1.78%	1.81%
N	323	147	83	52

v) risk-neutral	1-month	2-month	3-month	6-month
mean	0.64%	1.51%	1.79%	3.96%
st. deviation	0.94%	2.67%	1.74%	3.16%
N	323	147	83	52

vi) realized variance	1-month	2-month	3-month	6-month
	0.25%	0.56%	0.58%	1.19%

Panel C: Option-based physical skewness of log-returns across pricing kernels

i) $\gamma_1 r$	1-month	2-month	3-month	6-month
mean	-1.90	-2.06	-2.07	-1.64
st. deviation	0.96	1.03	1.02	0.54
N	323	147	83	52

ii) $\gamma_1 nvix^{\gamma_3} r$	1-month	2-month	3-month	6-month
mean	-1.90	-2.05	-2.05	-1.59
st. deviation	0.96	1.02	0.99	0.48
N	323	147	83	52

iii) $\gamma_1 r + \gamma_2 r^2$	1-month	2-month	3-month	6-month
mean	-1.54	-2.13	-2.32	-2.18
st. deviation	0.71	1.13	1.36	1.22
N	323	147	83	52

iv) $\gamma_1 nvix^{\gamma_3} r + \gamma_2 nvix^{\gamma_3} r^2$	1-month	2-month	3-month	6-month
mean	-0.86	-0.87	-1.02	-0.54
st. deviation	0.70	0.69	0.93	0.37
N	323	147	83	52

v) risk-neutral	1-month	2-month	3-month	6-month
mean	-1.96	-2.17	-2.21	-2.02
st. deviation	0.93	1.09	1.15	0.92
N	323	147	83	52

vi) realized skewness	1-month	2-month	3-month	6-month
	-1.78	-2.39	-1.44	-1.37

Panel D: Option-based physical kurtosis of log-returns across pricing kernels

i) $\gamma_1 r$	1-month	2-month	3-month	6-month
mean	10.96	12.71	12.97	9.85
st. deviation	7.33	9.34	9.53	4.97
N	323	147	83	52

ii) $\gamma_1 nvix^{\gamma_3} r$	1-month	2-month	3-month	6-month
mean	10.48	12.84	13.04	9.59
st. deviation	6.69	9.44	9.48	4.60
N	323	147	83	52

iii) $\gamma_1 r + \gamma_2 r^2$	1-month	2-month	3-month	6-month
mean	8.81	13.36	14.85	13.86
st. deviation	4.80	10.88	12.85	11.53
N	323	147	83	52

iv) $\gamma_1 nvix^{\gamma_3} r + \gamma_2 nvix^{\gamma_3} r^2$	1-month	2-month	3-month	6-month
mean	5.54	5.56	6.41	3.97
st. deviation	3.35	3.59	5.57	1.18
N	323	147	83	52

v) risk-neutral	1-month	2-month	3-month	6-month
mean	10.17	11.73	11.99	10.49
st. deviation	6.01	7.96	8.41	6.63
N	323	147	83	52

vi) realized kurtosis	1-month	2-month	3-month	6-month
	11.72	13.89	5.76	6.26

Table A.3 Coefficient of Determination for Log-return Moments under the Physical Measure across Pricing Kernels

This table reports coefficients of determination (R^2) from regressing the corresponding option-based moments for log-returns across the different pricing kernels from equations (1), (2), (4), and (6). Option-based physical moments for log-returns are derived according to equation (14). The pricing kernels are classified according to the their exponents: $\gamma_1 r$ (equation (1)), $\gamma_1 nvix^{\gamma_3} r$ (equation (2)), $\gamma_1 r + \gamma_2 r^2$ (equation (4)), and $\gamma_1 nvix^{\gamma_3} r + \gamma_2 nvix^{\gamma_3} r^2$ (equation (6)), where r denotes log returns, and $nvix$ is the normalized VIX, which is the VIX divided by its 1986-1995 average (to avoid look-ahead bias) and appropriately scaled for each expiration. The estimation of the various pricing kernels is based on the GMM system of equation (13), and the results are reported in Table 2 through Table 5. *risk-neutral* denotes the moments of the risk-neutral density. Panel A reports R^2's for option-based moment regressions for the 1-month expiration. Panel B reports R^2's for option-based moment regressions for the 2-month expiration. Panel C reports R^2's for the 3-month expiration, and Panel D shows R^2's for the 6-month expiration. N is the number of observations. The sample is from January 1996 to December 2022 for 1-month expiration options, May 1998 to November 2022 for 2-month expiration, January 2002 to October 2022 for 3-month expiration, and June 1996 to June 2022 for 6-month expiration options.

Panel A: 1-month expiration

R^2's of option-based expected log-returns regressions (average R^2 = 43.80%; excl. risk-neutral: 57.19%)

	$\gamma_1 r$	$\gamma_1 nvix^{\gamma_3} r$	$\gamma_1 r + \gamma_2 r^2$	$\gamma_1 nvix^{\gamma_3} r + \gamma_2 nvix^{\gamma_3} r^2$
$\gamma_1 nvix^{\gamma_3} r$	62.28%			
$\gamma_1 r + \gamma_2 r^2$	91.20%	59.22%		
$\gamma_1 nvix^{\gamma_3} r + \gamma_2 nvix^{\gamma_3} r^2$	31.42%	53.89%	45.17%	
risk-neutral	0.47%	26.34%	6.63%	61.46%

R^2's of option-based log-return variances regressions (average R^2 = 83.53%; excl. risk-neutral: 82.55%)

	$\gamma_1 r$	$\gamma_1 nvix^{\gamma_3} r$	$\gamma_1 r + \gamma_2 r^2$	$\gamma_1 nvix^{\gamma_3} r + \gamma_2 nvix^{\gamma_3} r^2$
$\gamma_1 nvix^{\gamma_3} r$	79.10%			
$\gamma_1 r + \gamma_2 r^2$	94.38%	82.69%		
$\gamma_1 nvix^{\gamma_3} r + \gamma_2 nvix^{\gamma_3} r^2$	94.05%	59.08%	86.04%	
risk-neutral	95.10%	65.74%	82.55%	96.60%

R^2's of option-based log-return skewness regressions (average R^2 = 53.54%; excl. risk-neutral: 43.85%)

	$\gamma_1 r$	$\gamma_1 nvix^{\gamma_3} r$	$\gamma_1 r + \gamma_2 r^2$	$\gamma_1 nvix^{\gamma_3} r + \gamma_2 nvix^{\gamma_3} r^2$
$\gamma_1 nvix^{\gamma_3} r$	97.35%			
$\gamma_1 r + \gamma_2 r^2$	75.55%	77.83%		
$\gamma_1 nvix^{\gamma_3} r + \gamma_2 nvix^{\gamma_3} r^2$	5.34%	3.27%	3.77%	
risk-neutral	99.02%	95.08%	69.86%	8.41%

R^2's of option-based log-return kurtosis regressions (average R^2 = 55.35%; excl. risk-neutral: 44.85%)

	$\gamma_1 r$	$\gamma_1 nvix^{\gamma_3} r$	$\gamma_1 r + \gamma_2 r^2$	$\gamma_1 nvix^{\gamma_3} r + \gamma_2 nvix^{\gamma_3} r^2$
$\gamma_1 nvix^{\gamma_3} r$	98.72%			
$\gamma_1 r + \gamma_2 r^2$	72.28%	70.96%		
$\gamma_1 nvix^{\gamma_3} r + \gamma_2 nvix^{\gamma_3} r^2$	12.69%	13.63%	0.87%	
risk-neutral	99.13%	98.08%	73.78%	13.41%

Panel B: 2-month expiration

R^2's of option-based expected log-returns regressions (average R^2 = 27.22%; excl. risk-neutral: 22.28%)

	$\gamma_1 r$	$\gamma_1 nvix^{\gamma_3} r$	$\gamma_1 r + \gamma_2 r^2$	$\gamma_1 nvix^{\gamma_3} r + \gamma_2 nvix^{\gamma_3} r^2$
$\gamma_1 nvix^{\gamma_3} r$	65.82%			
$\gamma_1 r + \gamma_2 r^2$	4.27%	5.69%		
$\gamma_1 nvix^{\gamma_3} r + \gamma_2 nvix^{\gamma_3} r^2$	22.76%	0.58%	34.53%	
risk-neutral	0.14%	26.95%	41.93%	69.55%

R^2's of option-based log-return variances regressions (average R^2 = 79.83%; excl. risk-neutral: 74.92%)

	$\gamma_1 r$	$\gamma_1 nvix^{\gamma_3} r$	$\gamma_1 r + \gamma_2 r^2$	$\gamma_1 nvix^{\gamma_3} r + \gamma_2 nvix^{\gamma_3} r^2$
$\gamma_1 nvix^{\gamma_3} r$	97.23%			
$\gamma_1 r + \gamma_2 r^2$	41.64%	55.75%		
$\gamma_1 nvix^{\gamma_3} r + \gamma_2 nvix^{\gamma_3} r^2$	85.57%	94.90%	74.44%	
risk-neutral	87.12%	94.35%	71.90%	95.39%

R^2's of option-based log-return skewness regressions (average R^2 = 61.95%; excl. risk-neutral: 52.58%)

	$\gamma_1 r$	$\gamma_1 nvix^{\gamma_3} r$	$\gamma_1 r + \gamma_2 r^2$	$\gamma_1 nvix^{\gamma_3} r + \gamma_2 nvix^{\gamma_3} r^2$
$\gamma_1 nvix^{\gamma_3} r$	99.52%			
$\gamma_1 r + \gamma_2 r^2$	97.99%	98.82%		
$\gamma_1 nvix^{\gamma_3} r + \gamma_2 nvix^{\gamma_3} r^2$	4.34%	6.58%	8.25%	
risk-neutral	96.74%	98.16%	99.11%	10.02%

R^2's of option-based log-return kurtosis regressions (average R^2 = 65.54%; excl. risk-neutral: 57.12%)

	$\gamma_1 r$	$\gamma_1 nvix^{\gamma_3} r$	$\gamma_1 r + \gamma_2 r^2$	$\gamma_1 nvix^{\gamma_3} r + \gamma_2 nvix^{\gamma_3} r^2$
$\gamma_1 nvix^{\gamma_3} r$	99.71%			
$\gamma_1 r + \gamma_2 r^2$	97.55%	96.93%		
$\gamma_1 nvix^{\gamma_3} r + \gamma_2 nvix^{\gamma_3} r^2$	14.88%	16.20%	17.46%	
risk-neutral	97.01%	98.00%	96.04%	21.65%

Panel C: 3-month expiration

R^2's of option-based expected log-returns regressions (average R^2 = 37.35%; excl. risk-neutral: 41.17%)

	$\gamma_1 r$	$\gamma_1 nvix^{\gamma_3} r$	$\gamma_1 r + \gamma_2 r^2$	$\gamma_1 nvix^{\gamma_3} r + \gamma_2 nvix^{\gamma_3} r^2$
$\gamma_1 nvix^{\gamma_3} r$	60.65%			
$\gamma_1 r + \gamma_2 r^2$	92.07%	72.60%		
$\gamma_1 nvix^{\gamma_3} r + \gamma_2 nvix^{\gamma_3} r^2$	14.08%	3.10%	4.50%	
risk-neutral	6.61%	56.39%	20.92%	42.56%

R^2's of option-based log-return variances regressions (average R^2 = 92.45%; excl. risk-neutral: 92.82%)

	$\gamma_1 r$	$\gamma_1 nvix^{\gamma_3} r$	$\gamma_1 r + \gamma_2 r^2$	$\gamma_1 nvix^{\gamma_3} r + \gamma_2 nvix^{\gamma_3} r^2$
$\gamma_1 nvix^{\gamma_3} r$	98.33%			
$\gamma_1 r + \gamma_2 r^2$	89.79%	90.22%		
$\gamma_1 nvix^{\gamma_3} r + \gamma_2 nvix^{\gamma_3} r^2$	92.52%	96.35%	89.70%	
risk-neutral	90.75%	90.35%	98.66%	87.78%

R^2's of option-based log-return skewness regressions (average R^2 = 63.85%; excl. risk-neutral: 54.82%)

	$\gamma_1 r$	$\gamma_1 nvix^{\gamma_3} r$	$\gamma_1 r + \gamma_2 r^2$	$\gamma_1 nvix^{\gamma_3} r + \gamma_2 nvix^{\gamma_3} r^2$
$\gamma_1 nvix^{\gamma_3} r$	98.66%			
$\gamma_1 r + \gamma_2 r^2$	91.91%	95.01%		
$\gamma_1 nvix^{\gamma_3} r + \gamma_2 nvix^{\gamma_3} r^2$	7.97%	14.11%	21.28%	
risk-neutral	96.96%	98.69%	97.42%	16.55%

R^2's of option-based log-return kurtosis regressions (average R^2 = 69.04%; excl. risk-neutral: 61.19%)

	$\gamma_1 r$	$\gamma_1 nvix^{\gamma_3} r$	$\gamma_1 r + \gamma_2 r^2$	$\gamma_1 nvix^{\gamma_3} r + \gamma_2 nvix^{\gamma_3} r^2$
$\gamma_1 nvix^{\gamma_3} r$	99.55%			
$\gamma_1 r + \gamma_2 r^2$	95.00%	95.73%		
$\gamma_1 nvix^{\gamma_3} r + \gamma_2 nvix^{\gamma_3} r^2$	19.85%	23.52%	33.49%	
risk-neutral	98.47%	99.08%	97.46%	28.20%

Panel D: 6-month expiration

R^2's of option-based expected log-returns regressions (average R^2 = 33.82%; excl. risk-neutral: 38.92%)

	$\gamma_1 r$	$\gamma_1 nvix^{\gamma_3} r$	$\gamma_1 r + \gamma_2 r^2$	$\gamma_1 nvix^{\gamma_3} r + \gamma_2 nvix^{\gamma_3} r^2$
$\gamma_1 nvix^{\gamma_3} r$	52.72%			
$\gamma_1 r + \gamma_2 r^2$	79.44%	74.41%		
$\gamma_1 nvix^{\gamma_3} r + \gamma_2 nvix^{\gamma_3} r^2$	8.19%	18.77%	0.00%	
risk-neutral	0.02%	35.25%	15.09%	54.36%

R^2's of option-based log-return variances regressions (average R^2 = 85.53%; excl. risk-neutral: 84.31%)

	$\gamma_1 r$	$\gamma_1 nvix^{\gamma_3} r$	$\gamma_1 r + \gamma_2 r^2$	$\gamma_1 nvix^{\gamma_3} r + \gamma_2 nvix^{\gamma_3} r^2$
$\gamma_1 nvix^{\gamma_3} r$	97.42%			
$\gamma_1 r + \gamma_2 r^2$	76.73%	79.97%		
$\gamma_1 nvix^{\gamma_3} r + \gamma_2 nvix^{\gamma_3} r^2$	85.95%	94.40%	71.38%	
risk-neutral	87.88%	89.60%	92.92%	79.05%

R^2's of option-based log-return skewness regressions (average R^2 = 50.41%; excl. risk-neutral: 39.64%)

	$\gamma_1 r$	$\gamma_1 nvix^{\gamma_3} r$	$\gamma_1 r + \gamma_2 r^2$	$\gamma_1 nvix^{\gamma_3} r + \gamma_2 nvix^{\gamma_3} r^2$
$\gamma_1 nvix^{\gamma_3} r$	81.72%			
$\gamma_1 r + \gamma_2 r^2$	65.41%	82.65%		
$\gamma_1 nvix^{\gamma_3} r + \gamma_2 nvix^{\gamma_3} r^2$	2.22%	3.54%	2.29%	
risk-neutral	86.11%	88.81%	91.31%	0.02%

R^2's of option-based log-return kurtosis regressions (average R^2 = 54.78%; excl. risk-neutral: 44.16%)

	$\gamma_1 r$	$\gamma_1 nvix^{\gamma_3} r$	$\gamma_1 r + \gamma_2 r^2$	$\gamma_1 nvix^{\gamma_3} r + \gamma_2 nvix^{\gamma_3} r^2$
$\gamma_1 nvix^{\gamma_3} r$	91.73%			
$\gamma_1 r + \gamma_2 r^2$	76.42%	88.34%		
$\gamma_1 nvix^{\gamma_3} r + \gamma_2 nvix^{\gamma_3} r^2$	0.05%	4.22%	4.21%	
risk-neutral	91.12%	95.57%	94.060%	1.53%

Table A.4 Coefficient of Determination for 3rd and 4th Moments under the Physical Measure across Pricing Kernels

This table reports coefficients of determination (R^2) from regressing option-based third and fourth central moments across the different pricing kernels from equations (1), (2), (4), (6). Option-based physical moments are derived according to equation (14). The pricing kernels are classified according to the their exponents: $\gamma_1 r$ (equation (1)), $\gamma_1 nvix^{\gamma_3} r$ (equation (2)), $\gamma_1 r + \gamma_2 r^2$ (equation (4)), and $\gamma_1 nvix^{\gamma_3} r + \gamma_2 nvix^{\gamma_3} r^2$ (equation (6)), where r denotes log returns, and $nvix$ is the normalized VIX, which is the VIX divided by its 1986-1995 average (to avoid look-ahead bias) and appropriately scaled for each expiration. The estimation of the various pricing kernels is based on the GMM system of equation (13), and the results are reported in Table 2 through Table 5. *risk-neutral* denotes the moments of the risk-neutral density. Panel A reports R^2's for option-based moment regressions for the 1-month expiration. Panel B reports R^2's for option-based moment regressions for the 2-month expiration. Panel C reports R^2's for the 3-month expiration, and Panel D shows R^2' for the 6-month expiration. N is the number of observations. The sample is from January 1996 to December 2022 for 1-month expiration options, May 1998 to November 2022 for 2-month expiration, January 2002 to October 2022 for 3-month expiration, and June 1996 to June 2022 for 6-month expiration options.

Panel A: 1-month expiration

R^2's of option-based third central moment regressions (average R^2 = 53.65%; excl. risk-neutral: 46.38%)

	$\gamma_1 r$	$\gamma_1 nvix^{\gamma_3} r$	$\gamma_1 r + \gamma_2 r^2$	$\gamma_1 nvix^{\gamma_3} r + \gamma_2 nvix^{\gamma_3} r^2$
$\gamma_1 nvix^{\gamma_3} r$	24.80%			
$\gamma_1 r + \gamma_2 r^2$	73.90%	37.73%		
$\gamma_1 nvix^{\gamma_3} r + \gamma_2 nvix^{\gamma_3} r^2$	86.24%	3.31%	52.28%	
risk-neutral	92.81%	11.50%	57.36%	96.60%

R^2's of option-based fourth central moment regressions (average R^2 =54.22%; excl. risk-neutral: 46.67%)

	$\gamma_1 r$	$\gamma_1 nvix^{\gamma_3} r$	$\gamma_1 r + \gamma_2 r^2$	$\gamma_1 nvix^{\gamma_3} r + \gamma_2 nvix^{\gamma_3} r^2$
$\gamma_1 nvix^{\gamma_3} r$	18.95%			
$\gamma_1 r + \gamma_2 r^2$	82.17%	24.31%		
$\gamma_1 nvix^{\gamma_3} r + \gamma_2 nvix^{\gamma_3} r^2$	89.44%	4.48%	60.70%	
risk-neutral	92.01%	9.05%	62.12%	98.95%

Panel B: 2-month expiration

R^2's of option-based third central moment regressions (average R^2 = 85.06%; excl. risk-neutral: 81.08%)

	$\gamma_1 r$	$\gamma_1 nvix^{\gamma_3} r$	$\gamma_1 r + \gamma_2 r^2$	$\gamma_1 nvix^{\gamma_3} r + \gamma_2 nvix^{\gamma_3} r^2$
$\gamma_1 nvix^{\gamma_3} r$	92.10%			
$\gamma_1 r + \gamma_2 r^2$	55.48%	78.65%		
$\gamma_1 nvix^{\gamma_3} r + \gamma_2 nvix^{\gamma_3} r^2$	72.64%	92.63%	94.97%	
risk-neutral	79.53%	94.46%	92.64%	97.53%

R^2's of option-based fourth central moment regressions (average R^2 = 88.88%; excl. risk-neutral: 86.23%)

	$\gamma_1 r$	$\gamma_1 nvix^{\gamma_3} r$	$\gamma_1 r + \gamma_2 r^2$	$\gamma_1 nvix^{\gamma_3} r + \gamma_2 nvix^{\gamma_3} r^2$
$\gamma_1 nvix^{\gamma_3} r$	90.72%			
$\gamma_1 r + \gamma_2 r^2$	67.13%	90.24%		
$\gamma_1 nvix^{\gamma_3} r + \gamma_2 nvix^{\gamma_3} r^2$	75.11%	95.23%	98.94%	
risk-neutral	77.68%	95.77%	98.48%	99.51%

Panel C: 3-month expiration

R^2's of option-based third central moment regressions (average R^2 = 83.46%; excl. risk-neutral: 81.73%)

	$\gamma_1 r$	$\gamma_1 nvix^{\gamma_3} r$	$\gamma_1 r + \gamma_2 r^2$	$\gamma_1 nvix^{\gamma_3} r + \gamma_2 nvix^{\gamma_3} r^2$
$\gamma_1 nvix^{\gamma_3} r$	92.78%			
$\gamma_1 r + \gamma_2 r^2$	77.78%	76.04%		
$\gamma_1 nvix^{\gamma_3} r + \gamma_2 nvix^{\gamma_3} r^2$	77.02%	91.76%	75.02%	
risk-neutral	89.35%	83.32%	95.84%	75.67%

R^2's of option-based fourth central moment regressions (average R^2 = 81.30%; excl. risk-neutral: 79.01%)

	$\gamma_1 r$	$\gamma_1 nvix^{\gamma_3} r$	$\gamma_1 r + \gamma_2 r^2$	$\gamma_1 nvix^{\gamma_3} r + \gamma_2 nvix^{\gamma_3} r^2$
$\gamma_1 nvix^{\gamma_3} r$	92.11%			
$\gamma_1 r + \gamma_2 r^2$	72.73%	70.92%		
$\gamma_1 nvix^{\gamma_3} r + \gamma_2 nvix^{\gamma_3} r^2$	75.05%	90.59%	72.69%	
risk-neutral	87.76%	81.35%	94.94%	74.90%

Panel D: 6-month expiration

R^2's of option-based third central moment regressions (average R^2 = 72.35%; excl. risk-neutral: 68.86%)

	$\gamma_1 r$	$\gamma_1 nvix^{\gamma_3} r$	$\gamma_1 r + \gamma_2 r^2$	$\gamma_1 nvix^{\gamma_3} r + \gamma_2 nvix^{\gamma_3} r^2$
$\gamma_1 nvix^{\gamma_3} r$	92.48%			
$\gamma_1 r + \gamma_2 r^2$	61.48%	63.17%		
$\gamma_1 nvix^{\gamma_3} r + \gamma_2 nvix^{\gamma_3} r^2$	68.00%	87.65%	40.38%	
risk-neutral	85.48%	81.78%	87.29%	55.81%

R^2's of option-based fourth central moment regressions (average R^2 = 70.71%; excl. risk-neutral: 66.85%)

	$\gamma_1 r$	$\gamma_1 nvix^{\gamma_3} r$	$\gamma_1 r + \gamma_2 r^2$	$\gamma_1 nvix^{\gamma_3} r + \gamma_2 nvix^{\gamma_3} r^2$
$\gamma_1 nvix^{\gamma_3} r$	93.41%			
$\gamma_1 r + \gamma_2 r^2$	59.37%	56.43%		
$\gamma_1 nvix^{\gamma_3} r + \gamma_2 nvix^{\gamma_3} r^2$	71.79%	89.14%	30.93%	
risk-neutral	86.76%	80.33%	85.47%	53.51%

Appendix C Proofs

A.1 Pricing Kernels and Log-normal Densities

This section derives the resulting probability densities from combining linear or quadratic pricing kernels with log-normal or skew log-normal distributions. The log-normal probability density function is proportional to

$$\frac{1}{y}Exp\Big[\frac{(lny+\omega)^2}{2\sigma^2}\Big].$$

The constants ω and σ^2 are the location and scale parameters of the distribution.

The skew log-normal probability density function is proportional to

$$\frac{1}{y}Exp\Big[\frac{(lny+\omega)^2}{2\sigma^2}\Big]\Phi\Big(\lambda\frac{lny-\omega}{\sigma}+\xi\Big),$$

where $\Phi()$ is the standard normal cumulative distribution function. The constants ω and σ^2 are the location and scale parameters. The parameters λ and ξ are the skewness and kurtosis parameters for $R>0$. Based on the probability density functions above for the log-normal and the skew log-normal distributions, the distributions resulting from the linear and quadratic pricing kernels can be easily calculated.

Linear Pricing Kernel and Log-normal Distribution

$$\frac{1}{y}Exp\Big[\gamma_1 lny-\frac{(lny-\omega)^2}{2\sigma^2}\Big]\propto\frac{1}{y}Exp\Big[-\frac{\big(lny-(\omega+\gamma_1\sigma^2)\big)^2}{2\sigma^2}\Big].$$

Quadratic Pricing Kernel and Log-normal Distribution

$$\frac{1}{y}Exp\Big[\gamma_1 lny+\gamma_2 ln^2y-\frac{(lny-\omega)^2}{2\sigma^2}\Big]\propto\frac{1}{y}Exp\Big[-\frac{\big(lny-\frac{\omega+\gamma_1\sigma^2}{1-2\gamma_2\sigma^2}\big)^2}{2\frac{\sigma^2}{1-2\gamma_2\sigma^2}}\Big].$$

Linear Pricing Kernel and Skew Log-normal Distribution

$$\frac{1}{y}Exp\Big[\gamma_1 lny-\frac{(lny-\omega)^2}{2\sigma^2}\Big]\Phi\Big(\lambda\frac{lny-\omega}{\sigma}+\xi\Big)\propto$$
$$\frac{1}{y}Exp\Big[-\frac{\big(lny-(\omega+\gamma_1\sigma^2)\big)^2}{2\sigma^2}\Big]\Phi\Big(\lambda\frac{lny-(\omega+\gamma_1\sigma^2)}{\sigma}+\xi+\lambda\gamma_1\sigma\Big).$$

$$\frac{1}{y}Exp\Big[\gamma_1 lny + \gamma_2 ln^2 y - \frac{(lny-\omega)^2}{2\sigma^2}\Big]\Phi\Big(\lambda\frac{lny-\omega}{\sigma}+\xi\Big) \propto$$
$$\frac{1}{y}Exp\Big[-\frac{\big(lny-\frac{\omega+\gamma_1\sigma^2}{1-2\gamma_2\sigma^2}\big)^2}{2\frac{\sigma^2}{1-2\gamma_2\sigma^2}}\Big]\Phi\Big(\frac{\lambda}{\sqrt{1-2\gamma_2\sigma^2}}\frac{lny-\frac{\omega+\gamma_1\sigma^2}{1-2\gamma_2\sigma^2}}{\frac{\sigma}{\sqrt{1-2\gamma_2\sigma^2}}}+\xi+\lambda\frac{\gamma_1+2\omega\gamma_2}{1-2\gamma_2\sigma^2}\sigma\Big).$$

A.2 Location-Scale Moments

Let Y be a location-scale transformation of a standardized random variable r:

$$Y = \omega + Z\sigma,$$

where ω and σ are the location and scale parameters. Then, it follows that

$$\begin{aligned}
&E[Y] = \omega + E[Z]\sigma \\
&E[(Y-E[Y])^2] = E[(Z-E[Z])^2]\sigma^2 \\
&E[(Y-E[Y])^3] = E[(Z-E[Z])^3]\sigma^3 \\
&E[(Y-E[Y])^4] = E[(Z-E[Z])^4]\sigma^4.
\end{aligned}$$

A.3 Truncated Normal Moments

This section derives the moments of a standard normal variable, T, truncated below the point $-\frac{\xi}{\sqrt{1+\lambda^2}}$:

$$T \sim \frac{N(0,1)}{1-\Phi\big(-\frac{\xi}{\sqrt{1+\lambda^2}}\big)},\ T > -\frac{\xi}{\sqrt{1+\lambda^2}}.$$

The first moment is

$$E[T] = \frac{\phi\big(-\frac{\xi}{\sqrt{1+\lambda^2}}\big)}{1-\Phi\big(-\frac{\xi}{\sqrt{1+\lambda^2}}\big)}.$$

The second and third moments are respectively

$$E[T^2] = 1 - \frac{\xi}{\sqrt{1+\lambda^2}}\frac{\phi\big(-\frac{\xi}{\sqrt{1+\lambda^2}}\big)}{1-\Phi\big(-\frac{\xi}{\sqrt{1+\lambda^2}}\big)}$$

and

$$E[T^3] = \frac{\Big(2 + \Big(\frac{\xi}{\sqrt{1+\lambda^2}}\Big)^2\Big)\phi\big(-\frac{\xi}{\sqrt{1+\lambda^2}}\big)}{1-\Phi\big(-\frac{\xi}{\sqrt{1+\lambda^2}}\big)}.$$

Hence, the second and third central moments are respectively

$$E[(T-E[T])^2] = 1 - \frac{\xi}{\sqrt{1+\lambda^2}}\frac{\phi\big(-\frac{\xi}{\sqrt{1+\lambda^2}}\big)}{1-\Phi\big(-\frac{\xi}{\sqrt{1+\lambda^2}}\big)} - \frac{\phi\big(-\frac{\xi}{\sqrt{1+\lambda^2}}\big)^2}{\big(1-\Phi\big(-\frac{\xi}{\sqrt{1+\lambda^2}}\big)\big)^2}$$

and

$$\begin{aligned}
E[(T-E[T])^3] &= \frac{\Big(2 + \Big(\frac{\xi}{\sqrt{1+\lambda^2}}\Big)^2\Big)\phi\big(-\frac{\xi}{\sqrt{1+\lambda^2}}\big)}{1-\Phi\big(-\frac{\xi}{\sqrt{1+\lambda^2}}\big)} \\
&-3\frac{\phi\big(-\frac{\xi}{\sqrt{1+\lambda^2}}\big)}{1-\Phi\big(-\frac{\xi}{\sqrt{1+\lambda^2}}\big)}\Big(1 - \frac{\xi}{\sqrt{1+\lambda^2}}\frac{\phi\big(-\frac{\xi}{\sqrt{1+\lambda^2}}\big)}{1-\Phi\big(-\frac{\xi}{\sqrt{1+\lambda^2}}\big)}\Big) + 2\frac{\phi\big(-\frac{\xi}{\sqrt{1+\lambda^2}}\big)^3}{(1-\Phi\big(-\frac{\xi}{\sqrt{1+\lambda^2}}\big))^3} \\
&\frac{\Big(\Big(\frac{\xi}{\sqrt{1+\lambda^2}}\Big)^2 - 1\Big)\phi\big(-\frac{\xi}{\sqrt{1+\lambda^2}}\big)}{1-\Phi\big(-\frac{\xi}{\sqrt{1+\lambda^2}}\big)} + 3\frac{\xi}{\sqrt{1+\lambda^2}}\frac{\phi\big(-\frac{\xi}{\sqrt{1+\lambda^2}}\big)^2}{\big(1-\Phi\big(-\frac{\xi}{\sqrt{1+\lambda^2}}\big)\big)^2} + 2\frac{\phi\big(-\frac{\xi}{\sqrt{1+\lambda^2}}\big)^3}{\big(1-\Phi\big(-\frac{\xi}{\sqrt{1+\lambda^2}}\big)\big)^3}.
\end{aligned}$$

.

A.4 Standard Skew-Normal Moments

The standard skew-normal random variable, r, can be derived as the linear combination of a truncated standard normal variable, T, which is truncated above the point $-\frac{\xi}{\sqrt{1+\lambda^2}}$, and a standard normal variable, V:

$$Z = \frac{\lambda}{\sqrt{1+\lambda^2}}T + \frac{1}{\sqrt{1+\lambda^2}}V,\ T \sim \frac{N(0,1)}{1-\Phi\big(-\frac{\xi}{\sqrt{1+\lambda^2}}\big)},\ T > -\frac{\xi}{\sqrt{1+\lambda^2}},\ V \sim N(0,1).$$

Using the binomial expansion, the general formula for the moments of r as a function of the moments of T and V is given by

$$E[Z^n] = \sum_{i=0}^{n}\binom{n}{i}\Big(\frac{\lambda}{\sqrt{1+\lambda^2}}\Big)^i\Big(\frac{1}{\sqrt{1+\lambda^2}}\Big)^{n-i}E[T^i]E[V^{n-i}].$$

Hence, the first moment of r is

$$E[Z^1] = \frac{\lambda}{\sqrt{1+\lambda^2}}E[T^1] = \frac{\lambda}{\sqrt{1+\lambda^2}}\frac{\phi\big(-\frac{\xi}{\sqrt{1+\lambda^2}}\big)}{1-\Phi\big(-\frac{\xi}{\sqrt{1+\lambda^2}}\big)},$$

where $\phi()$ is the standard normal density function. The second moment of r is given by

$$E[Z^2] = \frac{1}{1+\lambda^2} + \frac{\lambda^2}{1+\lambda^2}\Big(1 - \frac{\xi}{\sqrt{1+\lambda^2}}\frac{\phi\big(-\frac{\xi}{\sqrt{1+\lambda^2}}\big)}{1-\Phi\big(-\frac{\xi}{\sqrt{1+\lambda^2}}\big)}\Big),$$

and its variance is equal to

$$var(Z) = 1 - \frac{\lambda^2}{1+\lambda^2}\frac{\xi}{\sqrt{1+\lambda^2}}\frac{\phi\big(-\frac{\xi}{\sqrt{1+\lambda^2}}\big)}{1-\Phi\big(-\frac{\xi}{\sqrt{1+\lambda^2}}\big)} - \frac{\lambda^2}{1+\lambda^2}\frac{\phi\big(-\frac{\xi}{\sqrt{1+\lambda^2}}\big)^2}{\Big(1-\Phi\big(-\frac{\xi}{\sqrt{1+\lambda^2}}\big)\Big)^2}.$$

Similarly, the third central moment of r is

$$E[(Z-E[Z])^3] =$$
$$\frac{\lambda^3}{(1+\lambda^2)^{3/2}}\Big[\frac{\Big(\Big(\frac{\xi}{\sqrt{1+\lambda^2}}\Big)^2 - 1\Big)\phi\big(-\frac{\xi}{\sqrt{1+\lambda^2}}\big)}{1-\Phi\big(-\frac{\xi}{\sqrt{1+\lambda^2}}\big)} + 3\frac{\xi}{\sqrt{1+\lambda^2}}\frac{\phi\big(-\frac{\xi}{\sqrt{1+\lambda^2}}\big)^2}{\big(1-\Phi\big(-\frac{\xi}{\sqrt{1+\lambda^2}}\big)\big)^2} + 2\frac{\phi\big(-\frac{\xi}{\sqrt{1+\lambda^2}}\big)^3}{\big(1-\Phi\big(-\frac{\xi}{\sqrt{1+\lambda^2}}\big)\big)^3}\Big].$$

A.5 Derivative of the Inverse Mills Ratio

The inverse Mills ratio for a standard normal variable is

$$\frac{\phi(x)}{1-\Phi(x)}.$$

Its derivative is

$$\frac{\phi(x)}{1-\Phi(x)}\Big(-x + \frac{\phi(x)}{1-\Phi(x)}\Big).$$

From Appendix A.3, if $\widetilde{T}$ is a standard normal variable truncated from below at x, then

$$E[\widetilde{T}|\widetilde{T} \geq x] = \frac{\phi(x)}{1-\Phi(x)}.$$

Thus, for a standard normal variable, truncated from below at x the following holds

$$E[\widetilde{T}|\widetilde{T} \geq x] = \frac{\phi(x)}{1-\Phi(x)} > x,$$

and the inverse Mills ratio for a standard normal variable is strictly increasing.

A.6 Moments of Location-Scale Skew-Normal Distribution

Let the risk-neutral density for the random variable, Y, be skew log-normal with location, scale, and shape parameters ω, σ, λ, and ξ. In this case, based on the results from Appendices

A.2 and A.3, the density function, mean and variance are respectively given by

$$dQ_Y(y) \propto \frac{1}{y} Exp\Big[- \frac{\big(lny - \omega\big)^2}{2\sigma^2}\Big] \Phi\Big(\lambda \frac{lny - \omega}{\sigma} + \xi\Big)$$

$$E[lnY]^{RND} = \omega + \frac{\lambda}{\sqrt{1+\lambda^2}} \frac{\phi\big(-\frac{\xi}{\sqrt{1+\lambda^2}}\big)}{1 - \Phi\big(-\frac{\xi}{\sqrt{1+\lambda^2}}\big)} \sigma$$

$$var\big(lnY\big)^{RND} = \Big[1 - \frac{\lambda^2}{1+\lambda^2} \frac{\xi}{\sqrt{1+\lambda^2}} \frac{\phi\big(-\frac{\xi}{\sqrt{1+\lambda^2}}\big)}{1 - \Phi\big(-\frac{\xi}{\sqrt{1+\lambda^2}}\big)} - \frac{\lambda^2}{1+\lambda^2} \frac{\phi\big(-\frac{\xi}{\sqrt{1+\lambda^2}}\big)^2}{\Big(1 - \Phi\big(-\frac{\xi}{\sqrt{1+\lambda^2}}\big)\Big)^2}\Big] \sigma^2.$$

Linear Pricing Kernel

According to Appendix A.1, after applying the linear pricing kernel to the skew-normal RND, the density function, mean, and variance respectively become

$$dP_Y(y) \propto \frac{1}{y} Exp\Big[- \frac{\big(lny - (\omega + \gamma_1\sigma^2)\big)^2}{2\sigma^2}\Big] \Phi\Big(\lambda \frac{lny - (\omega + \gamma_1\sigma^2)}{\sigma} + \xi + \lambda\gamma_1\sigma\Big) \tag{a.1}$$

$$E[lnY] = \omega + \gamma_1\sigma^2 + \frac{\lambda}{\sqrt{1+\lambda^2}} \frac{\phi\big(-\frac{\xi+\lambda\gamma_1\sigma}{\sqrt{1+\lambda^2}}\big)}{1 - \Phi\big(-\frac{\xi+\lambda\gamma_1\sigma}{\sqrt{1+\lambda^2}}\big)} \sigma \tag{a.2}$$

$$var(lnY) = \Big[1 - \frac{\lambda^2}{1+\lambda^2} \frac{\xi+\lambda\gamma_1\sigma}{\sqrt{1+\lambda^2}} \frac{\phi\big(-\frac{\xi+\lambda\gamma_1\sigma}{\sqrt{1+\lambda^2}}\big)}{1 - \Phi\big(-\frac{\xi+\lambda\gamma_1\sigma}{\sqrt{1+\lambda^2}}\big)} - \frac{\lambda^2}{1+\lambda^2} \frac{\phi\big(-\frac{\xi+\lambda\gamma_1\sigma}{\sqrt{1+\lambda^2}}\big)^2}{\Big(1 - \Phi\big(-\frac{\xi+\lambda\gamma_1\sigma}{\sqrt{1+\lambda^2}}\big)\Big)^2}\Big] \sigma^2 \tag{a.3}$$

According to the last equation above, when the risk-neutral density deviates from normality, the linear pricing kernel alters both the expected return and the variance of the risk-neutral density by changing the shape parameter in the inverse Mills ratio from ξ to $\xi + \lambda\gamma_1\sigma$. Hence, the linear pricing kernel with positive risk aversion parameter γ_1 increases the mean of the risk-neutral distribution by the term $\gamma_1\sigma^2$, as in the case of normal RND (Appendix A.1), and also by decreasing in absolute value the negative term

$$\frac{\lambda}{\sqrt{1+\lambda^2}} \frac{\phi\big(-\frac{\xi+\lambda\gamma_1\sigma}{\sqrt{1+\lambda^2}}\big)}{1 - \Phi\big(-\frac{\xi+\lambda\gamma_1\sigma}{\sqrt{1+\lambda^2}}\big)} \sigma,$$

since λ is negative for a negatively skewed RND and the inverse Mills ratio, $\frac{\phi(x)}{1-\Phi(x)}$, is strictly increasing (Appendix A.5).

Quadratic Pricing Kernel

According to Appendix A.1, after applying the quadratic pricing kernel to the skew-normal

RND, the density function, mean, and variance respectively become

$$dP_Y(y) \propto \frac{1}{R} Exp\Big[- \frac{\big(lny - \frac{\omega+\gamma_1\sigma^2}{1-2\gamma_2\sigma^2}\big)^2}{2\frac{\sigma^2}{1-2\gamma_2\sigma^2}}\Big] \tag{a.4}$$

$$\times\Phi\Big(\frac{\lambda}{\sqrt{1-2\gamma_2\sigma^2}}\frac{lny - \frac{\omega+\gamma_1\sigma^2}{1-2\gamma_2\sigma^2}}{\frac{\sigma}{\sqrt{1-2\gamma_2\sigma^2}}} + \xi + \frac{\lambda}{\sigma}\frac{2\omega\gamma_2\sigma^2+\gamma_1\sigma^2}{1-2\gamma_2\sigma^2}\Big)$$

$$E[lnY] = \frac{\omega+\gamma_1\sigma^2}{1-2\gamma_2\sigma^2} + \frac{\frac{\lambda}{\sqrt{1-2\gamma_2\sigma^2}}}{\sqrt{1+\frac{\lambda^2}{1-2\gamma_2\sigma^2}}}\frac{\phi\Big(-\frac{\xi+\frac{\lambda}{\sigma}\frac{2\omega\gamma_2\sigma^2+\gamma_1\sigma^2}{1-2\gamma_2\sigma^2}}{\sqrt{1+\frac{\lambda^2}{1-2\gamma_2\sigma^2}}}\Big)}{1-\Phi\Big(-\frac{\xi+\frac{\lambda}{\sigma}\frac{2\omega\gamma_2\sigma^2+\gamma_1\sigma^2}{1-2\gamma_2\sigma^2}}{\sqrt{1+\frac{\lambda^2}{1-2\gamma_2\sigma^2}}}\Big)}\sigma$$

$$var(lnY) = \Big[1 - \frac{\frac{\lambda^2}{1-2\gamma_2\sigma^2}}{1+\frac{\lambda^2}{1-2\gamma_2\sigma^2}}\frac{\xi+\frac{\lambda}{\sigma}\frac{2\omega\gamma_2\sigma^2+\gamma_1\sigma^2}{1-2\gamma_2\sigma^2}}{\sqrt{1+\frac{\lambda^2}{1-2\gamma_2\sigma^2}}}\frac{\phi\Big(-\frac{\xi+\frac{\lambda}{\sigma}\frac{2\omega\gamma_2\sigma^2+\gamma_1\sigma^2}{1-2\gamma_2\sigma^2}}{\sqrt{1+\frac{\lambda^2}{1-2\gamma_2\sigma^2}}}\Big)}{1-\Phi\Big(-\frac{\xi+\frac{\lambda}{\sigma}\frac{2\omega\gamma_2\sigma^2+\gamma_1\sigma^2}{1-2\gamma_2\sigma^2}}{\sqrt{1+\frac{\lambda^2}{1-2\gamma_2\sigma^2}}}\Big)}$$

$$-\frac{\frac{\lambda^2}{1-2\gamma_2\sigma^2}}{1+\frac{\lambda^2}{1-2\gamma_2\sigma^2}}\frac{\phi\Big(-\frac{\xi+\frac{\lambda}{\sigma}\frac{2\omega\gamma_2\sigma^2+\gamma_1\sigma^2}{1-2\gamma_2\sigma^2}}{\sqrt{1+\frac{\lambda^2}{1-2\gamma_2\sigma^2}}}\Big)^2}{\Big(1-\Phi\Big(-\frac{\xi+\frac{\lambda}{\sigma}\frac{2\omega\gamma_2\sigma^2+\gamma_1\sigma^2}{1-2\gamma_2\sigma^2}}{\sqrt{1+\frac{\lambda^2}{1-2\gamma_2\sigma^2}}}\Big)\Big)^2}\Big]\frac{\sigma^2}{1-2\gamma_2\sigma^2}$$

For negative (positive) quadratic parameter γ_2, the scale parameter decreases (increases) from σ to $\sigma/\sqrt{1-2\gamma_2\sigma^2}$. Further, for positive linear parameter γ_1, the location parameter increases by the term $\frac{\gamma_1\sigma^2}{1-2\gamma_2\sigma^2}$ and by decreasing the absolute value of the negative term

$$\frac{\frac{\lambda}{\sqrt{1-2\gamma_2\sigma^2}}}{\sqrt{1+\frac{\lambda^2}{1-2\gamma_2\sigma^2}}}\frac{\phi\Big(-\frac{\xi+\frac{\lambda}{\sigma}\frac{2\omega\gamma_2\sigma^2+\gamma_1\sigma^2}{1-2\gamma_2\sigma^2}}{\sqrt{1+\frac{\lambda^2}{1-2\gamma_2\sigma^2}}}\Big)}{1-\Phi\Big(-\frac{\xi+\frac{\lambda}{\sigma}\frac{2\omega\gamma_2\sigma^2+\gamma_1\sigma^2}{1-2\gamma_2\sigma^2}}{\sqrt{1+\frac{\lambda^2}{1-2\gamma_2\sigma^2}}}\Big)}\sigma. \tag{a.5}$$

Interestingly, even if γ_1 is negative, such that the term $\gamma_1\sigma^2$ is negative, the mean of the physical density could still increase relatively to the mean of the RND as long as the quadratic parameter γ_2 is negative, and decreases the absolute magnitude of the negative term in equation (a.5).